ACTIVE-SITE DYNAMICS OF FLAVODOXINS

Promotor: Dr. C. Veeger, hoogleraar in de biochemie
Co-promotor: Dr. A. J. W. G. Visser, universitair hoofddocent

Rik Leenders

ACTIVE-SITE DYNAMICS OF FLAVODOXINS

Proefschrift
ter verkrijging van de graad van doctor
in de landbouw- en milieuwetenschappen
op gezag van de rector magnificus,
dr. C. M. Karssen,
in het openbaar te verdedigen
op dinsdag 28 september 1993
des namiddags te vier uur in de Aula
van de Landbouwuniversiteit te Wageningen.

ISN 506022

CIP-DATA KONINKLIJKE BIBLIOTHEEK, DEN HAAG

Leenders, Rik

Active-site dynamics of flavodoxins / Rik Leenders. -
[S.l. : s.n.]. - Ill.
Thesis Wageningen. - With ref. - With summary in Dutch.
ISBN 90-5485-160-0
Subject headings: flavodoxins / fluorescence.

Stellingen

1. Als gevolg van de verbeterde fluorescentie-detectiemogelijkheden lijken niet-fluorescente geoxideerde flavoproteinen niet te bestaan.

   - Moore, S. A., James, M. N. G., O'Kane, D. J & Lee, J. (1993) *EMBO Journal 12*, 1767-1774
   - dit proefschrift

2. De studie van Daggett et al. van poly-alanine geven een 'rijke' peptide-dynamica op nanoseconde tijdsschaal aan, welke mogelijk het gevolg is van het feit dat zij geen oplosmiddel-moleculen hebben meegenomen in hun berekeningen.

   - Daggett, V., Kollman, P. A. & Kuntz, I. D. (1991) *Biopolymers 31*, 1115-1134

3. De fluorescentie-techniek is uitstekend geschikt voor het bestuderen van thermodynamische parameters van complexe systemen.

   - Bastiaens, Ph., van Hoek, A., Benen, J. A. E., Brochon, J. C. & Visser, A. J. W. G. (1992) *Biophys. J. 63*, 839-853
   - LeTilly, V. & Royer, C. A. (1993) *Biochemistry 32*, 7753-7758
   - dit proefschrift

4. Het feit dat een blanco experiment, zoals in het geval van de afwezigheid van expressie van interleukine-6 mRNA in hepatocyten, leidt tot een op zichzelf staande publicatie, lijkt een geval van over-expressie.

   - Scotté, M., Daveau, M., Hiron, M., Ténière, P. & Lebreton, J. P. (1993) *FEBS Letters 315*, 159-162

5. Bij het interpreteren van mutatie-studies van eiwitten in het algemeen, en van metalloproteïnen in het bijzonder, dient gekeken te worden naar de conformatie-veranderingen in het gehele eiwit.

   - Farver, O., Skov, L. K., Pascher, T., Karlsson, B. G., Nordling, M., Lundberg, L. G., Vänngard, T. & Pecht, I. (1993) *Biochemistry 32*, 7317-7322

6. Bij het opschalen van een proces van laboratoriumschaal naar bulkhoeveelheden, wordt vaak geen onderscheid gemaakt tussen kritische parameters en chemische folklore.

7. Het valt te betwijfelen of het karakteriseren van eiwitten waarvan functie noch structuur bekend zijn wel wetenschap is.

8. Het is maar af te wachten of de prijs van nieuw ontwikkelde NMR-apparatuur evenredig is met de grootte van de moleculen waarvan de structuur opgehelderd kan worden.

9. Een moleculaire dynamica berekening van een eiwit zonder water is als een ei zonder wit.

10. Praten over het kappen van tropisch regenwoud is nooit afgezaagd.

Stellingen behorende bij het proefschrift
"Active-site dynamics of flavodoxins"

Rik Leenders
Wageningen, 28 september 1993

"No temple made with hands can compare with Yosemite. Every rock in its wall seems to glow with life as if into this one mountain mansion Nature had gathered her choicest treasures."

John Muir

Aan Antonet
en
mijn ouders

Voorwoord

Hierbij wil ik iedereen bedanken die op enigerlei wijze heeft bijgedragen tot het in dit proefschrift beschreven onderzoek.

In de eerste plaats wil ik mijn promotor professor C. Veeger bedanken omdat hij mij in de gelegenheid heeft gesteld mijn promotie-onderzoek in de vakgroep Biochemie te verrichten. Mijn co-promotor Ton Visser wil ik bedanken voor zijn hulp en steun tijdens de voortgang van het onderzoek.

Arie van Hoek van de vakgroep Moleculaire Fysica heeft de laser-opstelling in de kelder altijd in optima forma gehouden. Arie, nog bedankt voor je hulp en je prettig gezelschap gedurende de vele meetsessies. Martin Kooijman, Renata Sanders-Lunsche, Martijn van Iersel en Alex Rietveld hebben in het kader van een afstudeervak hun steentje aan het onderzoek bijgedragen.

Wilfred van Gunsteren (Laboratorium für Physikalische Chemie, ETH-Zürich) en Herman Berendsen (vakgroep Biofysische Chemie, R.U. Groningen) ben ik erkentelijk voor het ontwikkelen en beschikbaar stellen van hun dynamica simulatie pakket alsmede voor hun bijdrage aan hoofdstuk 4 van dit proefschrift. Jacob de Vlieg heeft geholpen met het opstarten van de eerste berekeningen.

Verder wil ik de stichting National Computer Faciliteiten (NCF) bedanken voor het beschikbaar stellen van rekentijd op de Cyber 205 en Cray Y-MP4/464 supercomputers en Bert van Corler van de Stichting Academisch Rekencentrum Amsterdam (SARA) voor zijn hulp bij het uitvoeren van de dynamica simulaties.

I would like to thank dr. Ralf Nystrom and Johnny Roslund for their help and hospitality during the synchrotron measurements at the MAX Laboratory in Lund, Sweden. The results of the experiments are described in Chapter 6.

Goede kamergenoten zijn een belangrijke voorwaarde voor het slagen van het onderzoek. Daarom wil ik graag Philippe Bastiaens en Eward Pap bedanken voor hun zeer opgewekte en constructieve aanwezigheid gedurende een groot deel van mijn promotieperiode. I thank Nina Visser-Shcherbatska for her pleasant company and consideration for a non-smoker like myself. Ook de prettige werksfeer op de vakgroep Biochemie en de hulp bij voor mij soms niet alledaagse bezigheden heb ik altijd bijzonder gewaardeerd. Verder kijk ik met veel genoegen terug op de gezellige lunches en constructieve koffiepauzes met Werner Stolle van de vakgroep Organische Chemie, waarbij we vele experimenten en berekeningen besproken hebben.

De interesse van mijn ouders in de voortgang van het onderzoek heb ik altijd als positief ervaren. Familie en vrienden dank ik voor hun getoonde interesse.

Mijn grootste dank gaat uit naar Antonet die mij altijd gestimuleerd en gesteund heeft tijdens het onderzoek en het schrijven van het proefschrift.

Contents

Chapter 1

General Introduction

Flavodoxins

Flavodoxins are small low-potential electron-transfering proteins (molecular weight 14-25 kDa). They can be isolated from a wide variety of organisms, including some algae and strictly anaerobic bacteria, as well as obligatory and facultatively aerobic bacteria. Flavodoxins are produced under iron-deficient conditions and can substitute efficiently for ferredoxins (for reviews on flavodoxins see: Mayhew and Ludwig, 1975; Simondson and Tollin, 1980; Tollin and Edmondson, 1980; Mayhew and Tollin, 1992). It has to be stressed that in some organisms flavodoxin is a constitutive component of the cell (Yoch and Valentine, 1972). Flavodoxins have not yet been found in plants and animals.

Flavodoxins promote electron transfer between two redox proteins as part of photosynthetic, nitrogen- or sulfate-reducing or hydrogen-evolving systems (IUPAC-IUB, 1970). Flavodoxins contain one non-covalently bound flavin mononucleotide (FMN) which can exist in three different oxidation states (see Figure 1), i.e. oxidized, one-electron reduced (semiquinone) and two-electron reduced (hydroquinone). Under physiological conditions flavodoxins shuttle between the semiquinone and hydroquinone states and are thus one-electron-transfering proteins.

Amino acid composition and sequence have been determined for quite a number of flavodoxins, but the three-dimensional structure has been elucidated for only a few oxidized flavodoxins (Watenpaugh et al., 1973; Burnett et al., 1974; Smith et al., 1983; van Mierlo et al., 1990a; Fukuyama et al., 1990). Furthermore, the 3-dimensional structure of some flavodoxins has been determined in the semiquinone and reduced state (Smith et al., 1977; Ludwig et al., 1982; van Mierlo et al., 1990b; Watt et al., 1991). The overall structures of these flavodoxins in their different oxidation states are highly similar, except for some small variations in active site conformation and amino acid composition. It has been demonstrated that upon reduction of some flavodoxins the protein backbone undergoes a conformational change near the flavin facilitating hydrogen bonding between the flavin molecule and the protein (Ludwig et al., 1982; Watt et al., 1991).

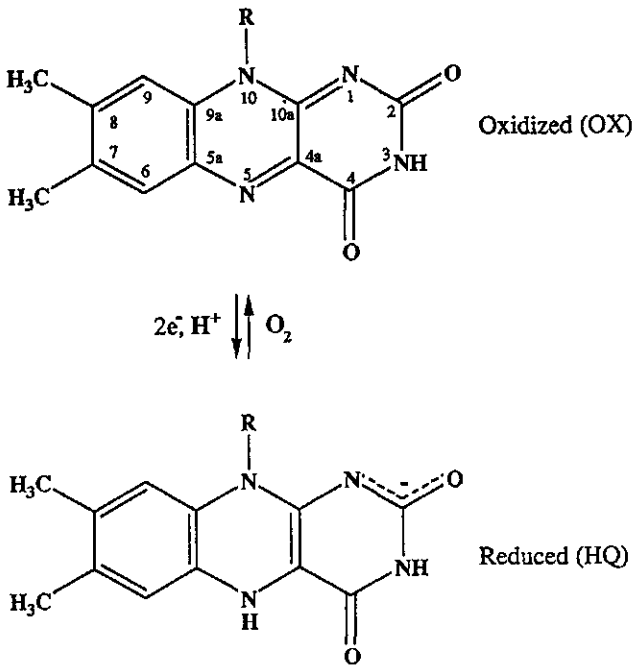

Figure 1. *The molecular structure of oxidized and two-electron-reduced protein-bound flavin mononucleotide (R is ribityl 5'-phosphate).* Upon reduction the flavin atom N(1) remains unhydrogenated and the resulting negative charge is delocalized (see text for details).

Internal dynamics of proteins

Early high-resolution X-ray crystal structure determinations gave the impression that globular proteins were densely packed bodies with precisely defined structures. Consequently one thought that proteins were fairly rigid with no or little internal mobility. This picture had to be modified, when experimental evidence accumulated showing that proteins have substantial flexibility which allows for considerable internal motion. Such motions could occur either in response to thermal forces or in response to specific or non-specific interactions with other molecules, e.g. ligand or substrate binding (Williams, 1977; Careri et al., 1979). Experimental evidence for the flexible nature of proteins came from several methods.

It was realized that packing defects are essential in order to produce channels through which oxygen can diffuse to and from the oxygen-binding sites in haemoglobin and myoglobin (Perutz and Mathews, 1966). Oxygen-quenching studies of protein fluorescence pointed in the same direction, i.e. oxygen can

reach basically any location in a protein with a diffusion coefficient that is only slightly less than in the surrounding water (Lakowicz and Weber, 1973). Further evidence for protein flexibility came from the study of allosteric effects in haemoglobin (Perutz, 1970) and from studies of fluorescence polarization (Mendelson et al., 1973; Harvey and Cheung, 1977; Rigler, 1977) indicating much shorter rotational relaxation times of aromatic amino acids in proteins than would be expected from rotational motion of the whole protein. This internal mobility of aromatic sidechains was also observed with nuclear magnetic resonance measurements (Wagner, 1983; Wagner and Wüthrich, 1986; Wüthrich, 1986).

During the last decade nuclear magnetic resonance measurements, X-ray diffraction spectroscopy, time-resolved fluorescence and fluorescence anisotropy experiments and molecular dynamics simulations yielded detailed information with respect to the time scale of structural fluctuations in proteins. In our present picture of proteins both flexibility and rigidity play an important role. The combination of both properties are considered fundamental requirements for proteins to fulfil their wide range of functions (Gurd and Rothgeb, 1979; Huber, 1987). However, at present our knowledge about flexibility of proteins is incomparably smaller than that about the aspects of static protein structures. For this reason a strong interest exists in all methods capable of studying the dynamic aspects of protein flexibility. Two of these techniques (fluorescence spectroscopy and molecular dynamics simulations) are described here in some detail because they are used throughout this thesis.

Fluorescence and fluorescence anisotropy

The absorption of light excites a molecule from the lowest vibrational level of the singlet ground state to various vibrational levels of excited singlet states in about 10^{-15} sec. For molecules in solution the excess vibrational energy is lost in about 10^{-12} sec by internal conversion (nonradiative). Fluorescence emission occurs when the molecule returns from the lowest vibrational level of the first excited singlet state to one of the vibrational levels of the ground electronic state. The absorption and emission of light is illustrated by a Jablonski diagram (Figure 2), where the ground, first, and second electronic states are depicted by S_0 , S_1 , and S_2 , respectively.

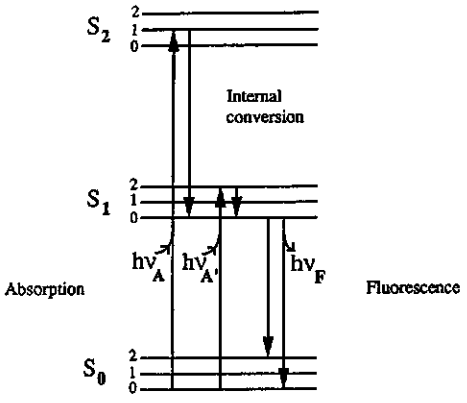

Figure 2. *Jablonski diagram illustrating the absorption and emission of light.* S_0, S_1, and S_2 are the ground, first, and second electronic states, respectively. Each electronic state is sub-divided into several vibrational levels. After the absorbtion of light ($h\nu_A$ and $h\nu_{A'}$) the system rapidly relaxes to the lowest vibrational level of the first excited state (partially via internal conversion). Fluorescence ($h\nu_F$) occurs when the molecule returns from this excited state to one of the vibrational levels of the ground electronic state.

The frequency of the light emitted in fluorescence, ν, is given by the equation:

$$\nu = \frac{\Delta E}{h} \tag{1}$$

where ΔE is the energy change associated with the emission and h is Planck's constant. Because of nonradiative losses of vibrational energy, fluorescence obviously occurs at a longer wavelength than absorbance. The main cause of this so-called Stokes' shift is the rapid decay to the lowest vibrational level of S_1 or to excited vibrational levels of S_0. In addition to these effects, fluorophores can undergo excited-state reactions or can interact with solvent molecules leading to an additional red-shift of the emission. The fluorescence quantum yield, Q, defined as the ratio of the number of photons emitted to absorbed, is not equal to unity because of these nonradiative processes.

From the depopulation of the excited state information can be obtained about the characteristics of the environment of the fluorophore. The decay process can be described by:

$$\frac{d(D^*)}{dt} = -(k_F + k_{NR}) \cdot (D^*) \tag{2}$$

where D^* is the population of the excited state, k_F is the fluorescence decay rate and k_{NR} represents the decay rate of all nonradiative processes. Eq. 2 can also be written as:

$$D^* = D_0^* e^{-t/\tau} \tag{3}$$

where D_0^* is the initial population of the excited state and τ is the fluorescence lifetime, $\tau = 1/(k_F + k_{NR})$. The rate constant k_F is the spontaneous transition probability, and $1/k_F$ is the natural lifetime, τ_0. This natural lifetime can be calculated from the spectral properties of the fluorescent species, e.g. according to Strickler and Berg (1962). Often the decay of fluorescence cannot be described by a single first-order rate process because, for example, two or more species with different lifetimes are present in the sample or the excited molecule undergoes an excited-state reaction, like quenching. A simplified way to describe the time dependence of the fluorescence decay is given by:

$$F(t) = \sum_i^N \alpha_i e^{-t/\tau_i} \qquad \text{(with } i=1,2,...N\text{)} \tag{4}$$

where $F(t)$ is the multi-exponential time-dependent fluorescence intensity, and α_i and τ_i are the amplitude parameter and relaxation times of component i, respectively. The decay parameters can be determined by a nonlinear least-squares curve-fitting procedure as described by Vos et al. (1987). A more realistic way to approach fluorescence decays is by treating them as distributions. It is known that the excited-state lifetime of a fluorophore in a protein is very sensitive to the physical properties of its environment. As described above protein environments often are very flexible, which will be reflected in a range of fluorescence lifetimes, rather than a few discrete lifetimes. The recently developed Maximum Entropy Method (Livesey and Brochon, 1987) approaches the fluorescence decay by a distribution of lifetimes τ, which are equally distributed in $\log(\tau)$ space. By using the Shannon-Jaynes information entropy an optimal spectrum of decay times is recovered by maximizing this entropy and minimizing χ^2 statistics.

Fluorophores preferentially absorb photons whose electric vectors are aligned parallel to the transition moment of the fluorophore. The transition moment has a defined orientation in the fluorophore. Upon excitation of an isotropic solution with polarized light, one selectively excites those fluorophores

whose absorption transition dipole is parallel to the electric vector of the exciting light. This selective excitation (photoselection) of an oriented population of fluorophores results in a polarized fluorescence emission. The time-resolved fluorescence anisotropy is defined as (Jablonski, 1960):

$$r(t) = \frac{I_{\parallel}(t) - I_{\perp}(t)}{I_{\parallel}(t) + 2I_{\perp}(t)} \tag{5}$$

where $I_{\parallel}(t)$ and $I_{\perp}(t)$ are the time-dependent parallel and perpendicular polarized components of emission, relative to the polarization direction of the exciting beam. Since the anisotropy decay is superimposed on the excited state decay, the time dependence of the anisotropic fluorescence contains information on both excited state decay and rotational motion of molecules as well as on energy transfer (Perrin, 1936; Ehrenberg and Rigler, 1972; Rigler and Ehrenberg, 1973; Szabo, 1984a; Bastiaens et al., 1991, 1992).

Assuming that the absorption and emission transition transition moments have fixed orientations within the fluorophore, the fundamental anisotropy, r_0, is given by:

$$r_0 = \frac{0.4\ (3cos^2\delta - 1)}{2} \tag{6}$$

where the factor 0.4 originates from photoselection and δ is the angle between absorption and emission transition moment; the maximum value of r_0 is therefore 0.4 (colinear transition moments).

Fluorescence spectroscopy is a powerful tool to study macromolecular structure and dynamics. For many years information has been obtained using steady-state fluorescence intensity measurements, but in the last two decades, time-resolved fluorescence and fluorescence anisotropy studies enjoy an increased interest because of instrumental and theoretical developments (van Hoek et al., 1983; Chang et al., 1985; van Hoek and Visser, 1992). The availability of high-quality laser and synchrotron systems as excitation sources now permit subnanosecond measurements on a routine basis with high reliability (this is especially true for time-correlated single-photon counting fluorimetry (TCSPC)). Furthermore, theoretical studies provide a new basis for the interpretation of fluorescence data (Lipari and Szabo, 1980; Szabo, 1984b; Bajzer et al., 1990; Janssens et al., 1990; Ameloot et al., 1991). It has been

suggested that heterogeneous fluorescence intensity decays in chemical and biological systems might be better interpreted in terms of a distribution of fluorescent lifetimes (James et al., 1985; Alcala et al., 1987a, 1987b; Livesey and Brochon, 1987), as compared to analysis in discrete exponential terms. It has been stressed that, whenever possible, the results of different analytical methods should be checked with simulations based on parameters recovered from the original experimental data (Ludescher et al., 1987; Prendergast et al., 1991).

These developments enable researchers to examine the dynamics of ultrafast physical and chemical processes at a molecular level. Applications are in the fields of photophysics and photochemistry where it is now possible to probe electronic and vibrational processes on a sub-nanosecond time scale. Extremely fast femtosecond lasers even allow us to study biological processes that are 'non-photochemical' in nature (for reviews on femtosecond laser spectroscopy see: Fleming, 1986; Shank, 1988).

Key technical factors in the development of picosecond fluorescence instrumentation have been: the availability of stable laser systems that can deliver excitation pulses of short duration (<10 ps for dye lasers) and of sufficient peak power, the existence of non-linear optical systems for 'frequency doubling' of dye laser outputs (particularly useful with UV excitation), and the availability of ultrafast optical detection systems, mostly through the use of microchannel plate photomultiplier tubes. The improvement of fluorescence techniques and methodology continues and will further enhance the accuracy of quantitation of fluorescence parameters that helps revealing the details of the intrinsically complex photophysics of fluorophores, such as for instance the (naturally occurring) fluorophores tyrosine, tryptophan and flavin.

Molecular dynamics simulations

Since a part of this thesis concerns molecular dynamics (MD) simulations a brief description of the method will be given here (for a recent review see: van Gunsteren and Mark, 1992). MD simulations can be used to model the conformational dynamics of a variety of systems, ranging from small organic molecules to large proteins in different environments (in vacuo, crystals or in solution). In combination with information obtained with spectroscopic techniques computer simulations can be used for tracing conformational differences between molecules in solution and in the crystalline state (solvent effects). MD simulations can also be used in solving unknown 3-dimensional

structures using starting configurations of comparable molecules. Simulations are a very useful tool to do time series analysis of structural and energetic properties and one thus can gain insight in the internal dynamics of a molecule.

Before performing any calculations the appropriate simulation program and force field has to be chosen. Three MD programs are generally available and frequently used: AMBER (Weiner and Kollman, 1981), CHARMm (Brooks et al., 1983), and GROMOS (van Gunsteren and Berendsen, 1987). Each program has its advantages and disadvantages and the actual choice is not only determined by fully scientific considerations but is also based on experience of colleagues, ease of use, availability and support. The standard MD programs provide a limited number of potential functions to describe the models and the interaction function is always a simplification of reality. In some cases standard MD programs have to be modified for specific use or one even has to write a new simulation program. In our case, in which we studied *clostridial* flavodoxin in different oxidation states, the GROMOS program was selected for it is known to describe protein dynamics adequately. The procedures as well as conditions used in our MD simulations will be described here.

First a protein structure file (PSF) has to be created from a residue topology file (RTF). This residue topology file contains information about the molecular topology of each of the amino acid residues as well as all kinds of small organic molecules (like for example porphyrin or flavin mononucleotide). It also contains information on atom names, atom types, atomic masses, and partial atomic charges as well as lists of bonds, angles, dihedral angles and improper dihedral angles for each of the individual protein building blocks. The protein structure file contains information about the amino acid sequence (primary structure) and chromophoric groups and is completed by patching the amino and carboxyl ends and adding information where disulphide bridges are located within the protein. All interaction parameters for the protein are read from the interaction function parameter file (IFP). Reduction of computational demands is established using united atom representations in which hydrogens attached to non-polar carbons are not treated explicitly. Only the so-called polar hydrogens defined as those bonded to oxygen, nitrogen, olefin carbon, or carbonyl carbon atoms are taken into account. Cartesian coordinates can be taken from crystallographically obtained structures, as well as from 'hand-built' structures.

In the early stages MD simulations were mainly performed in vacuo (McCammon et al., 1977; Northrup et al., 1980; Levitt, 1980; Ichiye and Karplus, 1983; Levy, 1985; Åqvist et al., 1985, 1986; Henry and Hochstrasser, 1987). However, under these conditions the characteristics of the surface

residues are distorted. The classical way to minimize these edge effects in a finite system is to use periodic boundary conditions in systems with or without solvent molecules surrounding the molecule of interest. When simulations are performed in solvent environment this means that the atoms of the system are placed in a rectangular box with solvent molecules, and is surrounded by 26 identical translated images of itself. As a consequence of the large number of atoms involved, this approach is very expensive for proteins. An alternative and much cheaper way to simulate in solvent environment is the use of spherical boundary conditions. This means that the region of interest is surrounded by a sphere of solvent molecules. Vacuum distortions are then minimized by position-restraining the solvent molecules located in the outer sphere (Figure 3). The size of the system is then significantly smaller than the rectangular box and simulations can be performed in convenient periods of time. Another way to reduce the needed computer time is to apply bond-length constraints using the SHAKE method (Ryckaert et al., 1977; van Gunsteren and Berendsen, 1977; Berendsen and van Gunsteren, 1983). By constraining the degrees of freedom with highest frequencies, the time step can be larger, reducing the required computation time.

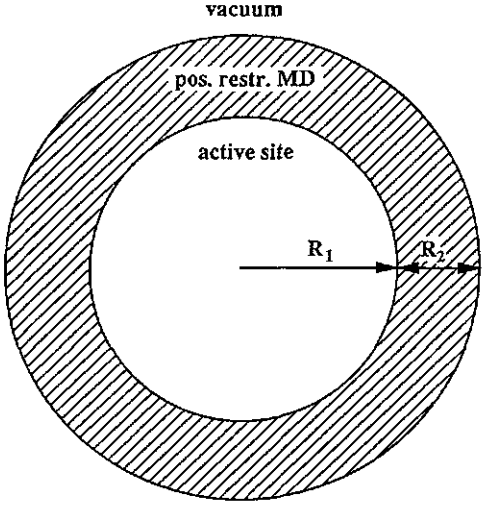

Figure 3. *Schematic drawing of spherical boundary conditions.* The region of interest (active site) is surrounded by a sphere (R_1+R_2) of solvent molecules. The atoms in the inner sphere (R_1) are allowed full motion, whereas the atoms in the surrounding shell (R_2) are position restrained in order to reduce the deforming influence of the nearby vacuum.

Prior to the MD simulation the potential energy of the molecular structure has to be minimized to eliminate local strains. The most widely used methods are the Steepest Descent and Conjugate Gradient energy minimizations. The former method is a simple first derivative method, which is very useful for small conformational shifts to reduce local unfavorable steric contacts. It performs well far from a minimum, but converges slowly near a minimum. The latter method searches along directions corresponding to the local quadratic approximation to the potential energy function, usually converging superlinearly. Since it does not require manipulation and storage of large matrices with dimensions equal to the number of degrees of freedom, it is most appropriate for large systems, like proteins.

After minimizing the energy the MD simulation can be started by randomly assigning atomic velocities (taken from a Maxwellian distribution) with total kinetic energy according to:

$$\sum_{i=1}^{N_{at}} \frac{1}{2} m_i \vec{v}_i^{\,2} = \frac{1}{2} N_{df} kT \qquad (7)$$

where m_i and $\vec{v}_i$ are the mass and velocity of atom i, respectively, and the summation extends over all atoms. k is the Boltzmann constant (k is $8.314*10^{-3}$ $kJ.mol^{-1}.K^{-1}$), T is the simulation temperature in Kelvin, and N_{df} is the number of degrees of freedom in the system denoted by:

$$N_{df} = 3\, N_{at} - N_c \qquad (8)$$

with N_{at} and N_c are the number of atoms in the simulated system and the number of constraints, respectively. The number of constraints comprise local constraints (e.g. bond lengths) as well as global constraints (due to removal of translational and/or rotational motion). Constant temperature of the simulated system is achieved by weakly coupling to an external bath of constant temperature, T_0 (Berendsen et al., 1984):

$$\left(\frac{dT(t)}{dt}\right) = \frac{1}{\tau_T} \{T_0 - T(t)\} \qquad (9)$$

where the adjustable relaxation time τ_T determines the thermal energy exchange between the system and the heat bath. A value of 0.1 ps was used in order to

obtain reliable dynamics as fluctuations of global properties are strongly influenced when smaller time constants are applied (Berendsen et al., 1984). Similarly, when periodic boundary conditions are used, coupling to a bath of constant reference pressure can be established.

In the MD simulation method a series of molecular configurations as a function of time (a trajectory) is generated by integration of Newton's equation of motion for all atoms in the molecular system:

$$\frac{\vec{F}_i(t)}{m_i} = \frac{d\vec{v}_i(t)}{dt} = \frac{d^2\vec{r}_i(t)}{dt^2} = \vec{a}_i(t) \tag{10}$$

where $\vec{r}_i$, $\vec{v}_i$, $\vec{a}_i$ and m_i are the coordinates, velocity, acceleration and atomic mass of atom i, respectively. The force $\vec{F}_i$ exerted on atom i is given by the negative gradient of the atomic interaction function V and depends on the coordinates of all N atoms in the system:

$$\vec{F}_i(t) = \frac{-\partial V[\vec{r}_1(t),\vec{r}_2(t),.....,\vec{r}_N(t)]}{\partial \vec{r}_i(t)} \tag{11}$$

Given the acceleration, approximate atomic velocities (see Eq. 10) can be computed after a small time step, Δt:

$$\vec{v}_i(t+\tfrac{1}{2}\Delta t) = \vec{v}_i(t-\tfrac{1}{2}\Delta t) + \frac{\vec{F}_i[\vec{r}_1(t),\vec{r}_2(t),.....\vec{r}_N(t)]}{m_i}.\Delta t \tag{12}$$

New coordinates are then given by:

$$\vec{r}_i(t+\Delta t) = \vec{r}_i(t) + \vec{v}_i(t+\tfrac{1}{2}\Delta t)\Delta t \tag{13}$$

Equations 12 and 13 form the so-called leap-frog scheme by which Eq. 10 can be integrated in small time steps. Smaller time steps enhance the quality of the approximation, on the other hand the time step should be taken large enough to simulate longer time spans. In practice values of 0.5 fs (when high-frequency bond vibration is allowed) to 2 fs are used (when constraining bond lengths to preset values).

The GROMOS force field used in our MD simulations consisted of bonded and non-bonded terms:

$$V(\vec{r}_1,\vec{r}_2,\ldots,\vec{r}_N) = \sum_{bonds} \tfrac{1}{2}K_b(b-b_0)^2 + \sum_{angles} \tfrac{1}{2}K_\theta(\theta-\theta_0)^2 +$$

$$\sum_{\substack{improper\\dihedrals}} \tfrac{1}{2}K_\zeta(\zeta-\zeta_0)^2 + \sum_{dihedrals} K_f(1+cos(n\phi-\delta)) +$$

$$\sum_{all\ pairs\ (i,j)} [\frac{C_{12}(i,j)}{r_{ij}^{12}} - \frac{C_6(i,j)}{r_{ij}^{6}} + \frac{q_i \cdot q_j}{4\pi\varepsilon_0\varepsilon_R r_{ij}}]. S(r_{ij}) \qquad (14)$$

The first term describes the bond-stretching interaction along covalent bond, b. It is a harmonic potential in which the minimum energy bond length, b_0, and the force constant, K_b, vary with the particular type of bond. The second term represents the bond-angle (θ) bending interaction in an analogous way. The third and fourth terms describe the dihedral angle interactions; the former term is the harmonic for the so-called improper dihedrals (torsion angles ζ that are not allowed to make transitions, e.g. dihedrals within aromatic rings or dihedrals to maintain chirality) and the latter term is for the proper dihedrals, described by a sinusoidal, which may make 360° turns. The last term is a summation over all pairs of non-bonded atoms i and j at distance r_{ij} and is controlled by a switching function, $S(r_{ij})$, which is added to these interactions in order to allow for a smooth behaviour of the interaction function when a cut-off radius is used. The summation models intramolecular interactions (between atoms that are 3 or more bonds apart) as well as all intermolecular interactions and is composed of repulsive (C_{12}) and attractive (C_6) van der Waals interactions and Coulomb interactions (between atoms with charges q_i and q_j), respectively. The repulsive and attractive van der Waals interactions are inversely proportional to the twelfth and sixth power of the distance r_{ij}, respectively (Lennard-Jones parametrization). In the GROMOS force field, the $C_{12}(i,j)$ and $C_6(i,j)$ of pairs of hydrogen bond donors and acceptors are chosen such that proper hydrogen bond geometry and energetics are obtained, given the charges q_i and ε_r=1. For two dissimilar atoms the $C_{12}(i,j)$ and $C_6(i,j)$ parameters are taken to be the geometrical mean of the parameters for the constituting atoms.

Coupling of fluorescence anisotropy experiments with MD simulations

One of the challenging applications of time-resolved fluorescence anisotropy measurements is to validate conclusions drawn from molecular dynamics simulations. Although relatively few picosecond-resolved anisotropy measurements with coupling to MD simulations have been reported thus far (Ichiye and Karplus, 1983; Henry and Hochstrasser, 1987; MacKerell et al., 1987, 1988; Chen et al., 1988; Axelsen et al., 1988, 1991; Axelsen and Prendergast, 1989), a consensus is growing that fluorescence anisotropy decay data can be valuable in corroborating MD simulations.

When the overall rotation is diffusional and isotropic the experimental anisotropy (Eq. 5) can be written as a simple correlation function (Tao, 1969; Kinosita et al., 1977; Zannoni, 1981):

$$r(t) = \frac{2}{5} <P_2[\hat{\mu}_a(0) \cdot \hat{\mu}_e(t)]> \cdot e^{-t/\phi_r} \tag{15}$$

where $P_2[...]$ is the second-order Legendre polynomial, $\hat{\mu}_a$ and $\hat{\mu}_e$ are the unit transition dipole vectors with components defined in a local coordinate system fixed in the molecule, the brackets (<...>) denote an ensemble average, and ϕ_r is the correlation time for the isotropic rotation of the molecule. When the MD calculations are performed in vacuo or with spherical boundary conditions, no rotation (and translation) of the whole molecule is present and Eq. 15 can be simplified:

$$r(t) \cong \frac{2}{5} <P_2[\hat{\mu}_a(0) \cdot \hat{\mu}_e(t)]> \tag{16}$$

Under these conditions the quantity $<P_2[\hat{\mu}_a(0) \cdot \hat{\mu}_e(t)]>$ is calculated directly, so that the internal motional contribution to the time dependence of $r(t)$ is obtained independent of the overall molecular motion. The ensemble average of the correlation function at time t_m is estimated from a time average over the simulation by:

$$<P_2[\hat{\mu}_a(0) \cdot \hat{\mu}_e(t_m)]> \cong \frac{1}{(N-m)} \sum_{n=1}^{N-m} P_2[\hat{\mu}_a(t_n) \cdot \hat{\mu}_e(t_m)] \tag{17}$$

where N is the number of datasets in the simulation, t_n is the time coordinate of the n^{th} dataset and t_m is the time interval to m dynamic time steps; the vectors $\hat{\mu}_a$ and $\hat{\mu}_e$ at times t_n and t_m, respectively, are calculated from the trajectory. When

cylindrical symmetry of the probe and azimuthal symmetry of its motion within the macromolecule is assumed (Lipari and Szabo, 1980; Brainard and Szabo, 1981; Ichiye and Karplus, 1983) the anisotropy given by Eq. 15 becomes:

$$r(t) = \frac{2}{5}\ e^{-t/\phi_r} \cdot P_2(cos\delta) \cdot \langle P_2[\hat{\mu}_a(0) \cdot \hat{\mu}_a(t)]\rangle \qquad (18)$$

where δ is the angle between absorption and emission transition dipole moments.

Outline of this thesis

The transfer of electrons involving proteins has been studied for many years. It is assumed that protein structure and dynamics play an important role in this process. The aim of this thesis is to examine the active site dynamics of flavodoxins in different oxidation states. This has been performed by means of time-resolved fluorescence methods and molecular dynamics simulations. The results described in this thesis can be used as a first step in elucidating the possible effect of protein dynamics on electron transfer.

In Chapter 2 the time-resolved flavin fluorescence and fluorescence anisotropy characteristics of four reduced flavodoxins are described: *Desulfovibrio gigas*, *Desulfovibrio vulgaris*, *Clostridium beijerinckii*, and *Megasphaera elsdenii* flavodoxin. The results obtained with two different methods for analyzing the time-resolved polarized fluorescence decays are compared. The results obtained for protein-bound reduced flavin are compared to reduced flavin in solution.

Chapter 3 deals with the conformational dynamics of oxidized *Clostridium beijerinckii* flavodoxin. As in Chapter 2 the protein-bound flavin characteristics are examined, but now the decays are also analyzed using associative modeling of fluorescence and fluorescence anisotropy decay parameters. The dissociation constant for the equilibrium between protein-bound and free flavin is determined.

Chapter 4 provides a detailed description of flavin and tryptophan motional behaviour as obtained with molecular dynamics simulations. Both oxidized and reduced flavodoxin were simulated in a solvent environment using spherical boundary conditions. Comparison of the two oxidation states shows the effect of the flavin oxidation state on the conformational dynamics of the active site.

Chapter 5 describes a time-resolved tryptophan fluorescence and fluorescence anisotropy study of two *Desulfovibrio* flavodoxins, one of which

has an unknown three-dimensional structure (*D. gigas* flavodoxin). The results are discussed in the light of energy transfer from the tryptophan residues to the protein-bound flavin. From the three-dimensional structure of *D. vulgaris* flavodoxin energy transfer rates can be calculated. By comparison of steady state and time-resolved fluorescence experiments the location of a tryptophan residue in the *D. gigas* flavodoxin is determined.

In Chapter 6 the time-resolved tryptophan fluorescence characteristics are reported for a number of apo- and holo-flavodoxins. The decays are analyzed using the maximum entropy method.

Finally, Chapter 7 contains a description of the time-resolved fluorescence and fluorescence anisotropy characteristics of a number of oxidized flavin derivatives in aqueous solution. The effect of methylation of the isoalloxazine ring on rotational behaviour is shown.

References

Alcala, J. R., Gratton, E. & Prendergast, F. G. (1987a) *Biophys. J. 51*, 597-604.

Alcala, J. R., Gratton, E. & Prendergast, F. G. (1987b) *Biophys. J. 51*, 925-936.

Ameloot, M., Boens, N., Andriessen, R., Vandenbergh, V. & Deschryver, F. C. (1991) *J. Phys. Chem. 95*, 2041-2047.

Åqvist, J., van Gunsteren, W. F., Leijonmarck, M. & Tapia, O. (1985) *J. Mol. Biol. 183*, 461-477.

Åqvist, J., Sandblom, P., Jones, T. A., Newcomer, M. E., van Gunsteren, W. F. & Tapia, O. (1986) *J. Mol. Biol. 192*, 593-604.

Axelsen, P. H., Haydock, C. & Prendergast, F. G. (1988) *Biophys. J. 54*, 249-258.

Axelsen, P. H. & Prendergast, F. G. (1989) *Biophys. J. 56*, 43-66.

Axelsen, P. H., Gratton, E. & Prendergast, F. G. (1991) *Biochemistry 30*, 1173-1179.

Bajzer, Z., Sharp, J. C., Sedarous, S. S. & Prendergast, F. G. (1990) *Eur. Biophys. J. 18*, 101-115.

Bastiaens, P. I. H., Mayhew, S. G., O'Nualláin, E. M., van Hoek, A. & Visser, A. J. W. G. (1991) *J. of Fluorescence 1*, 95-103.

Bastiaens, P. I. H., van Hoek, A., Benen, J. A. E., Brochon, J.-C. & Visser, A. J. W. G. (1992) *Biophys. J. 63*, 839-853.

Berendsen, H. J. C., Postma, J. P. M., van Gunsteren, W. F., DiNola, A. & Haak, J. R. (1984) *J. Chem. Phys. 81*, 3684-3690.

Berendsen, H. J. C. & van Gunsteren, W. F. (1983) in *The Physics of Superionic Conductors and Electrode Materials* (Perran, J. W., Ed,), pp. 221-226, NATO ASI Series B, Plenum, New York.

Brainard, J. R. & Szabo, A. (1981) *Biochemistry 20*, 4618-4628.

Brooks, B. R., Bruccoleri, R. E., Olafson, B. D., States, D. J., Swaminathan, S. & Karplus, M. (1983) *J. Comp. Chem. 4*, 187-217.

Burnett, R. M., Darling, G. D., Kendall, D. S., LeQuesne, M. E., Mayhew, S. G., Smith, W. W. & Ludwig, M. L. (1974) *J. Biol. Chem. 249*, 4383-4392.

Careri, G., Fasella, P. & Gratton, E. (1979) *Ann. Rev. Biophys. Bioeng. 8*, 69-97.

Chang, M. C., Courtney, S. H., Cross, A. J., Gulotty, R. J., Petrich, J. W. & Fleming, G. R. (1985) *Anal. Instrum. 14*, 433-464.

Chen, L. X.-Q., Engh, R. A. & Fleming, G. R. (1988) *J. Phys. Chem. 92*, 4811-4816.

Ehrenberg, M. & Rigler, R. (1972) *Chem. Phys. Lett. 14*, 539-544.

Fleming, G. R. (1986) *Ann. Rev. Phys. Chem. 37*, 81-104.

Fukuyama, K., Wakabayashi, S., Matsubaru, H. & Rogers, L. J. (1990) *J. Biol. Chem. 265*, 15804-15812.

Gurd, F. R. N. & Rothgeb, M. (1979) *Advances in Protein Chemistry 33*, 73-165.

Harvey, S. C. & Cheung, H. C. (1977) *Biochemistry 16*, 5181-5187.

Henry, E. R. & Hochstrasser, R. M. (1987) *Proc. Natl. Acad. Sci. USA 84*, 6142-6146.

Hermans, J., Berendsen, H. J. C., van Gunsteren, W. F. & Postma, J. P. M. (1984) *Biopolymers 23*, 1513-1518.

Huber, R. (1987) *Biochem. Soc. Trans. 15*, 1009-1020.

Ichiye, T. & Karplus, M. (1983) *Biochemistry 22*, 2884-2893.

IUPAC-IUB commission on biochemical nomenclature (1970) *J. Biol. Chem. 245*, 6489-6497.

Jablonski, A. (1960) *Bull. Acad. Pol. Sci., Ser. Sci. Math. Astron. Phys. 8*, 259-264.

James, D. R., DeMayo, P. & Ware, W. R. (1985) *Chem. Phys. Lett. 120*, 460-465.

Janssens, L. D., Boens, N., Ameloot, M. & Deschryver, F. C. (1990) *J. Phys. Chem. 94*, 3564-3576.

Kinoshita, K., Kawato, S. & Ikegami, A. (1977) *Biophys. J. 20*, 289-305.

Lakowicz, J. R. & Weber, G. (1973) *Biochemistry 12*, 4171-4179.

Levitt, M. (1980) in *Protein Folding* (Jaenicke, R., Ed.), Elsevier/North-Holland, Amsterdam, pp. 17-39.

Levy, R. M. (1985) in *Proceedings of the Workshop on Molecular Dynamics and Protein Structure* (Hermans, J., Ed.), pp. 62-64, Polycrystal Book Service, Western Springs, IL.

Lipari, G. & Szabo, A. (1980) *Biophys. J. 30*, 489-508.

Livesey, A. K. & Brochon, J. C. (1987) *Biophys. J. 52*, 693-706.

Ludescher, R. D., Peting, L., Hudson, S. & Hudson, B. (1987) *Biophys. Chem. 28*, 59-75.

Ludwig, M. L., Pattridge, K. A., Smith, W. W., Jensen, L. H. & Watenpaugh, K. D. (1982) in *Flavins and Flavoproteins*, (Massey, V. & Williams, C. H., Eds.), pp. 19-28, Elsevier/North-Holland, Amsterdam.

MacKerell, A. D., Rigler, R., Nilsson, L., Hahn, U. & Saenger, W. (1987) *Biophys. Chem. 26*, 247-261.

MacKerell, A. D., Nilsson, L., Rigler, R. & Saenger, W. (1988) *Biochemistry 27*, 4547-4556.

Mayhew, S. G. & Ludwig, M. L. (1975) in *The Enzymes* (Boyer, P. D., Ed.), pp. 57-118, Academic Press, New York.

Mayhew, S. & Tollin, G. (1992) in *Chemistry and Biochemistry of Flavoenzymes, vol. III* (Müller, F., Ed.), pp. 389-426, CRC Press, Boca Raton, FL.

McCammon, J. A., Gelin, B. R. & Karplus, M. (1977) *Nature (London) 267*, 585-590.

Mendelson, R. A., Morales, M. F. & Botts, J. (1973) *Biochemistry 12*, 2250-2255.

Northrup, S. H., Pear, M. R., McCammon, J. A. & Karplus, M. (1980) *Nature (London) 286*, 304-305.

Perrin, F. (1936) *J. Phys. Radium VII 1*, 1-11.

Perutz, M. F. & Mathews, F. S. (1966) *J. Mol. Biol. 21*, 199-202.

Perutz, M. F. (1970) *Nature 228*, 726-734.

Prendergast, F. G. (1991) *Current Opinions in Structural Biology 1*, 1054-1059.

Prendergast, F. G., Bajzer, Z., Axelsen, P. H. & Haydock, C. (1991) in *Proteins: Structure, Dynamics and Design* (Renugopalokrishnan, V., Carey, P. R., Smith, I. C. P., Huang, S. G. & Sorer, A. C., Eds.), pp. 208-219, Escom, Leiden.

Rigler, R. & Ehrenberg, M. (1973) *Quart. Rev. Biophys. 6*, 139-199.

Rigler, R. (1977) *Trends Biochem. Sci 2*, 252-254.

Ryckaert, J.-P., Ciccotti, G. & Berendsen, H. J. C. (1977) *J. Comput. Phys. 23*, 327-341.

Shank, C. V. (1988) in *Ultrashort Laser Pulses and Applications* (Kaiser, W., Ed.), pp. 5-34, Springer Verlag, Berlin.

Simondson, R. P. & Tollin, G. (1980) *Mol. Cell. Biochem. 33*, 13-24.
Smith, W. W., Burnett, R. M., Darling, G. D. & Ludwig, M. L. (1977) *J. Mol. Biol. 117*, 195-225.
Smith, W. W., Pattridge, K. A., Ludwig, M. L., Petsko, G. A., Tsernoglou, D., Tanaka, M. & Yasunobo, K. T. (1983) *J. Mol. Biol. 165*, 737-755.
Strickler, S. J. & Berg, R. A. (1962) *J. Chem. Phys. 37*, 814-822.
Szabo, A. (1984a) *Biophys. J. 45*, 327a-327a.
Szabo, A. (1984b) *J. Chem. Phys. 81*, 150-167.
Tao, T. (1969) *Biopolymers 8*, 609-632.
Tollin, G. & Edmondson, D. E. (1980) *Methods Enzymol. 69*, 392-406.
van Gunsteren, W. F. & Berendsen, H. J. C. (1977) *Mol. Phys. 34*, 1311-1327.
van Gunsteren, W. F. & Berendsen, H. J. C. (1987) *Groningen molecular simulation (GROMOS) library manual*, Biomos, Groningen.
van Gunsteren, W. F. & Mark, A. E. (1992) *Eur. J. Biochem. 204*, 947-961.
van Hoek, A., Vervoort, J. & Visser, A. J. W. G. (1983) *J. Biochem. Biophys. Methods 7*, 243-254.
van Hoek, A. & Visser, A. J. W. G. (1992) in *Time-resolved Laser Spectroscopy in Biochemistry, vol. 1640* (Lakowicz, J. R., Ed.), pp. 325-329, Proceedings of SPIE-The International Society for Optical Engineering, Bellingham, WA.
van Mierlo, C. P. M., van der Sanden, B. P. J., van Woensel, P., Müller, F. & Vervoort, J. (1990a) *Eur. J. Biochem. 194*, 199-216.
van Mierlo, C. P. M., Lijnzaad, Ph., Vervoort, J., Müller, F., Berendsen, H. J. C. & de Vlieg, J. (1990b) *Eur. J. Biochem. 194*, 185-188.
Vos, K., van Hoek, A. & Visser, A. J. W. G. (1987) *Eur. J. Biochem. 165*, 55-63.
Wagner, G. (1983) *Quart. Rev. Biophys. 16*, 1-57.
Wagner, G. & Wüthrich, K. (1986) *Methods Enzymol. 131*, 307-326.
Watenpaugh, K. D., Sieker, L. C. & Jensen, L. H. (1973) *Proc. Nat. Acad. Sci. 70*, 3857-3860.
Watt, W., Tulinsky, A., Swenson, R. P. & Watenpaugh, K. D. (1991) *J. Mol. Biol. 218*, 195-208.
Weiner, P. & Kollman, P. A. (1981) *J. Comp. Chem. 2*, 287-303.
Williams, R. J. P. (1977) *Angew. Chem. 89*, 805-816.
Wüthrich, K. (1986) *NMR of Proteins and Nucleic Acids*, Wiley, New York.
Yoch, D. C. & Valentine, R. C. (1972) *Ann. Rev. Microbiol. 26*, 139-162.
Zannoni, C. (1981) *Mol. Phys. 42*, 1303-1320.

Chapter 2

Flavin dynamics in reduced flavodoxins: a time-resolved polarized fluorescence study

Rik Leenders, Martin Kooijman, Arie van Hoek, Cees Veeger, and Antonie J. W. G. Visser

published in: *European Journal of Biochemistry 211* (1993) 37-45

Abstract

The time-resolved fluorescence and fluorescence anisotropy characteristics of reduced flavin mononucleotide in solution as well as bound in flavodoxins isolated from the bacteria *Desulfovibrio gigas, Desulfovibrio vulgaris, Clostridium beijerinckii* and *Megasphaera elsdenii* have been examined. All fluorescence and fluorescence anisotropy decays were analyzed by two different methods: (a) least-squares fitting with a sum of exponentials and (b) the maximum entropy method to yield distributed lifetimes and correlation times. The results of both approaches are in excellent agreement. The fluorescence decay of the free as well as protein-bound reduced flavin chromophore is made up of three components. The shortest component proves to be relatively sensitive to the environment and can therefore be used as a diagnostic tool to probe the microenvironment of the reduced isoalloxazine ring system. The other two longer fluorescence lifetime components are insensitive to the chromophore environment and seem therefore related to intrinsic, photophysical properties of the reduced chromophore. Fluorescence anisotropy decays show that the flavin mononucleotide in all four reduced flavodoxins is immobilized within the protein matrix, as indicated by the recovery of a single rotational correlation time, reflecting the rotation of the whole protein. No indications are found that rapid structural fluctuations occur in reduced flavodoxins, and the mechanism of electron transfer from flavodoxin to other redox proteins seems to involve immobilized reduced flavin.

Introduction

Flavodoxins are small (14-25 kDa) electron-transfering proteins which can be isolated from some algae and several anaerobic and aerobic bacteria grown under iron-deficient conditions (Knight and Hardy, 1966; Mayhew, 1971), although some bacteria also produce flavodoxin under iron-containing conditions (Benemann et al., 1969; Vetter and Knappe, 1971; Hatchikian et al., 1972; van Lin and Bothe, 1972; Irie et al., 1973). Up to now, no flavodoxins have been found in higher animals or plants.

Flavodoxins promote electron transfer between two redox proteins as part of photosynthetic, nitrogen- or sulfate-reducing or hydrogen-evolving systems (for a review see: Mayhew and Ludwig, 1975). Based on biochemical and

spectroscopic differences, flavodoxins can be divided into two groups: the *rubrum*-type and *pasteurianum*-type of flavodoxins (D'Anna and Tollin, 1972).

Flavodoxins contain one non-covalently bound flavin mononucleotide (FMN) which can exist in three different oxidation states, i.e. oxidized, one-electron reduced (semiquinone), and two-electron-reduced (hydroquinone). Under physiological conditions flavodoxins shuttle between the semiquinone and hydroquinone states and are thus one-electron transferring proteins.

Chemical composition and amino acid sequence are known for quite a number of flavodoxins, while for a few flavodoxins in the oxidized state three-dimensional structures have been elucidated (Watenpaugh et al., 1973; Burnett et al., 1974; Smith et al., 1983; van Mierlo et al., 1990a). Furthermore, the structures of semiquinone and reduced *Clostridium beijerinckii* flavodoxin (Smith et al., 1977; Ludwig et al., 1982), semiquinone and reduced *Desulfovibrio vulgaris* flavodoxin (Watt et al., 1991) and reduced *Megasphaera elsdenii* flavodoxin (van Mierlo et al., 1990b) have been published. The overall structures of these flavodoxins in their different oxidation states are highly similar, except for some variations in protein conformation and amino acid composition around the flavin chromophore. It has been shown that in reduced *Cl. beijerinckii* flavodoxin the protein backbone of residue Gly57 is rotated towards the flavin facilitating hydrogen bonding between the apoprotein and the flavin molecule (Ludwig et al., 1982). Recently, Watt et al. (1991) demonstrated a similar conformational change for reduced *D. vulgaris* flavodoxin. Nuclear magnetic resonance studies of *D. vulgaris* flavodoxin have revealed a hydrogen bond between the flavin atom N(1) and residue Asp95 in all three oxidation states (Vervoort et al., 1986), implying that atom N(1) remains unprotonated upon reduction. These studies confirmed a similar finding in the three different oxidation states of *Cl. beijerinckii* flavodoxin (Ludwig et al., 1982).

Comparison of the structures of oxidized *D. vulgaris* and *Cl. beijerinckii* flavodoxin (Mayhew and Ludwig, 1975) shows a high degree of similarity between the folding of the polypeptide chains, but differences in the flavin binding sites exist. Firstly, the orientation of the isoalloxazine rings with respect to the otherwise aligned crystallographic protein structures are at 24° to each other. Secondly, the distance between the flavin N(5) and the carbonyl oxygen of the rotated glycine residue is somewhat shorter in *Cl. beijerinckii* flavodoxin (0.28 nm) as compared to *D. vulgaris* flavodoxin (0.30 nm). Furthermore, the tryptophan residue which is located near the active site in *D. vulgaris* flavodoxin is not stacked with the isoalloxazine of the flavin (the tryptophan-flavin center-to-center distance is 0.55 nm), whereas in *Cl. beijerinckii* flavodoxin residue

Trp90 seems to be stacked with the flavin chromophore (center-to-center distance is 0.31 nm). Based on nearly identical tryptophan fluorescence results it was noted that *Desulfovibrio gigas* and *D. vulgaris* flavodoxins have a very similar tryptophan residue in common (Leenders et al., 1990). Although only limited information about proton-proton distances between the flavin molecule and the *M. elsdenii* apoflavodoxin is available from 2-dimensional ^{1}H-NMR studies (van Mierlo et al., 1990a, b), it seems that in this flavodoxin the flavin is stacked with a tryptophan residue (Trp91).

The differences in flavin environment are reflected in the spectroscopic properties of the flavodoxins. Shifted absorption maxima and different ellipticity cross-over points in visible circular dichroism spectra between both classes of flavodoxins result in two clearly distinguishable flavodoxin-types (D'Anna and Tollin, 1972). Redox properties (Mayhew and Ludwig, 1975) and Raman spectroscopy also revealed significant differences in flavin vibrational frequencies in bacterial flavodoxins belonging to the two classes (Visser et al., 1983).

There is cumulating evidence for the existence of rapid structural fluctuations in proteins and attention is being focussed to relate these fluctuations with biochemical reactions (Karplus and McCammon, 1983; Kraut, 1988; Farnum et al., 1991). Such fluctuations may play an important role in the mechanism of electron transfer of flavodoxins.

Since crystallographically obtained structures contain only limited information about internal dynamics, other spectroscopic techniques have to be applied to obtain more detailed information. Time-resolved protein fluorescence is widely used to investigate structure and dynamics (for general references see Rigler and Ehrenberg, 1973, 1976; Cundall and Dale, 1983; Lakowicz, 1983; Beechem and Brand, 1985). Both segmental motion of a chromophore and isotropic rotation of a whole protein can be observed using high-resolution fluorescence techniques. The most intensively studied probe is tryptophan but also other intrinsic probes, like tyrosine and flavin, and extrinsic probes can be used to study protein dynamics. We have employed sensitive time-resolved fluorescence and fluorescence anisotropy techniques to obtain information on the dynamic characteristics of reduced flavin in flavodoxins. Reduced flavins are intrinsically fluorescent and their fluorescence properties have been globally investigated for several reduced model compounds and flavoproteins (Ghisla et al., 1974; Visser et al., 1979; Visser et al., 1991). The fluorescence of reduced (1,5-dihydro) flavins, free or bound in flavodoxin as dealt with in this article, have in general a rather low quantum yield, which is in contrast to the

fluorescence quantum yield of 4a,5-dihydroflavins (Lee et al., 1991). Four reduced flavodoxins were investigated: *D. gigas* and *D. vulgaris* flavodoxin as members of the *rubrum* class of flavodoxins and *Cl. beijerinckii* and *M. elsdenii* flavodoxin as members of the *pastaurianum* class of flavodoxins. The results are compared with the dynamic fluorescence properties of free reduced flavin mononucleotide.

Materials and Methods

Preparation of the flavodoxins

The preparation of flavodoxins from *D. gigas, D. vulgaris, Cl. beijerinckii,* and *M. elsdenii* was as described previously (Mayhew, 1971; Irie et al., 1973; LeGall and Hatchikian, 1967; Mayhew and Massey, 1969). Fluorescent grade flavin mononucleotide (FMN) was obtained from Merck. FMN and the flavodoxins were dissolved in 70 mM pyrophosphate buffer pH 8.3 at concentrations which varied from 50 to 150 μM. These, for optical spectroscopy, rather high concentrations were necessary because of the low absorbance of the reduced chromophore at the excitation wavelength. The anaerobic solutions were reduced by the addition of equimolar amounts of sodium dithionite as described by Ghisla et al. (1974). Substoichiometric amounts of dithionite would result in incomplete reduction and remaining small traces of oxidized flavodoxin would cause a disturbing signal because of its significantly higher quantum yield of fluorescence. All chemicals used were of the highest purity available and only Millipore-filtered water was used. All experiments were conducted between 4 °C and 37 °C.

Time-resolved fluorescence and fluorescence anisotropy measurements

Fluorescence and fluorescence anisotropy decays were measured using the time-correlated single photon counting technique (van Hoek et al., 1983, 1987; van Hoek and Visser, 1985, 1992; Visser et al., 1985; Vos et al., 1987). Reduced free and protein-bound flavin was excited at 444.0 nm with vertically polarized light. Erythrosin-B served as a reference compound to yield the instrumental response function (Erythrosin-B shows a single exponential fluorescence decay with a slightly temperature-dependent lifetime, which amounts to 80 ps at 20 °C).

After excitation the parallel and perpendicular polarized fluorescence intensities were monitored using a 557.9 nm line filter (Schott with half band width of 13.0 nm) in combination with a cut-off filter (Schott OG530). In this way the disturbing Raman scattering signal of water is not detected and only fluorescence photons are detected and accumulated in discrete channels of the multichannel analyzer. Due to the relatively low fluorescence quantum yields of the reduced flavodoxins, the background fluorescence arising from the buffer had to be subtracted, since it amounted to a few percent of the protein fluorescence. The fluorescence and fluorescence anisotropy decays were analyzed by two different methods. The total fluorescence decays were analyzed by nonlinear least-squares fitting of the experimental data with a sum of exponentials (Vos et al., 1987):

$$f(t) = i_{\parallel}(t) + 2g i_{\perp}(t) = \sum_{i=1}^{n} \alpha_i \, e^{-t/\tau_i} \qquad \text{with } i=1,2,.....n \qquad (1)$$

where $f(t)$ is the deconvoluted time-dependent fluorescence, $i_{\parallel}(t)$ and $i_{\perp}(t)$ are the parallel and perpendicular polarized fluorescence components, and g is the correction factor for the different responses of the instrumentation to parallel and perpendicular polarized light. Polarizers were aligned carefully, and when measuring reference samples of known anisotropy, it was found that no correction was needed (g-factor is 1). α_i and τ_i are the relative contribution and fluorescence lifetime of component i, respectively. The fluorescence anisotropy decays, $r(t)$, were globally analyzed in an analogous manner:

$$r(t) = \sum_{j=1}^{m} \beta_j \, e^{-t/\phi_j} \qquad \text{with } j=1,2,.....m \qquad (2)$$

where m is the number of rotational correlation time components, β_j and ϕ_j are the amplitude and rotational correlation time of component j, respectively. The sum of β_j corresponds to the initial anisotropy, $r(0)$. The parallel and perpendicular fluorescence decays were globally analyzed by minimizing the reduced χ^2 statistics:

$$\chi^2 = \frac{1}{N} \sum_{k=1}^{N} \frac{\{I_c(k) - I_o(k)\}^2}{\sigma_k^2} \qquad (3)$$

where N is the number of degrees of freedom, $I_c(k)$ and $I_o(k)$ are the calculated and observed number of photons in channel k, respectively. Furthermore, σ_k^2 is the variance in channel k.

The fluorescence decay as well as the fluorescence anisotropy decay were also analyzed in terms of a continuous distribution of decay times by means of the maximum entropy method (MEM, developed and distributed by Maximum Entropy Data Consultancy Ltd., Cambridge, U.K.). In this method Livesey et al., 1986; Livesey and Brochon, 1987), a spectrum of decay times, $\alpha(\tau)$, can be recovered by considering the total fluorescence, $I(t)$:

$$I(t) = I_{\parallel}(t) + 2gI_{\perp}(t) = E(t) * \int_0^{\infty} \alpha(\tau)\, e^{-t/\tau}\, d\tau \qquad (4)$$

where $I(t)$ is the sum of the polarized fluorescence intensities ($I_{\parallel}(t)$ and $I_{\perp}(t)$) which are convolved (represented by the symbol $*$) with the shape of the excitation pulse, $E(t)$. $\alpha(\tau)$ represents the number of fluorophores that decay with time constant τ. The image $\alpha(\tau)$, which is formally the inverse Laplace transform of the measured intensities deconvoluted from the excitation pulse $E(t)$, is calculated in such a way that it results in a maximum value of the Skilling-Jaynes entropy, S (Jaynes, 1983):

$$S = \int_0^{\infty} \alpha(\tau) - m(\tau) - \alpha(\tau)\, log\, \frac{\alpha(\tau)}{m(\tau)} d\tau \qquad (5)$$

where $m(\tau)$ is the starting model for the distribution of fluorescence lifetimes. The entropy is maximized under the condition that the reduced χ^2 (Eq. 3) is minimized (Jaynes, 1983). When no *a priori* knowledge about the shape of the distribution was available, $m(\tau)$ was set to a flat distribution in $\log(\tau)$ space as this introduces the least correlations between the $\alpha(\tau)$ parameters (Livesey and Brochon, 1987; Mérola et al., 1989).

From fluorescence anisotropy experiments one can recover the complete 3-dimensional image $\gamma(\tau,\phi,r_0)$, representing the number of fluorophores with lifetime τ, rotational correlation time ϕ, and initial anisotropy r_0 (Livesey and Brochon, 1987). If one assumes that τ and ϕ are uncorrelated (non-associative model) the images $\alpha(\tau)$ and $\beta(\phi)$ are independent as expressed by the deconvoluted polarized fluorescence intensity components:

$$i_{\parallel}(t) = \frac{1}{3} \int_0^{\infty} \alpha(\tau)\, e^{-t/\tau}\, d\tau \int_0^{\infty} \{1 + 2\beta(\phi)\}\, e^{-t/\phi}\, d\phi \qquad (6)$$

and

$$i_{\perp}(t) = \frac{1}{3} \int_0^{\infty} \alpha(\tau)\, e^{-t/\tau}\, d\tau \int_0^{\infty} \{1 - \beta(\phi)\}\, e^{-t/\phi}\, d\phi \qquad (7)$$

where the integrated amplitude $\beta(\phi)$ corresponds to the initial anisotropy r_0, which is dependent on the degree of non-coincidence of absorption and emission transition moments, and r_0 may be defined by an (average) angle δ between them:

$$r_0 = \frac{1}{5}(3cos^2\,\delta - 1) \qquad (8)$$

A spectrum of rotational correlation times ϕ, $\beta(\phi)$, is obtained for which it also applies that, if no *a priori* knowledge of the distribution is known, the initial spectrum should be taken flat in $\log(\phi)$ space.

In the analysis of the fluorescence decay an $\alpha(\tau)$ image consisting of 150 decay times equally spaced in $\log(\tau)$ space (ranging from 0.01 ns to 15 ns) was recovered. This image was then fixed in the anisotropy decay analysis where an image $\beta(\phi)$ consisting of 150 rotational correlation times equally spaced in $\log(\phi)$ space (from 0.05 ns to 30 ns) was recovered.

Results and Discussion

Time-resolved fluorescence

As an example the time-resolved fluorescence intensity of reduced *D. vulgaris* flavodoxin at 4 °C is presented in Figure 1. The fluorescence intensity of reduced free FMN, which is also given for comparison, initially decays much faster than the fluorescence intensity of the reduced protein. It is obvious from the semilogarithmic display in Figure 1 that the time-dependent fluorescence intensities exhibit a heterogeneous pattern. When the fluorescence decays of reduced free FMN and the reduced flavodoxins were analyzed by non-linear least-squares fitting procedures using a sum of exponentials (Eq. 1), at least three exponentials were needed to describe the experimental decay adequately. The fitting parameters obtained are listed in Table 1. It is to be noted that the relative contributions of the different fluorescence lifetime components are more or less independent of the flavodoxin species. In general, 80% of the total fluorescence decay is that of the shortest fluorescence lifetime component, τ_1, and lifetime components τ_2 and τ_3 are present with relative contributions of 19% and 1%, respectively. The shortest fluorescence lifetime in free reduced FMN is shorter than in reduced flavodoxins, where it seems to be class-dependent. Flavodoxins from the *rubrum* class (the two *Desulfovibrio* flavodoxins) have a significantly shorter τ_1 (about 400 ps) than flavodoxins from the *pasteurianum* class (τ_1 of about 750 ps). The values of τ_2 and τ_3 seem to be independent of the kind of flavodoxin and, hence, of the environment of the reduced flavin chromophore.

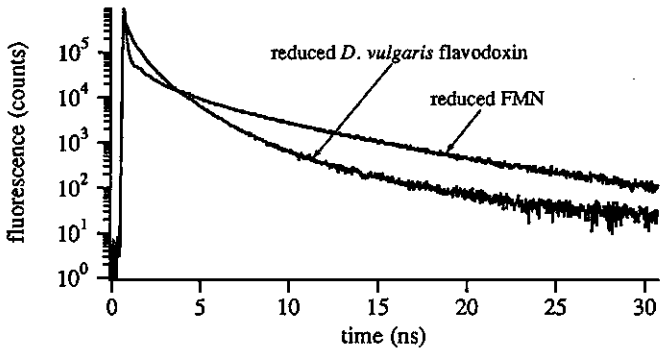

Figure 1. *Fluorescence decay curves of reduced D. vulgaris flavodoxin and reduced free FMN.* Both fluorescence decays were measured at 4 °C. Excitation and emission wavelengths were 444.0 nm and 557.9 nm, respectively (see text for details).

Table 1. *Fluorescence decay characteristics of reduced FMN and reduced flavodoxins (at 4 °C)* [a].

sample	α_1 [b]	τ_1 [b]	α_2	τ_2	α_3	τ_3	$\langle\tau\rangle$ [c]	χ^2 [d]	Q [e]
	(±0.02)	(±0.02) (ns)	(±0.02)	(±0.15) (ns)	(±0.02)	(±0.25) (ns)	(ns)		
FMN	0.80	0.12	0.19	1.41	0.01	5.27	0.30	1.02	0.005
D. gigas	0.80	0.44	0.19	1.71	0.01	4.40	0.72	1.16	0.013
D. vulgaris	0.79	0.39	0.19	1.41	0.02	4.11	0.66	1.13	0.012
Cl. beijerinckii	0.75	0.88	0.23	1.30	0.02	4.53	1.05	1.09	0.019
M. elsdenii	0.82	0.72	0.15	1.47	0.03	5.26	0.97	1.02	0.017

a) Parameters were obtained by least-squares fitting of the time-resolved fluorescence (Eq. 1). Excitation and emission wavelengths were 444.0 nm and 557.9 nm, respectively
b) the order of magnitude of the errors (given in parenthesis) is deduced from the results of multiple experiments
c) the average fluorescence lifetime is defined as: $\langle\tau\rangle = \Sigma \alpha_i \tau_i$ (Eq. 12)
d) see Eq. 3
e) calculated according to Eq. 9 using τ_0 is 56 ns (see text)

The fluorescence decay curves of all four reduced flavodoxins as well as free reduced flavin were analyzed using the maximum entropy method, in order to obtain information about the distribution of lifetimes in the decays. The results of these analyses are shown in Figure 2. From inspection of Figure 2 it is clear that indeed more than one component is present in the decays. A common feature in the distributions of reduced free and protein-bound flavin is the presence of three lifetime distributions in accordance with the results obtained with the least-squares fitting. The fluorescence decay of free reduced flavin is composed of a most intense distribution peaked at about 115 ps, and two other distributions with barycenters at about 1.3 ns and 4.5 ns (see Table 1). The relative contributions of these components are 82%, 17% and 1%, respectively. In the *Desulfovibrio* flavodoxins an intense distribution (about 77 % of the total fluorescence) of a shorter lifetime component is found at about 350 ps, and two other less intense distributions at about 1.3 ns and 3-4 ns (about 20 % and 3 % of the total fluorescence, respectively). In *Cl. beijerinckii* and *M. elsdenii* flavodoxin an intense lifetime distribution is found at about 800 ps, i.e. considerably longer than the corresponding short lifetimes in *Desulfovibrio* flavodoxins. The asymmetric form of this distribution (see Figure 2C) indicates an underlying

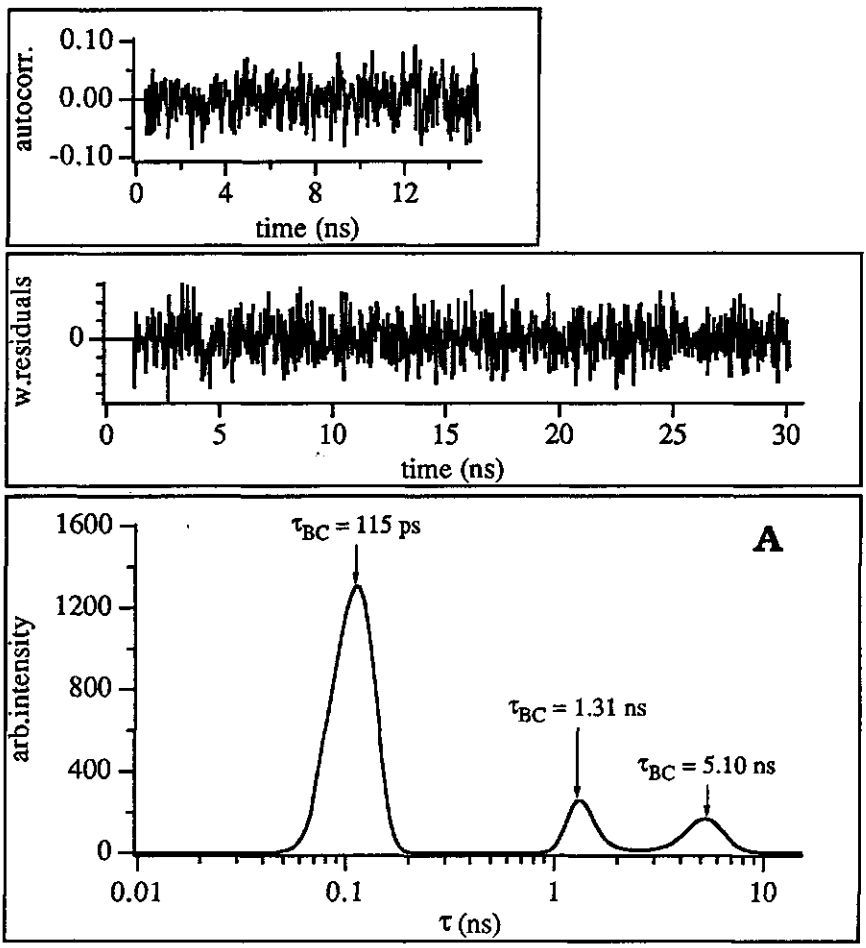

Figure 2. *Maximum entropy analyses of the time-resolved fluorescence intensities (at 4 °C)* . A: Free reduced FMN, B: reduced *D. vulgaris* flavodoxin, C: reduced *Cl. beijerinckii* flavodoxin. The positions of the barycenters, calculated according to $\tau_{BC} = \Sigma \alpha_i \tau_i / \Sigma \tau_i$, are indicated. In the top panels the weighted residuals and autocorrelations are given. The fit-quality is excellent: χ^2 is 1.02, 1.02, and 1.08 for A , B, and C, respectively.

lifetime component at about 1.5 ns. A third lifetime distribution is present which could not be very well resolved.

Fluorescence techniques with high time-resolution show that the fluorescence decays of reduced flavodoxins are not mono-exponential, in contrast to earlier findings in which the decay of reduced *M. elsdenii* flavodoxin appeared to be

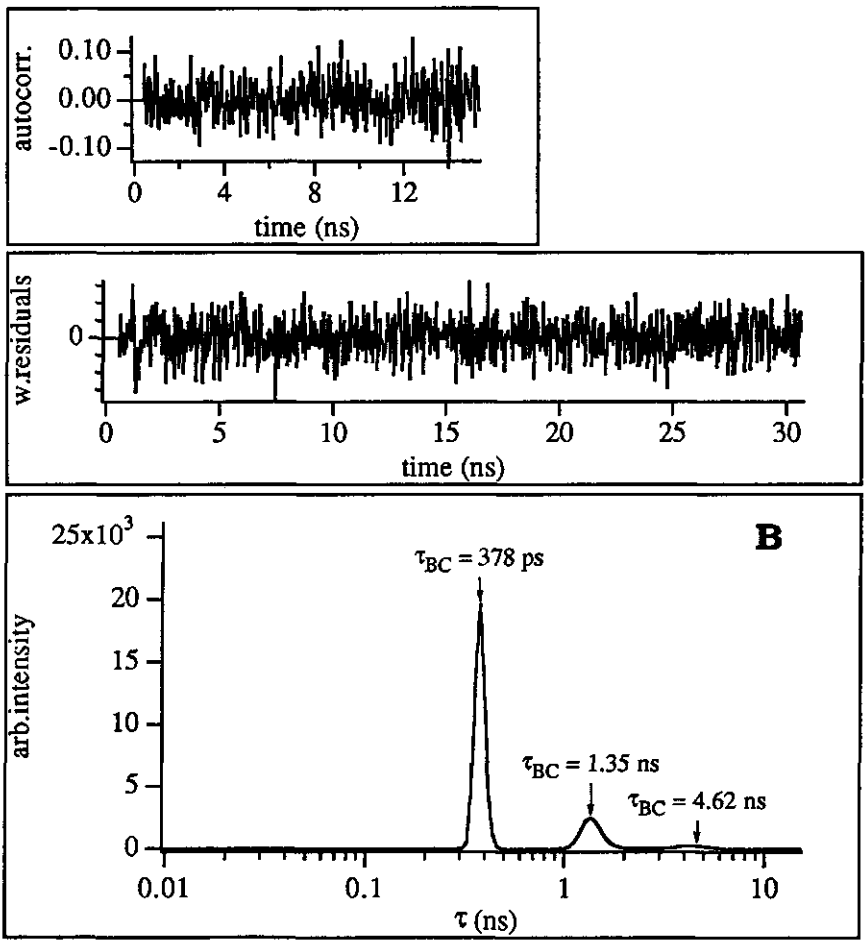

Figure 2B.

consistent with a single fluorescence lifetime of 2.1 ns (Visser et al., 1979). The existence of three fluorescence lifetime components is now demonstrated. It is difficult to explain the exact origin of this fluorescence lifetime heterogeneity, but the observation that the fluorescence is enhanced in more rigid structures (Visser et al., 1979) indicates that the shortest fluorescence lifetime (τ_1) is influenced by the environment of the flavin. It is noted that, because of the smaller distance between the flavin and the rotated glycine carbonyl oxygen, the reduced flavin in *Cl. beijerinckii* flavodoxin is probably bound more firmly than

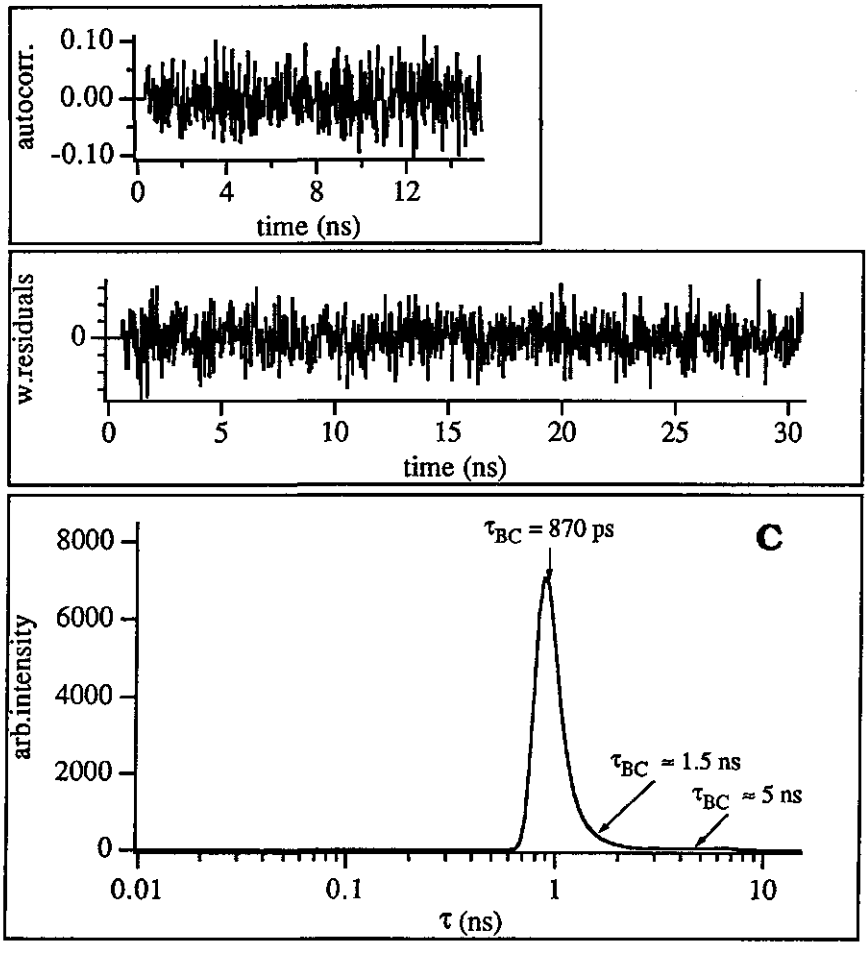

Figure 2C.

in *D. vulgaris* flavodoxin. The longer lifetimes (τ_2 and τ_3) possibly originate from flavin configurations which are almost or completely planar (*vide infra*). Comparison of the fluorescence decays of free and protein-bound reduced FMN indicates that no additional exponential components are introduced as a result of changes in micro-environment of the isoalloxazine ring system.

The results show that the position of the shortest lifetime distribution is influenced by the environment of the flavin chromophore. In free reduced FMN τ_1 is about 115 ps and in reduced flavodoxins τ_1 is significantly longer (about 400 ps in *rubrum* flavodoxins and about 800 ps in *pasteurianum* flavodoxins). Two

possible mechanisms both explaining this behaviour can be proposed. The reduced chromophore in solution is completely surrounded by water molecules. The excited state will therefore be immediately stabilized to a solvent-relaxed state which might be deactivated more efficiently by radiationless transition to the ground state (internal conversion) than is the unrelaxed excited state. This would mainly be reflected by a considerable shortening of the average lifetime of the excited state. An alternative and/or additional mechanism has been proposed which may also account for the multiplicity of decay times observed (Visser et al., 1991). Ultrafast (subpicosecond) collective vibrations are responsible for the fact that reduced flavin possesses multiple conformations of different planarity. Upon excitation most nonplanar states will return to the ground state via radiationless pathways which explains the picosecond lifetimes observed in most reduced flavin compounds in fluid solutions. In reduced flavodoxins the isoalloxazine ring system is (partially) surrounded by a more rigid protein environment resulting in a decreased rate of internal conversion and an increased τ_1. The so-called butterfly motion, i.e. inversion of the central ring as detected in reduced flavins in solution (Tauscher et al., 1973), will be hindered by the protein environment and may be expected to reduce the rate of radiationless transitions to the ground state (the energy dissipates better in more dynamic systems). As a result of the partial accessibility of the reduced protein-bound flavin, solvent relaxation will play a less important role as compared to reduced flavins in solution leading to longer lifetimes.

The value of τ_1 can be used as a diagnostic tool for probing the environment of reduced flavin chromophores. This influence is smaller in the *rubrum* class than in the *pasteurianum* class of flavodoxins: the flavin in the former proteins has dynamic properties which are more similar to reduced flavin in solution. The flavin in the latter class of flavodoxins is more restricted by the protein environment, probably as a result of a more intense hydrogen bonding between the flavin N(5) and H(5) atoms and the rotated glycine carbonyl oxygen.

An interesting feature is detected at increased temperatures and occurs in all four reduced flavodoxins, as well as in reduced FMN in solution. All fluorescence lifetimes shorten at higher temperature, but they do not converge, whereas their relative contributions (α_i) are clearly independent of temperature. This is illustrated in Figure 3 for reduced *D. gigas* flavodoxin. This appears to rule out excited-state processes such as exciplex formation or solvent relaxation on the time-scale of the emission itself, because the resultant lifetime changes would also affect the α terms. The fact that the α values do not vary with

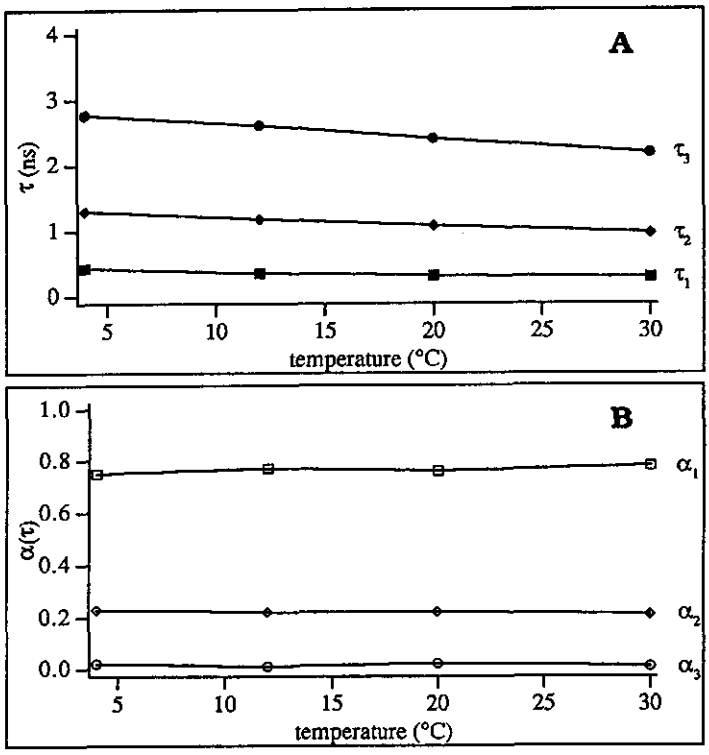

Figure 3. *Position of the barycenters, τ_i, and integrated amplitudes, α_i, of the separate fluorescence lifetimes in reduced D. vulgaris flavodoxin as a function of temperature.* **A**: position of the barycenters, **B**: integrated relative amplitudes.

temperature favours the excited-state kinetics in which there are three independently emitting species. These emitting conformers either result from three different ground states or are formed in parallel very rapidly (non-exchangeable) in the excited state by a temperature-independent mechanism both in free solution and when bound in flavodoxin. The lack of interconversion between the separate emitting forms indicates that the energy barrier between configurations is too high and therefore no major conformational changes occur (Bastiaens et al., 1992). Reduced flavodoxins were measured up to 37 °C and showed no sign of degradation, whereas fluorescence of reduced FMN in solution (above 20 °C) decreased to a non-detectable level.

The fluorescence quantum yield, Q, of an aromatic molecule exhibiting a monoexponential excited-state decay is related to its measured lifetime τ by:

$$Q = \frac{\tau}{\tau_0} \tag{9}$$

where τ_0 is the 'natural' fluorescence lifetime, i.e. that which would be observed in the absence of radiationless deactivation of the excited singlet state. This latter lifetime, also called the radiative lifetime, can be estimated from the first absorption and emission bands according to (Strickler and Berg, 1962):

$$\frac{1}{\tau_0} = 2.88 \,.\, 10^{-9}\, n^2 <\tilde{\nu}_F^{-3}>^{-1} \int_0^{\infty} \frac{\varepsilon(\tilde{\nu})}{\tilde{\nu}}\, d\tilde{\nu} \tag{10}$$

where n is the refractive index of the medium, ε is the extinction coefficient (given in $M^{-1}.cm^{-1}$) and $\tilde{\nu}$ is the wavenumber (cm^{-1}). $<\tilde{\nu}_F^{-3}>$ is the third moment of the fluorescence spectrum defined as:

$$<\tilde{\nu}_F^{-3}> = \frac{\int_0^{\infty} \tilde{\nu}^{-3} F(\tilde{\nu})\, d\tilde{\nu}}{\int_0^{\infty} F(\tilde{\nu})\, d\tilde{\nu}} \tag{11}$$

Using Eqs. 10 and 11 it was calculated for reduced *Cl. beijerinckii* flavodoxin that τ_0 is 56 ns. Assuming that τ_0 is invariant to the environment of the chromophore, any variation in quantum yield can be attributed to differing magnitudes of the rate constants for radiationless deactivation. For multi-exponential fluorescence decay the value for τ can be taken as the average fluorescence lifetime, $<\tau>$ (according to: Kulinski et al., 1987):

$$<\tau> = \sum_{i=1}^{n} \alpha_i\, \tau_i \qquad \text{(with } \sum_{i=1}^{n} \alpha_i = 1\text{)} \tag{12}$$

provided that each component arises from an independent monoexponentially decaying excited-state species with identical radiative lifetime and spectral distribution for each of the individual forms. The average excited-state lifetime of reduced FMN in solution ($<\tau>$ is 0.30 ns) is significantly smaller than for protein-bound reduced FMN ($<\tau>$ varies between 0.66 and 1.05 ns for the

different flavodoxins). This means that the quantum yield, calculated by substitution of $<\tau>$ and τ_0 in Eq. 9, increases upon binding of the reduced chromophore (Table 1), which is in agreement with steady-state fluorescence intensity measurements (data not shown). Therefore, for reduced flavodoxins the rate of radiationless deactivation of the excited state is smaller than for free reduced FMN.

Time-resolved fluorescence depolarization

We also performed time-resolved fluorescence depolarization experiments on members of the two classes of flavodoxins to investigate whether differences in flavin microenvironments are related to an altered motional behaviour. In Figure 4 it is demonstrated that the fluorescence anisotropy decay of free

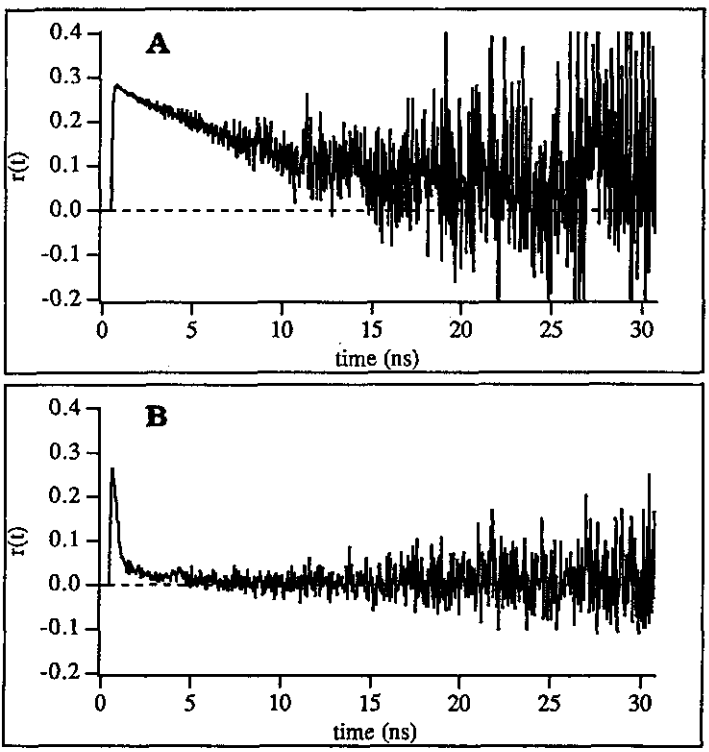

Figure 4. *Fluorescence anisotropy decays of reduced flavodoxin and reduced flavin in solution (at 4 °C).* **A**: reduced *D. vulgaris* flavodoxin, **B**: reduced FMN. The anisotropy of free reduced flavin decays much faster than that of reduced flavodoxin (see also Table 2).

Table 2. *Fluorescence anisotropy decay characteristics of reduced free FMN and reduced flavodoxins (at 4 °C)* [a].

sample	β[b]	ϕ[b]	χ^2
	(±0.01)	(±0.14) (ns)	
FMN	0.30[c]	0.22	1.14
D. gigas	0.29	11.96	1.01
D. vulgaris	0.28	11.18	1.16
Cl. beijerinckii	0.25	9.73	1.08
M. elsdenii	0.25	9.13	1.13

a) The parameters were obtained by least-squares fitting of the time-resolved fluorescence anisotropy (Eq. 2, j=1)
b) the order of magnitude of the errors (in parenthesis) is based on results obtained from multiple experiments
c) this value was fixed

reduced FMN (at 4 °C) is significantly faster than that of reduced *Cl. beijerinckii* flavodoxin. When the fluorescence anisotropy decay is analyzed using a sum of exponentials it is found that a single exponential is sufficient, yielding a 220 ps rotational correlation time for free reduced flavin at 4 °C (Table 2). This value is somewhat smaller than the rotational correlation time found for oxidized flavin mononucleotide at the same temperature (Chapter 3; Leenders et al., 1990b), which is possibly due to a reduced hydration sphere around the molecule. The fluorescence anisotropy decay of reduced flavodoxins could also be described with a single exponential (an additional anisotropy component did not result in better fits). The rotational correlation times of reduced flavodoxins as obtained with least-squares fitting are listed in Table 2.

The fluorescence anisotropy decays of the four reduced flavodoxins and free reduced flavin were also analyzed using the maximum entropy method. The results of these analyses at 20 °C are shown in Figure 5. It is clear that the anisotropy of all reduced flavodoxins can be described by a unimodal distribution of correlation times. Using the empirical formula (Visser et al., 1983b) describing the relation between the molecular mass of a protein and the

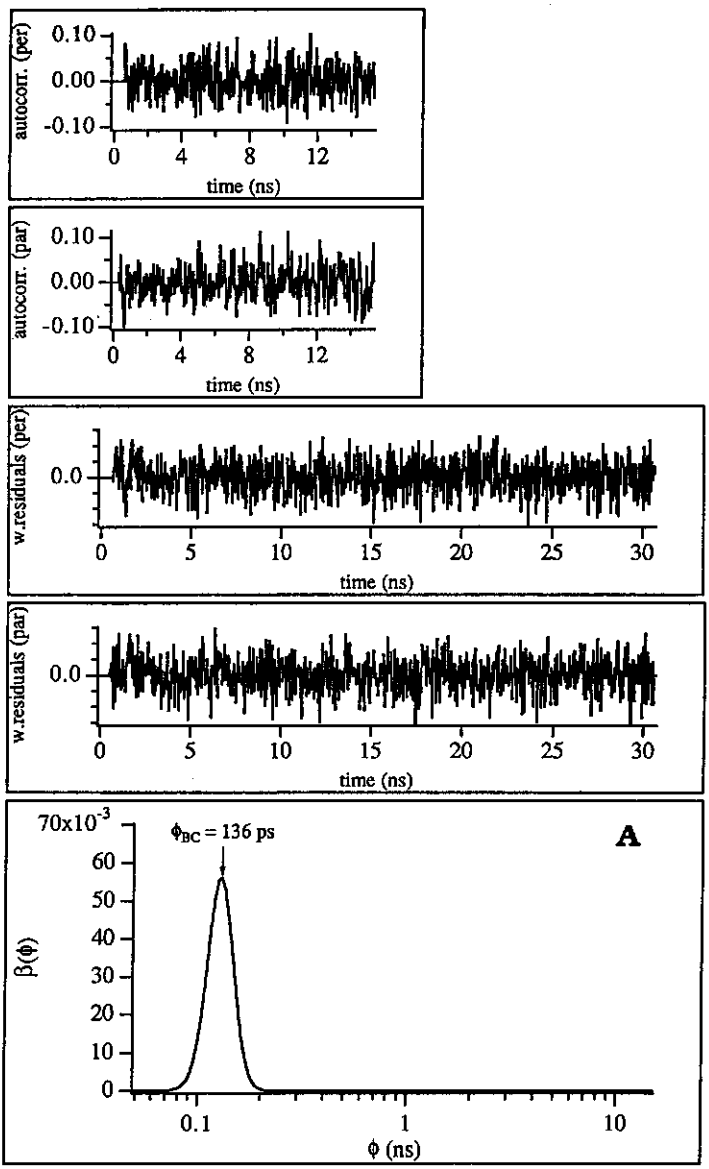

Figure 5. *Maximum entropy analyses of the time-resolved fluorescence anisotropies (at 20 °C).* **A**: reduced FMN in solution, **B**: reduced *D. vulgaris* flavodoxin, **C**: reduced *Cl. beijerinckii* flavodoxin. The positions of the barycenters, calculated according to $\phi_{BC} = \Sigma \beta_i \phi_i / \Sigma \phi_i$, are

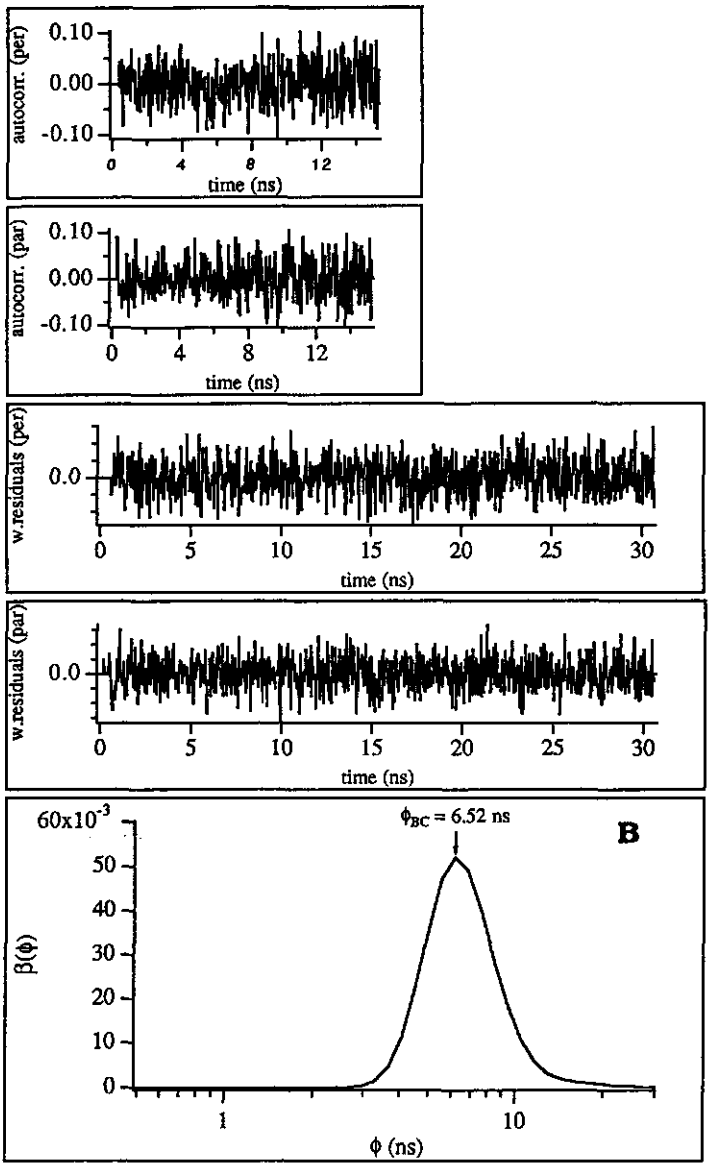

indicated. Integration of the amplitudes $\beta(\phi)$ yields different initial anisotropies for reduced *Cl. beijerinckii* and *D. vulgaris* flavodoxins of 0.249 ± 0.002 and 0.281 ± 0.003, respectively (the errors are standard deviations deduced from integration of 5 separate measurements). In the top

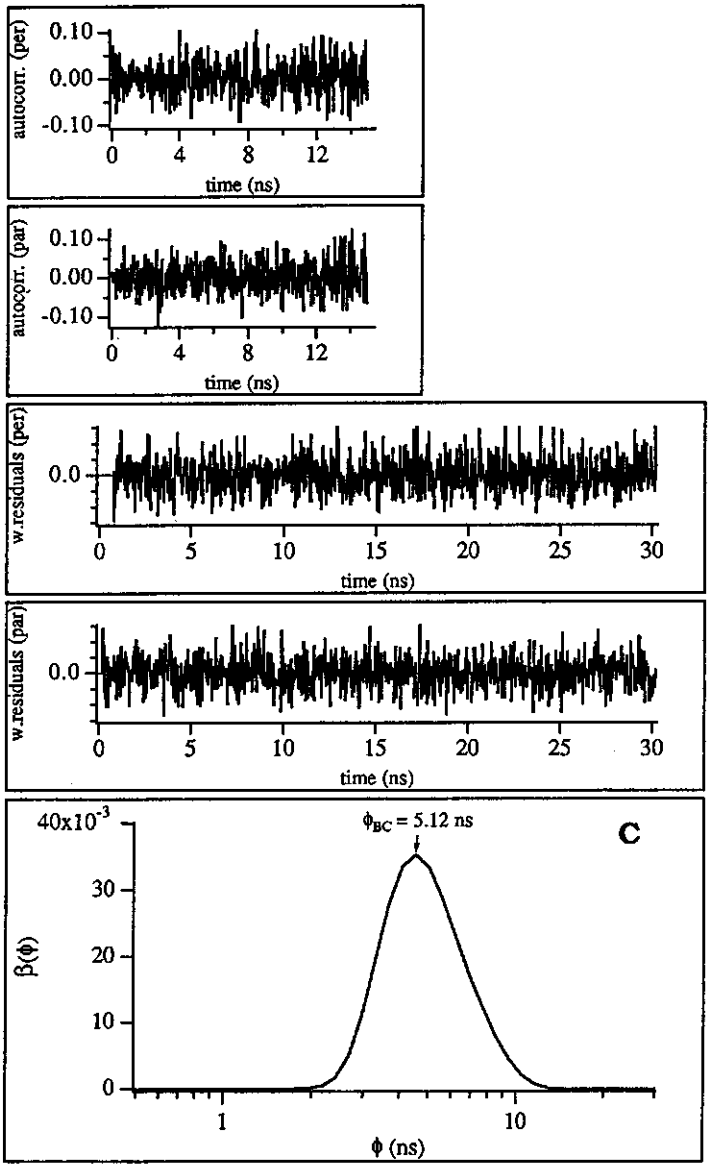

panels the weighted residuals and autocorrelations for the parallel and perpendicular components are given. The fit-quality of the presented analyses is excellent: χ^2 is 1.09, 1.05, and 1.06 for **A**, **B**, and **C**, respectively.

rotational correlation time, ϕ (in ns), at room temperature (20°C):

$$\phi = 3.84 \cdot 10^{-4} M_r \qquad (13)$$

where M_r is the molecular mass, a spherical protein like flavodoxin, with an M_r of 15000, would have a rotational correlation time of about 5.8 ns at 20 °C. In all four reduced flavodoxins the barycenters of the distribution of correlation times are of this order (Figure 5), indicating that the reduced flavin is immobilized within the protein matrix, and hence rotates with the whole protein. In the *pasteurianum* class of flavodoxins, a distribution of rotational correlation times is found which seems somewhat smaller than found in the *rubrum* class of flavodoxins. It is known that the *rubrum* class of flavodoxins contains about 10 extra amino acids and therefore the enlarged molecular mass will be reflected in the rotational correlation times. Analysis of temperature-dependent anisotropy decays using the maximum entropy method shows that the rotational correlation times of both classes of flavodoxins (Figure 6) shorten at higher temperature consistent with the Stokes-Einstein relation:

$$\phi = \frac{\eta V}{k T} \qquad (14)$$

where ϕ is the rotational correlation time, η is the relative viscosity, V is the volume of the spherical rotating unit, k is the Boltzmann constant ($1.38*10^{-23}$ $J.K^{-1}$) and T is the temperature in Kelvin. No indications were found that the reduced protein-bound flavin chromophore exhibits any internal flexibility at elevated temperatures (37 °C).

It should be noted that long fluorescence lifetime components are the carrier signals for the anisotropy. Since the average fluorescence lifetime of reduced flavodoxins is about an order of magnitude smaller than the rotational correlation times, the accuracy of the correlation times will be diminished resulting in broader distributions of the rotational correlation times as compared to free reduced FMN.

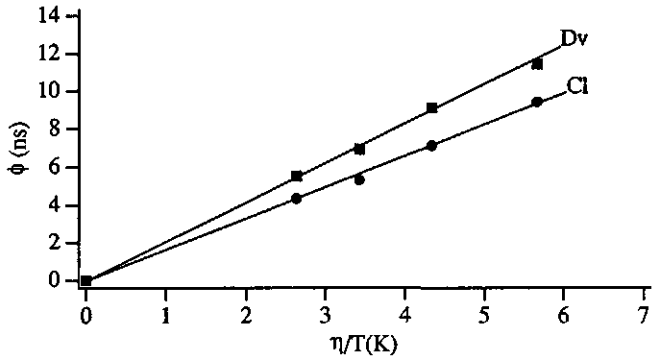

Figure 6. *Relative viscosity dependence of the rotational correlation times of reduced D. vulgaris* (**Dv**) *and Cl. beijerinckii* (**Cl**) *flavodoxin as obtained from the barycenters of the correlation time distribution.* A linear fit to the data is also given (with correlation coefficients of 0.99). The linear behaviour is consistent with the Stokes-Einstein relation (Eq. 14).

From crystallographic and two-dimensional NMR studies (Watenpaugh et al., 1973; Burnett et al., 1974; Smith et al., 1977, 1983; Ludwig et al., 1982; van Mierlo et al., 1990a,b; Watt et al., 1991) it is known that in flavodoxins aromatic amino acid residues are located within a small distance from the isoalloxazine ring of FMN. Furthermore, these studies indicated that upon reduction of the flavodoxins a polypeptide carbonyl group is rotated towards the reduced flavin and the reduced flavin becomes hydrogen bonded with the apoprotein. Therefore, the reduced isoalloxazine ring system is buried in the flavin binding site, resulting in immobilization of the flavin chromophore, consistent with the single correlation time found for whole protein rotation.

Integration of the amplitudes, $\beta(\phi)$, yields significantly different initial anisotropies for reduced *pasteurianum* and *rubrum* flavodoxins of 0.249 ± 0.002 and 0.281 ± 0.003, respectively (see Figure 5). These values are in excellent agreement with those obtained using least-squares fitting (Table 2). The reason that the initial anisotropies (r_0) are smaller than the theoretical maximum of 0.4, is certainly due to non-coincidence of absorption and emission transition moments. An average angle δ between these moments can be calculated from the initial anisotropies using Eq. 8. For the *rubrum* and *pasteurianum* class of reduced flavodoxins these angles are 26.4° ± 0.2° and 30.1° ± 0.3°, respectively, which is significantly larger than the angle found in oxidized flavodoxins (Chapter 3). These larger angles might be due to either overlapping of different electronic transitions or to differences in torsional vibrations (Jablonski, 1965) in

oxidized and reduced isoalloxazine systems. It is noted that fluorescence studies using oriented flavodoxin crystals would have to be performed to determine the exact (mean) location of the absorption and emission dipole moment in reduced flavin (Hansen et al., 1991).

The results described above may indicate that the rigidity of the reduced flavin chromophore observed and the spatial orientation that this implies is necessary for efficient oxidation of the reduced protein-bound flavin, after the flavodoxin is associated with other redox proteins (Pueyo et al., 1991). Further studies investigating flavin dynamics in multi-redox complexes will contribute to the elucidation of the electron transfer mechanism.

Conclusions

The fluorescence intensity decay of reduced free FMN differed from that of reduced protein-bound FMN. However, similar peaks in the fluorescence lifetime distributions found in free reduced FMN were recovered in the reduced protein-bound flavins. Comparison of the fluorescence lifetimes/lifetime distributions showed that the lifetime of the shortest component is influenced by the protein environment, whereas the position of the other components is hardly affected. The results indicate that the environment of the reduced flavin in the *Desulfovibrio* flavodoxins resembles that of free reduced flavin more than in the other two flavodoxins examined. Therefore, also on the basis of the time-resolved fluorescence characteristics of reduced flavodoxin this protein can be classified into two groups: *rubrum*-like and *pasteurianum*-like. Temperature-dependent fluorescence decay studies revealed that in the temperature range used (4 °C to 37 °C) no interconversion on the fluorescence time scale between the different fluorescent states occurs.

The fluorescence anisotropy decays of the four reduced flavodoxins were measured and analyzed at different temperatures. The recovered rotational correlation times are in good agreement with those expected from the Stokes-Einstein relation for rotation of a spherical protein, indicating that the reduced protein-bound flavin is immobilized within the apoprotein matrix. The rotational correlation times of the *rubrum* class of reduced flavodoxins are somewhat longer than in *pasteurianum* flavodoxins, consistent with the larger molecular mass of the former class.

The dynamic properties of reduced flavins bound in flavodoxins as obtained from this study indicate that a specific fixed orientation of the flavin may be required for efficient electron transfer from flavodoxins to other redox proteins.

The motional behaviour of reduced flavins within the protein matrix is somewhat different from flavin bound in oxidized flavodoxins, where part of the protein population is characterized by a flavin which has a certain degree of motional freedom within the protein matrix.

Acknowledgements

The authors wish to thank Dr. Ph. Bastiaens for critically reading the manuscript. Furthermore, the Netherlands Organisation for Scientific Research (N.W.O.) is thanked for partial financial support.

References

Bastiaens, P. I. H., van Hoek, A., Wolkers, W. F., Brochon, J. C. & Visser, A. J. W. G. (1992) *Biochemistry 31*, 7050-7060.

Beechem, J. M. & Brand, L. (1985) *Ann. Rev. Biochem. 54*, 43-71.

Benemann, J. R., Yoch, D. C., Valentine, R. C. & Arnon, D. I. (1969) *Proc. Nat. Acad. Sci. U.S. 64*, 1079-1086.

Burnett, R. M., Darling, G. D., Kendall, D. S., LeQuesne, M. E., Mayhew, S. G., Smith, W. W. & Ludwig, M. L. (1974) *J. Biol. Chem. 249*, 4383-4392.

Cundall, R. B. & Dale, R. E. (Eds.) (1983) *Time-resolved fluorescence spectroscopy in biochemistry and biology*, NATO ASI series, Ser. A: Life Sciences, Vol. 69, Plenum Press, New York.

D'Anna, J. A., Jr. & Tollin, G. (1972) *Biochemistry 11*, 1073-1080.

Farnum, M. F., Magde, D., Howell, E. E., Hirai, J. T., Warren, M. S., Grimsley, J. K. & Kraut, J. (1991) *Biochemistry 30*, 11567-11579.

Ghisla, S., Massey, V., Lhoste, J.-M. & Mayhew, S. G. (1974) *Biochemistry 13*, 589-597.

Hansen, L. K., Christoph, G. W., Hofrichter, J. & Ludwig, M. L. (1991) in *Flavins and Flavoproteins*, (Curti, B., Ronchi, S. & Zanetti, G., Eds.), pp. 405-408, Walter de Gruyter, Berlin.

Hatchikian, E. C., LeGall, J., Bruschi, M. & Dubourdieu, M. (1972) *Biochim. Biophys. Acta 258*, 701-708.

Irie, K., Kobayashi, K., Kobayashi, M. & Ishimoto, M. (1973) *J. Biochem. 73*, 353-366.

Jablonski, A. (1965) *Acta Phys. Polonica 28*, 717-725.

Jaynes, E. T. (1983) *Papers on Probability, Statistics and Statistical Physics*, (Reidel, D., Ed.), Dordrecht, The Netherlands.

Karplus, M. & McCammon, J.A. (1983) *Ann. Rev. Biochem. 53*, 263-300.

Kraut, J. (1988) *Science 242*, 534-560.

Knight, E., Jr. & Hardy, R. W. F. (1966) *J. Biol. Chem. 241*, 2752-2756.

Kulinski, T., Visser, A. J. W. G., O'Kane, D. J. & Lee, J. (1987) *Biochemistry 26*, 540-549.

Lakowicz, J. R. (1983) *Principles of fluorescence spectroscopy*, Plenum Press, New York.

Lee, J., Matheson, I. B. C., Müller, F., O'Kane, D. J., Vervoort, J. & Visser, A. J. W. G. (1991) in *Chemistry and Biochemistry of Flavoenzymes*, Vol. II (Müller, F., Ed.), pp. 109-151, CRC Press, Boca Raton, FL.

Leenders, H. R. M., Vervoort, J., van Hoek, A. & Visser, A. J. W. G. (1990a) *Eur. Biophys. J. 18*, 43-55

Leenders, R., Bastiaens, Ph., Lunsche, R., van Hoek, A. & Visser, A. J. W. G. Visser (1990b) *Chem. Phys. Lett. 165*, 315-322.

LeGall, J. & Hatchikian, E. C. (1967) *C. R. Acad. Sc. Paris 264*, 2580-2583.

Livesey, A. K., Licinio, P. & Delaye, M. (1986) *J. Chem. Phys. 84*, 5102-5107.

Livesey, A. K. & Brochon, J. C. (1987) *Biophys. J. 52*, 693-706.

Ludwig, M. L., Pattridge, K. A., Smith, W. W., Jensen, L. H. & Watenpaugh, K. D. (1982) in *Flavins and Flavoproteins*, (Massey, V. & Williams, C. H., Eds.), pp. 19-28, Elsevier/North-Holland, Amsterdam.

Mayhew, S. G. & Massey, V. (1969) *J. Biol. Chem. 244*, 794-802.

Mayhew, S. G. (1971) *Biochim. Biophys. Acta 235*, 289-302.

Mayhew, S. G. & Ludwig, M. L. (1975) in *The Enzymes*, Vol. XII, (Boyer, P. D., Ed.), pp. 57-118, Academic Press, New York.

Mérola, F., Rigler, R., Holmgren, A. & Brochon, J. C. (1989) *Biochemistry 28*, 3383-3398.

Pueyo, J. J., Walker, M. C., Tollin, G. & Gómez-Moreno, C. (1991) in *Flavins and Flavoproteins*, (Curti, B., Ronchi, S. & Zanetti, G., Eds.), pp. 483-486, Walter de Gruyter, Berlin.

Rigler, R. & Ehrenberg, M. (1973) *Q. Rev. Biophys. 6*, 139-199.

Rigler, R. & Ehrenberg, M. (1976) *Q. Rev. Biophys. 9*, 1-19.

Smith, W. W., Burnett, R. M., Darling, G. D. & Ludwig, M. L. (1977) *J. Mol. Biol. 117*, 195-225.

Smith, W. W., Pattridge, K. A., Ludwig, M. L., Petsko, G. A., Tsernoglou, D., Tanaka, M. & Yasunobu, K. T. (1983) *J. Mol. Biol. 165*, 737-755.

Strickler, S. J., & Berg, R. (1962) *J. Chem. Phys. 37*, 814-822.

Tauscher, L., Ghisla, S. & Hemmerich, P. (1973) *Helv. Chim. Acta 56*, 630-644.

van Hoek, A., Vervoort, J. & Visser, A. J. W. G. (1983) *J. Biochem. Biophys. Methods 7*, 243-254.

van Hoek, A. & Visser, A. J. W. G. (1985) *Anal. Instrum. 14*, 359-372.

van Hoek, A., Vos, K. & Visser, A. J. W. G. (1987) *IEEE J. Quantum Electron. QE-23*, 1812-1820.

van Hoek, A. & Visser, A. J. W. G. (1992) in *Time-resolved Laser Spectroscopy in Biochemistry, vol. 1640* (Lakowicz, J. R. , Ed.), pp. 325-329, Proceedings of SPIE-The International Society for Optical Engineering, Bellingham, WA.

van Lin, B. & Bothe, H. (1972) *Arch. Mikrobiol. 82*, 155-172.

van Mierlo, C. P. M., Lijnzaad, Ph., Vervoort, J., Müller, F., Berendsen, H. J. C. & de Vlieg, J. (1990a) *Eur. J. Biochem. 194*, 185-198.

van Mierlo, C. P. M., van der Sanden, B. P. J., van Woensel, P., Müller, F. & Vervoort, J. (1990b) *Eur. J. Biochem. 194*, 199-216.

Vervoort, J., van Berkel, W. J. H., Mayhew, S. G., Müller, F., Bacher, A., Nielsen, P., LeGall, J. (1986) *Eur. J. Biochem. 161*, 749-756.

Vetter, H., Jr. & Knappe, J. (1971) *Hoppe-Seyler's Z. Physiol. Chem. 352*, 433-446.

Visser, A. J. W. G., Ghisla, S., Massey, V., Müller, F. & Veeger, C. (1979) *Eur. J. Biochem. 101*, 13-21.

Visser, A. J. W. G., Vervoort, J., O'Kane, D. J., Lee, J. & Carreira, L. A. (1983a) *Eur. J. Biochem. 131*, 639-645.

Visser, A. J. W. G., Penners, N. H. G., & Müller, F. (1983b) in *Mobility and recognition in cell biology*, (Sund, H. & Veeger, C., Eds.), pp. 137-152, Walter de Gruyter, Berlin.

Visser, A. J. W. G., Ykema, T., van Hoek, A., O'Kane, D. J. & Lee, J. (1985) *Biochemistry 24*, 1489-1496.

Visser, A. J. W. G., Ghisla, S. & Lee, J. (1991) in *Flavins and Flavoproteins*, (Curti, B., Ronchi, S. & Zanetti, G., Eds.), pp. 49-54, Walter de Gruyter, Berlin.

Vos, K., van Hoek, A. & Visser, A. J. W. G. (1987) *Eur. J. Biochem. 165*, 55-63.

Watenpaugh, K. D., Sieker, L. C. & Jensen, L. H. (1973) *Proc. Nat. Acad. Sci. U.S. 70*, 3857-3860.

Watt, W., Tulinsky, A., Swenson, R. P. & Watenpaugh, K. D. (1991) *J. Mol. Biol. 218*, 195-208.

Chapter 3

Flavin dynamics in oxidized *Clostridium beijerinckii* flavodoxin as assessed by time-resolved polarized fluorescence

Rik Leenders, Arie van Hoek, Martijn van Iersel, Cees Veeger, and Antonie J. W. G. Visser

submitted to: *European Journal of Biochemistry*

Abstract

The time-resolved fluorescence characteristics of flavin in oxidized flavodoxin isolated from the anaerobic bacterium *Clostridium beijerinckii* have been examined. The fluorescence intensity decays were analyzed using the maximum entropy method (MEM). It is demonstrated that there exist large differences in fluorescence behaviour between free and protein-bound flavin mononucleotide (FMN). Three fluorescence lifetime components are found in oxidized flavodoxin, two of which are not present in the fluorescence intensity decay of free FMN. The main component is distributed at 30 ps, with relative contribution of 90%. Another minor component (4% contribution) is distributed at 0.5 ns. The third component is distributed at 4.8 ns (6%), coinciding with the main distribution present in the fluorescence decay of free FMN. The results allowed us to determine the dissociation constant, $K_D = 2.61*10^{-10}$ (at 20 °C).

Collisional fluorescence quenching experiments revealed that the flavin moiety responsible for the longest fluorescence lifetime is, at least partially, exposed to the solvent. The shortest lifetime is not affected significantly, indicating that it possibly originates from an active site conformation in which the flavin is more or less buried in the protein and not accessible for iodide.

The fluorescence anisotropy behaviour of free and protein-bound FMN was examined and analyzed with the maximum entropy method. It was found that an excess of apoflavodoxin is required to detect differences between free and protein-bound FMN. In free FMN one single distribution of rotational correlation times is detected, whereas in flavodoxin the anisotropy decay is composed of more than one distribution.

Associative analysis of fluorescence anisotropy decays shows that part of the 4.8 ns fluorescence lifetime present in the flavodoxin fluorescence decay, is coupled to a rotational correlation time similar to that of free FMN in solution, while another part of this lifetime is coupled to a longer correlation time of about 1 ns. This finding is in accordance with earlier studies (Barman and Tollin (1972) *Biochemistry 11*, 4746-4754) in which it was proposed that the first binding step of the flavin to the protein involves the phosphate group rather than another part of the flavin mononucleotide.

The two shortest fluorescence lifetimes, which do not carry information on the long-term rotational behaviour of the protein, seem nonetheless to be associated with a longer rotational correlation time which is comparable to overall protein tumbling. These lifetime components probably originate from a

complex in which the flaving ring system is more or less immobilized within the protein matrix.

Introduction

Flavodoxins are low molecular weight electron-transport proteins (M_r 14-25 kDa) which can substitute for ferredoxin in a number of reactions (Mayhew, 1971; Mayhew and Ludwig, 1975). Flavodoxins can be isolated from some algae and several anaerobic and aerobic bacteria grown under iron-containing or iron-deficient conditions (Knight and Hardy, 1966; Benemann et al., 1969; Mayhew, 1971; Vetter and Knappe, 1971; Hatchikian et al., 1972; van Lin and Bothe, 1972; Irie et al., 1973). The redox-active centre of flavodoxins is the non-covalently bound flavin mononucleotide (FMN). Flavodoxins can exist in different oxidation states, i.e. oxidized, one-electron reduced (semiquinone), and two-electron-reduced (hydroquinone). The physiologically relevant redox states are the semiquinone and hydroquinone ones.

In the seventies the three-dimensional structure of oxidized *Clostridium beijerinckii* flavodoxin was resolved using X-ray crystallography (Burnett et al., 1974). The structures of the semiquinone and reduced *clostridial* flavodoxin show a large overall similarity with the oxidized protein (Smith et al., 1977; Ludwig et al., 1982). The major difference between these two oxidation states is the direction of the carbonyl group of residu Gly57. Upon reduction the carbonyl rotates towards the flavin facilitating hydrogen bonding between the carbonyl oxygen and the hydrogen attached to flavin atom N(5). Recently the structure of *Megasphaera elsdenii* flavodoxin in different oxidation states was determined using two-dimensional nuclear magnetic resonance and restrained molecular dynamics simulations (van Mierlo et al., 1990a,b). The overall structures of *Cl. beijerinckii* and *M. elsdenii* flavodoxin were shown to be highly similar. These three-dimensional structures mainly yield information about the static properties of the flavodoxins. However, knowledge of the dynamic behaviour of proteins is essential in understanding the way in which they function (Karplus and McGammon, 1983; Kraut, 1988; Farnum et al., 1991).

Spectroscopic techniques in general, and fluorescence measurements in particular, have been widely used to characterize microenvironments of intrinsicly and extrinsicly bound chromophores (Rigler and Ehrenberg, 1973, 1976; Cundall and Dale, 1983; Lakowicz, 1983; Beechem and Brand, 1985;

Leenders et al., 1990, 1993; Bastiaens et al., 1992a,b,c)). In this respect tryptophan residues are the most intensively studied chromophores in proteins. These fluorescence techniques can also be applied to study other chromophores, like for example flavins in various flavoproteins. In this paper we used time-resolved fluorescence and fluorescence anisotropy techniques to obtain information about the dynamic characteristics of flavin bound in oxidized *Cl. beijerinckii* flavodoxin. The time-resolved fluorescence studies of reduced flavodoxins have been reported (Chapter 2; Leenders et al., 1993). Although *clostridial* flavodoxin has a low flavin fluorescence quantum yield, it has the advantage that it contains several intrinsic chromophoric groups which are located in or near the active site of the protein (the flavin and a number of tryptophan residues). These chromophores are ideally suited for fluorescence studies in which information about the flexibility of the active site can be obtained.

In this contribution attention is focussed on the fluorescence properties of the oxidized prosthetic group FMN bound in flavodoxin. As a result of the equilibrium between protein-bound and dissociated FMN, differences in fluorescence behaviour between free and protein-bound FMN can be used to study the association process and binding properties of the FMN, and the obtained insight in motional behaviour may contribute to the understanding of the process of electron transfer of flavodoxins.

Materials and Methods

Preparation of the flavodoxins

The preparation of *Cl. beijerinckii* flavodoxin was as described previously (Leenders and Visser, 1991). The flavodoxins were dissolved in 0.1 M KP_i pH 7.0 at protein concentrations of about 10 μM (determined spectrophotometrically). At these concentrations reabsorption effects are eliminated. All chemicals used were of the highest purity available and only Millipore-filtered water was used. Apoflavodoxins were prepared as described by Wassink and Mayhew (1975). Experiments were conducted between 4 °C and 30 °C.

Fluorescence quenching experiments

Collisional fluorescence quenching experiments using KI were performed as described by Lehrer (1971). Samples containing *Cl. beijerinckii* flavodoxin were quenched as well as samples containing free FMN in solution (quenched for comparison). The effects of KI quenching were studied by means of steady-state and time-resolved fluorescence experiments.

Time-resolved fluorescence and fluorescence anisotropy measurements

Fluorescence decay measurements using a mode-locked argon-ion laser/synchronously-pumped dye laser system as the source of excitation, have been described extensively (van Hoek et al., 1983, 1987; van Hoek and Visser, 1985,; Visser et al., 1985; Vos et al., 1987). The most recent update in description of the system has been given by van Hoek and Visser (1992). The protein-bound FMN as well as the FMN in aqueous buffer solution were excited (457.9 nm) in their first absorption band. Erythrosin-B was used as a reference compound to describe the instrumental response (Erythrosin-B fluorescence decays single-exponentially with a typical lifetime of about 80 ps at 4 °C). After excitation the polarized fluorescence was monitored using a Schott (Mainz, Germany) line filter (Schott 557.6, with half band width of 12.6 nm) in combination with a Schott cut-off filter (KV550).

The fluorescence and fluorescence anisotropy decays were analyzed in terms of continuous lifetime distributions by means of the maximum entropy method (MEM). In this method (Livesey et al., 1986; Livesey and Brochon, 1987), a distribution of lifetimes, $\alpha(\tau)$, is calculated which results in a maximum value of the entropy, S (Jaynes, 1983):

$$S = -\int_0^\infty \alpha(\tau)\, log\frac{\alpha(\tau)}{m(\tau)}\, d\tau \qquad (1)$$

where $m(\tau)$ is the initial guess for the distribution of fluorescence lifetimes. In all cases the entropy, S, is maximized under the condition that χ^2 is minimized to unity:

$$\chi^2 = \frac{1}{N} \sum_{k=1}^{N} \frac{\{I_c(k) - I_o(k)\}^2}{I_o(k)} \qquad (2)$$

where N is the number of channels, $I_c(k)$ and $I_o(k)$ are the calculated and observed number of photons in channel k, respectively. Furthermore, $I_o(k)$ is an estimate for the variance in channel k. The obtained distribution will yield the most uncorrelated solution. When no *a priori* knowledge about the shape of the distribution was available, $m(\tau)$ was set to a flat distribution in $\log(\tau)$ space (Livesey and Brochon, 1987; Mérola et al., 1988; Bastiaens et al., 1992c). Since fluorescence intensities and anisotropy contributions are only represented correctly in $\log(\tau)$ and $\log(\phi)$ space, respectively, we divided the logarithmic time axis in 150 equally spaced intervals. $\mathrm{Log}(\tau)$ space ranged from 0.01 to 15 ns, whereas $\log(\phi)$ space ranged from 0.05 to 30 ns. Integration of the amplitudes $\beta(\phi)$ yields the initial anisotropy, $r(0)$.

The time-resolved fluorescence anisotropy behaviour was also analyzed using the maximum entropy method in an associative manner (for details see: Bastiaens et al., 1992d). In this analysis of the fluorescence and fluorescence anisotropy decay the entropy of the cross-product $\alpha \cdot \beta$ is maximized (again under the constraint of minimum χ^2):

$$S = -\int_0^\infty \alpha(\tau)\,\beta(\phi)\,\log\frac{\alpha(\tau)\,\beta(\phi)}{m(\tau)}\,d\tau \qquad (3)$$

where $m(\tau)$ is the initial guess of the $\alpha(\tau)\cdot\beta(\phi)$ distribution. The logarithmic time axes were divided in 40 equally spaced intervals. Since this type of analysis yields information about specific correlations between fluorescence lifetimes and rotational correlation times it can substantially contribute to the understanding of multi-exponential fluorescence and fluorescence anisotropy decays. All analyses were performed on a Silicon Graphics 4D/35 computer.

Results and Discussion

Quenching of flavin fluorescence in flavodoxin

It is known from earlier studies that flavin fluorescence can be quenched significantly upon binding with the apoflavoprotein (see review Mayhew and Ludwig, 1975). Steady-state fluorescence experiments showed that the reason for this quenching must be the interaction of the isoalloxazine ring system with specific parts of the protein. In particular, disulfide bridges and aromatic amino acid sidechains are potential quenchers of flavin fluorescence in flavoproteins. In case of tryptophan sidechains, using flavinyl-tryptophan model compounds, it was shown by steady-state fluorescence measurements (MacKenzie et al., 1969) and proton magnetic resonance experiments (Föry et al., 1970; Johnson and McCormick, 1973) that the isoalloxazine and indole rings are coplanar. This ground-state complex clearly influences fluorescence characteristics of the flavin ring system. This is the basis for the so-called static quenching of flavin fluorescence (Lakowicz, 1983).

Time-resolved fluorescence

The time-resolved fluorescence decays of *Cl. beijerinckii* flavodoxin and free FMN in solution were measured at different temperatures. The fluorescence decays recorded at 4 °C are presented in Figure 1A. The protein-bound FMN fluorescence initially decays much faster than the fluorescence of free FMN, indicating the influence of the protein environment upon FMN fluorescence. The decay curves were analyzed using the maximum entropy method (MEM), to obtain information about the distribution of lifetimes in the fluorescence decays. The results of these analyses are shown in Figures 1B and 1C. The quality of the fits was excellent, $1.02 \leq \chi^2 \leq 1.06$. It is clear that two short lifetime components (about 30 ps and 0.5 ns) are distributed in the protein-bound FMN fluorescence which are not present in the fluorescence decay of free FMN. This difference in lifetime distributions directly results from binding of the FMN to the protein, leading to quenching by the protein environment. The very short lifetime (30 ps) has already been noticed for *Desulfovibrio* flavodoxins (Visser et al., 1987) and glutathione reductase (Bastiaens et al., 1992c). It has been ascribed to exciplex formation and energy transfer from a donor to the flavin, which brings the

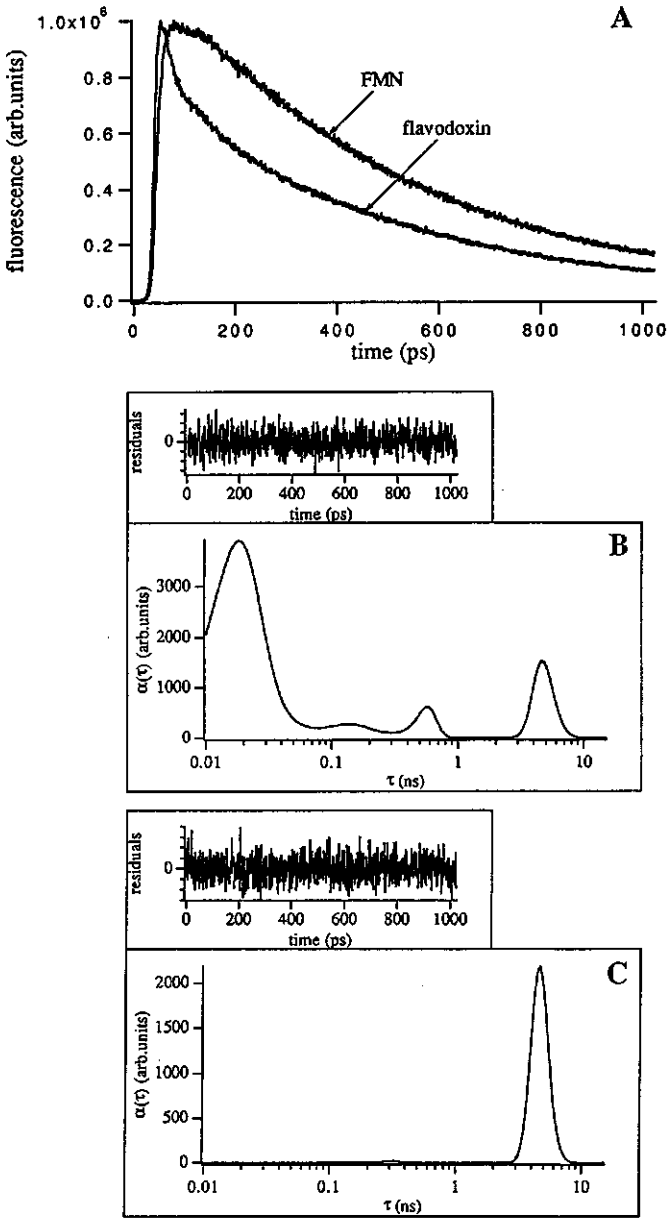

Figure 1. *Fluorescence decays (at 4 °C) of clostridial flavodoxin and free FMN in solution* (**A**). The results of the maximum entropy analysis is also presented: **B**, *clostridial* flavodoxin; **C**, FMN in solution. The fit quality was excellent: χ^2 is 1.02 and 1.06, for flavodoxin and FMN, respectively.

flavin excited-state lifetime in the picosecond range. A third fluorescence lifetime distribution is found in flavodoxin which coincides with the main lifetime distribution found in free FMN in solution (4.8 ns).

It is known that an equilibrium exists between free and protein-bound FMN. Therefore, the 4.8 ns fluorescence lifetime in flavodoxin may well originate from dissociated FMN. Barman and Tollin (1972) examined the relaxation kinetics of flavin analogs binding to *Azotobacter vinelandii* apoflavodoxin and it was demonstrated that binding of phosphorylated flavin analogs has to be described by a two-step mechanism:

$$P + F \rightleftharpoons X \rightleftharpoons FP \qquad (4)$$

with P is the apoflavodoxin, F is the flavin analog, FP is the flavodoxin in which the flavin is firmly bound, and X is an intermediate structure in which the flavin is bound to the apoflavodoxin in some way. Because of the relatively small dissociation constant K_D (*vide infra*), only a very small fraction of dissociated FMN is present in a flavodoxin solution. However, because of its much higher fluorescence quantum yield, as compared to protein-bound FMN, it will contribute significantly to the decay of flavin fluorescence in flavodoxin samples. In order to demonstrate this, the effect of temperature on the fluorescence behaviour of flavin and flavodoxin was examined. At higher temperatures (≥20 °C) the barycenter of the lifetime distribution of the flavin slightly decreases (from 4.8 ns to 4.7 ns). The temperature dependence of the fluorescence decay of *clostridial* flavodoxin, given in terms of lifetime distributions, is illustrated in Figure 2. It is obvious that the contribution of the short lifetime component decreases at higher temperatures, in favour of the contribution of the 4.8 ns fluorescence lifetime component. The most reasonable explanation is that at higher temperatures part of the population of the non-covalently bound FMN chromophores dissociates from the protein (Eq. 4), resulting in a larger contribution of the 4.8 ns fluorescence lifetime component. To examine if this distribution at 4.8 ns originates from dissociated FMN, apoflavodoxin was added to the *clostridial* flavodoxin sample (the apoprotein does not absorb light at the excitation wavelength). Addition of apoflavodoxin resulted in a significant decrease of the contribution of 4.8 ns fluorescence lifetime component (see Figure 2B), which is the result of a shift in the equilibrium. The dissociated flavin binds to the added apoflavodoxin to form holoflavodoxin. Addition of an excess of apoflavodoxin, however, did not result in complete loss of the 4.8 ns fluorescence lifetime component. In most flavodoxin samples used in the experiments a slight excess of apoflavodoxin was present.

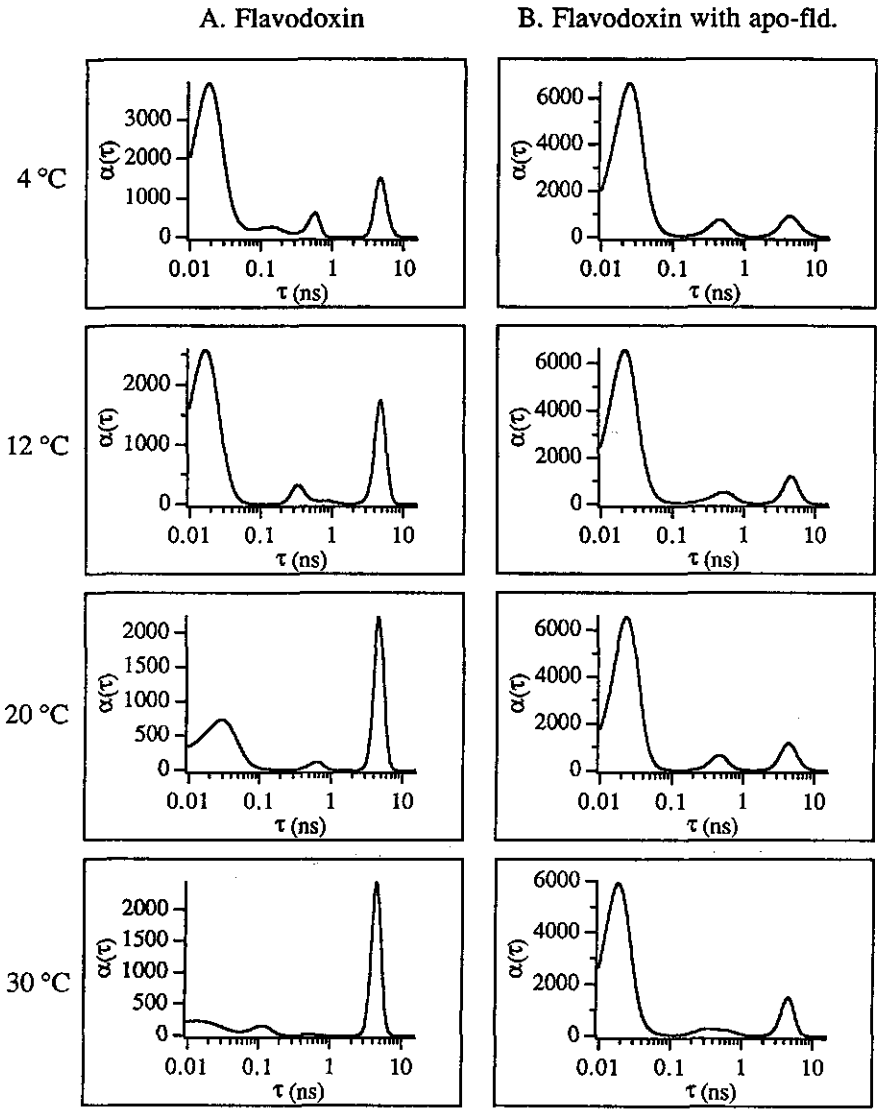

Figure 2. *Temperature dependence of the flavodoxin fluorescence decay (A).* The fluorescence lifetime distributions are calculated with the maximin entropy method. Addition of apoflavodoxin to the flavodoxin sample clearly influences the lifetime distribution at different temperatures (B). The fit quality was very good: χ^2's between 1.01 and 1.08.

Analysis of the fluorescence decays of flavodoxin samples containing apoflavodoxin demonstrated that the lifetime distribution is no longer temperature dependent. Only at 30 °C the contribution of the 4.8 ns component somewhat increases, indicating a small shift of the equilibrium. The short lifetime component is always predominantly present (about 80 to 90 %), whereas the intermediate lifetime (distributed between 0.2 and 1.0 ns) contributes for only about 4 %. The rest of the flavodoxin fluorescence decay is composed of the 4.8 ns component.

Another piece of evidence for the equilibrium between protein-bound and dissociated flavin is given by KI-quenching experiments with flavodoxin samples to which no apoflavodoxin was added (Figure 3). The 4.8 ns fluorescence lifetime is quenched significantly in both flavodoxin and FMN in solution, indicating that both samples contain a similar flavin moiety.

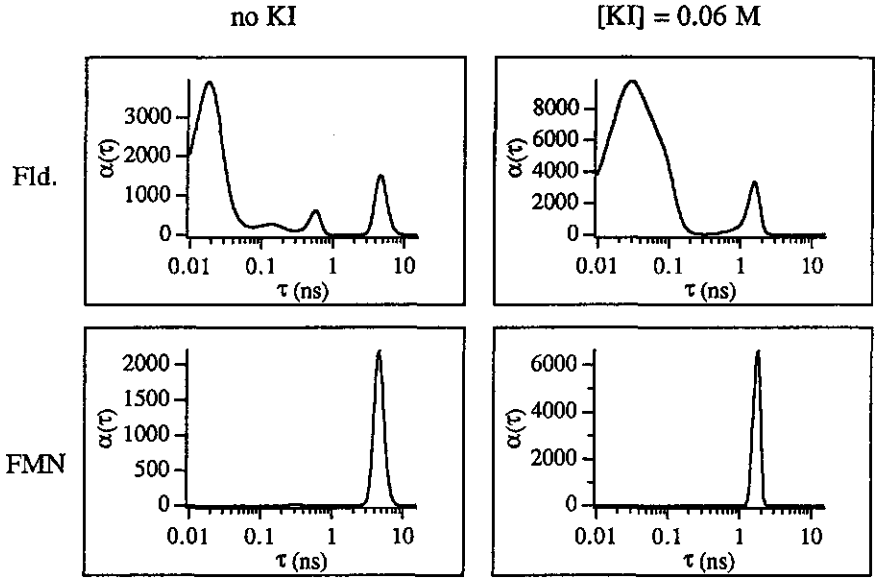

Figure 3. *Quenching experiments with clostridial flavodoxin* ([KI] is 0.06 M; no apoflavodoxin was added). The results of KI-quenching of FMN in solution are given for comparison. It is clear that both samples contain a similar flavin moiety. The intermediate lifetimes in the flavodoxin (Fld) also seem to be quenched by the iodide.

Determination of the dissociation constant

For the ease of calculation it is assumed that the 4.8 ns fluorescence lifetime distribution in flavodoxin completely originates from dissociated flavin (Figure 2; flavodoxin with no added apoprotein) and the other predominant lifetime is related to flavin bound in the flavodoxin. Relative fluorescence quantum yields can then be obtained from the ratio of lifetimes:

$$\frac{Q_F}{Q_f} = \frac{\tau_F}{\tau_f} \tag{5}$$

where Q_F and Q_f are the quantum yields of FMN and flavodoxin, respectively, and the corresponding lifetimes are calculated from the barycenters of the lifetime distributions. From the ratio of these barycenters (4.8 ns and 30 ps for FMN and flavodoxin, respectively) the relative quantum yield can be calculated, Q_F/Q_f is 160. Integration of the lifetime distribution at 20 °C yields that 55% of the total fluorescence originates from flavodoxin and 45% from dissociated flavin. When these values are corrected for the quantum yield ratio, 99.49% of the flavin is bound in flavodoxin and 0.51% is dissociated. When the reaction in Eq. 4 is considered to occur via a one step mechanism (no intermediate state X) and apoflavodoxin and dissociated flavin are present in equimolar concentrations (the total flavin concentration is 10 μM), the dissociation constant K_D at equilibrium is then given by:

$$K_D = \frac{[P].[F]}{[PF]} \tag{6}$$

The dissociation constant at 20 °C can then be calculated, K_D=2.61*10^{-10} M. This value is in good agreement with the one determined for *M. elsdenii* flavodoxin, K_D is 4.3*10^{-10} M (Mayhew, 1971). The standard enthalpy change of the dissociation reaction, ΔH^0, is determined by measuring the dissociation constant at various temperatures and using the van 't Hoff equation:

$$\frac{d\ln K_D}{d(1/T)} = -\frac{\Delta H^0}{R} \tag{7}$$

where R is the gas constant (8.31 J.K^{-1}.mol^{-1}) and T is the temperature in Kelvin. From the slope of the van 't Hoff plot (Figure 4) the standard enthalpy

change of the dissociation reaction, ΔH^0, was calculated to be 144.8 ± 12.4 kJ.mol^{-1}.

Table 1. The thermodynamic parameters describing the equilibrium of flavin, free and bound in clostridial flavodoxin, as a function of temperature.

T (°C)	[FMN]	[fld]	K_D	ΔG^0
	(μM)	(μM)	(M^{-1})	(kJ/mol)
4	0.009	9.991	$1.01*10^{-11}$	58.7
12	0.022	9.978	$3.25*10^{-11}$	56.2
20	0.051	9.949	$2.61*10^{-10}$	53.7
30	0.137	9.863	$1.90*10^{-9}$	50.6

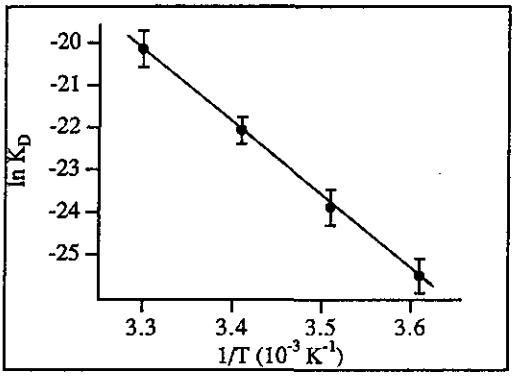

Figure 4. *van 't Hoff plot of the equilibrium constant of flavin dissociating from clostridial flavodoxin.* The solid line is a linear fit to the experimental data. Standard deviations are estimated from multiple experiments.

The standard entropy difference, ΔS^0, is obtained from the temperature dependence of the free energy ΔG^0:

$$\frac{d\Delta G^0}{dT} = -\Delta S^0 \qquad (8)$$

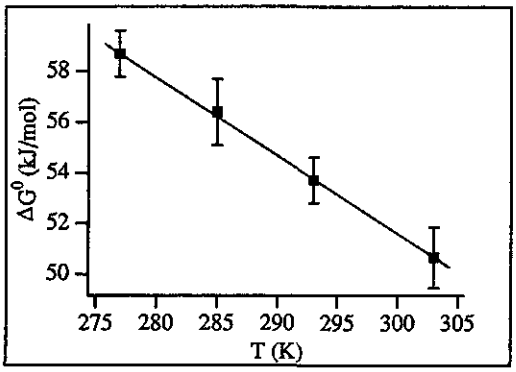

Figure 5. *Free energy of flavin dissociation as a function of temperature.* The solid line is a linear fit to the experimental data. Standard deviations are estimated from multiple experiments.

From the slope of the plot of ΔG^0 (Figure 5) the standard entropy difference, ΔS^0, was determined as 311 ± 27 J.mol^{-1}.K^{-1}. By comparing values at 20 °C (ΔH^0 = 144.8 kJ.mol^{-1} and TΔS^0 = 91.1 kJ.mol^{-1}) it is suggested that the enthalpy contribution prevails in the dissociation reaction.

Time-resolved fluorescence is one of the very few techniques with which dissociation constants, K_D, can be determined directly in very dilute solutions (thermodynamically ideal).

Time-resolved fluorescence anisotropy

The time-resolved fluorescence anisotropy decays of oxidized *Cl. beijerinckii* flavodoxin did not differ significantly from the anisotropy decay of free FMN unless an amount of apoflavodoxin was added to the flavodoxin samples. This difference in anisotropy decay is illustrated in Figure 6. The fluorescence anisotropy decay of flavodoxin is 'delayed' as compared to the anisotropy decay of free FMN, indicating that in flavodoxin the rotation is more hindered than in free flavin (both decays are nonetheless very rapid). The fluorescence anisotropy decays of free FMN in solution, analyzed using the maximum entropy method, is presented in Figure 7. It is obvious that the rotational correlation time, ϕ, of free FMN in solution behaves according to the Stokes-Einstein relationship,

$$\phi = \frac{\eta V}{k T} \tag{9}$$

where η is the viscosity, V is the molecular volume, k is Boltzmann's constant, and T is the temperature.

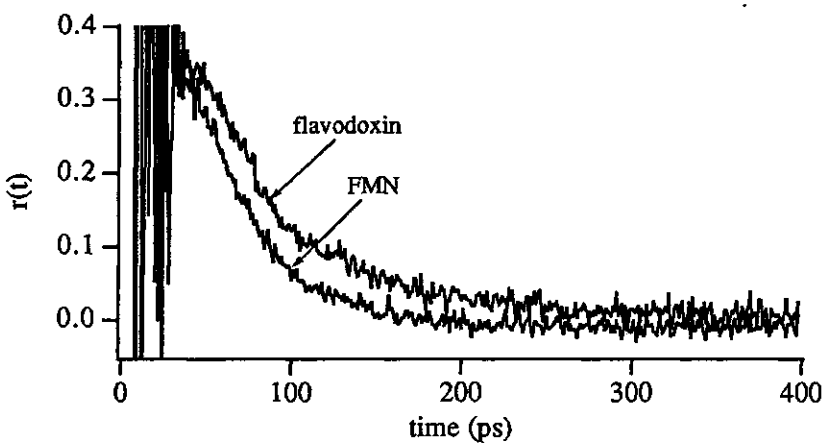

Figure 6. *The anisotropy decays of free FMN and Cl. beijerinckii flavodoxin at 20 °C.*

Analysis of the *clostridial* flavodoxin anisotropy decay using the maximum entropy method, shows that the decay has to be described by more than one distribution (Figure 7). At 4 °C a distribution is found at 290 ps, which is ascribed to partially dissociated FMN. A second distribution is found at about 1.2 ns. According to the Stokes-Einstein relation in combination with the empirically determined relation of Visser et al. (1983):

$$\phi(T) = \eta(T)\ 3.8*10^{-4} M_r \qquad (10)$$

a protein with a molecular weight (M_r) of 15 kDa has a rotational correlation time of about 8.5 ns (at 4 °C). No significant distribution is found corresponding to protein tumbling, indicating that FMN which is bound to the apoflavodoxin is not immobilized within the protein matrix, but has a certain degree of motional flexibility. This is expressed by the rotational correlation time of about 1.2 ns. Integration of the amplitudes, $\beta(\phi)$, yields initial anisotropies of 0.35 for both the FMN and flavodoxin. For other flavoproteins identical initial anisotropies have been demonstrated (Bastiaens et al., 1992b).

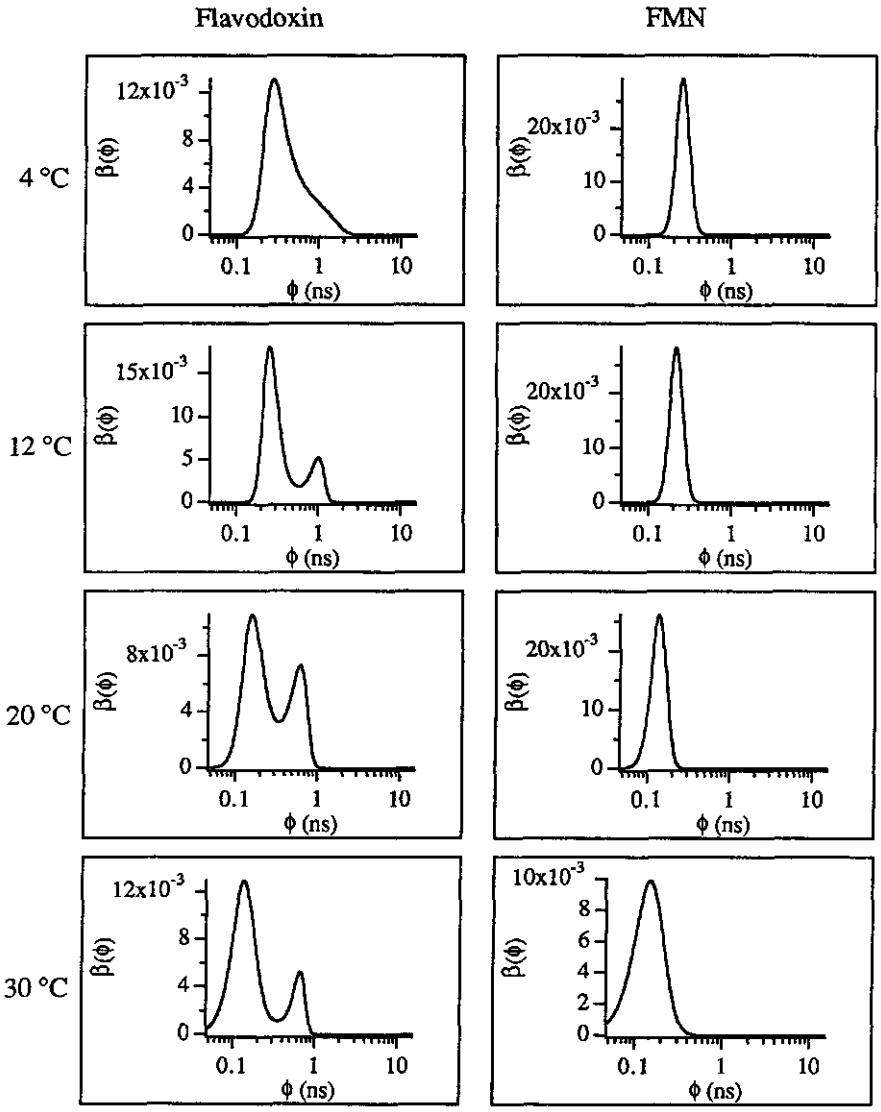

Figure 7. *Maximum entropy analyses of the anisotropy decay of clostridial flavodoxin and free FMN in solution.* Measurements are performed between 4 °C and 30 °C. The position of the shortest distribution in the *clostridial* flavodoxin anisotropy decay is clearly identical to that in free FMN. A longer rotational correlation time is only present in flavodoxin.

One should keep in mind that the very short fluorescence lifetime, which may be coupled to an immobilized flavin moiety, decays so fast that information about the relatively long rotational correlation time is completely lost, irrespective of temperature.

Associative analyses of polarized fluorescence decays

To interpret the polarized fluorescence decays in an unambiguous way we have carried out associative analyses of both flavodoxin and FMN in solution. In this way more information is obtained about the components present in the anisotropy decay of *clostridial* flavodoxin at different temperatures. The decays were analyzed in terms of rotational correlation times which are coupled to specific fluorescence lifetimes (Eq. 3). The initial anisotropy was fixed at 0.35 in the analysis of both flavodoxin and free FMN. The results of the analyses are given in Figure 8.

Some very interesting details can be extracted from Figure 8. First of all we notice that indeed more than one distribution can be found in the flavodoxin anisotropy decay. One of the most pronounced features is the fact that the very short fluorescence lifetime (30 ps) can hardly be coupled specificly with certain rotational correlation times. As expected, accurate information about longer rotational correlation times cannot be retrieved from picosecond fluorescence lifetimes. Only at 4 °C it is valid to remark that this ultrashort lifetime seems correlated with a larger rotational correlation time (more than 5 ns) possibly corresponding with the one expected from overall protein tumbling (8.5 ns). This implies that this associative behaviour originates from a flavin moiety which is immobilized within the protein matrix. Another very pronounced feature (at 4 °C) is the presence of a correlation between the fluorescence lifetime distributed at 4.8 ns and the rotational correlation time distributed at 280 ps. Since this correlation exactly corresponds with the one found in the associative analysis of free FMN and since the size of its rotational correlation time perfectly matches the one expected from extrapolation of the already published correlation time of 155 ps at 20 °C, it is ascribed to dissociated FMN. So, even at lower temperatures (between 4 °C and 20 °C), where no significant dissociation is expected there seems always some dissociated FMN present. Furthermore, another correlation is detected between the 4.8 ns fluorescence lifetime distribution and a rotational correlation time which is longer than the

one found for free FMN. This is best illustrated with measurements at 20 °C (Figure 8).

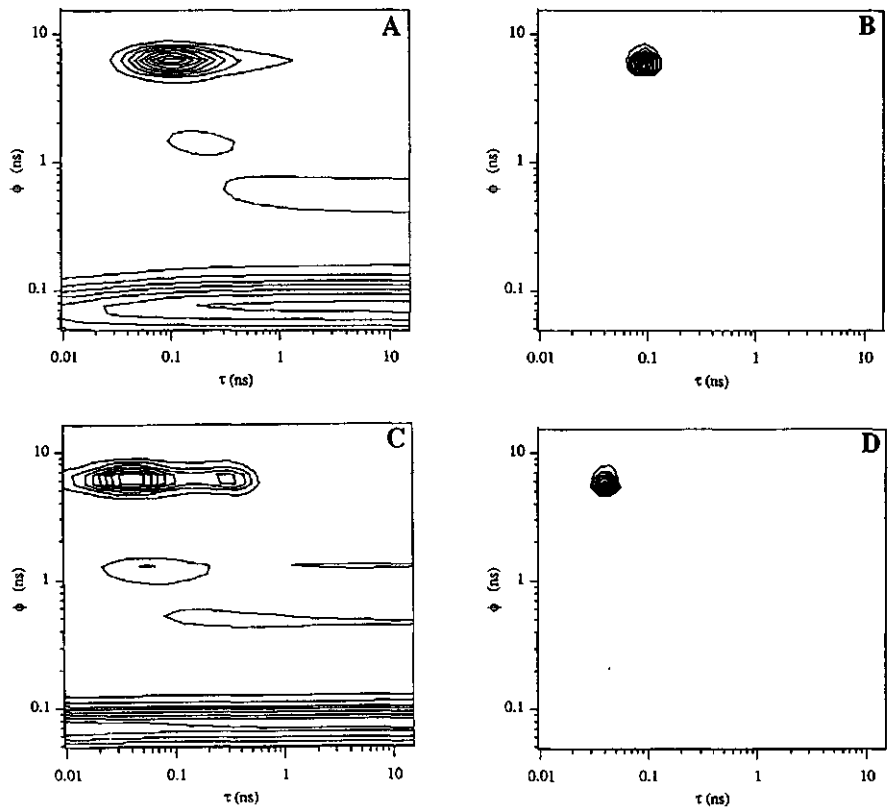

Figure 8. *Contour plots of the associative analysis of the fluorescence and fluorescence anisotropy decays of clostridial flavodoxin at different temperatures, 4 °C and 20 °C* (see text for details). The initial anisotropy was fixed at 0.35 during the analyses. The results for FMN in solution are also given. **A**, flavodoxin at 4 °C; **B**, FMN at 4 °C; **C**, flavodoxin at 20 °C; **D**, FMN at 20 °C.

The origin of this correlation can be ascribed to a flavin moiety which is flexibly bound to the protein in such a way that the electronic structure of the flavin chromophore is not influenced and therefore no effect on the fluorescence characteristics of the chrompohore is detected. The rotational correlation time is larger than for free FMN because the motion of the isoalloxazine ring system is somewhat hindered by the protein environment. A possible explanation is that binding of this moiety occurs via the phosphate group of the FMN. Since earlier

studies (Barman and Tollin, 1972) demonstrated that the presence of the phosphate group is indispensable for FMN binding to the protein matrix, it might therefore be that the correlation found between the 4.8 ns fluorescence lifetime and the 1 ns rotational correlation time originates from an intermediate step in the binding process. The correlations found in flavodoxin associated with lifetimes between 0.1 ns and 1.5 ns may originate from iso-κ solutions ($1/\kappa = 1/\tau_1 + 1/\phi_2 = 1/\tau_2 + 1/\phi_1$).

Conclusions

In the fluorescence decay of *clostridial* flavodoxin a trimodal lifetime distribution is demonstrated. The shortest component of about 30 ps originates from the interaction between flavin and the closely located tryptophan residue (Trp90). The fluorescence lifetime component of about 4.8 ns, present in the flavodoxin decay, coincides with the only distribution present in the fluorescence decay of free FMN. A third lifetime component is distributed at about 0.5 ns. The presence of tens of picosecond fluorescence lifetimes in flavodoxins with heavily quenched flavin fluorescence ('nonfluorescent flavoproteins') seems to be a general property.

The relative contribution of the fluorescence lifetimes is clearly temperature-dependent, in agreement with the existing equilibrium between protein-bound and dissociated flavin. From these experiments the dissociation constant could be determined, $K_D = 2.61*10^{-10}$ M^{-1} (at 20 °C). A titration study, in which *clostridial* apoflavodoxin was added to the protein sample, resulted in a significant change in the distribution of fluorescence lifetimes, reflecting the shifted equilibrium between protein-bound and dissociated FMN. Addition of an excess of apoflavodoxin did not result in complete loss of the 4.8 ns fluorescence component.

Collisional fluorescence quenching experiments with flavodoxin samples that did not contain added apoflavodoxin, showed that the 4.8 ns fluorescence component is affected significantly by iodide. This indicates that a population of flavin molecules, responsible for the 4.8 ns fluorescence lifetime, is accessible to iodide.

The fluorescence anisotropy decays were also analyzed in an associative way, and it was found that in free FMN one single distribution of rotational correlation times is present, whereas in flavodoxin the anisotropy decay is composed of more than one distribution. In flavodoxin it was demonstrated that

part of the 4.8 ns fluorescence lifetime is specifically coupled to the rotational correlation time of free (dissociated) FMN, but another part of this lifetime is coupled to a longer correlation time (about 1.2 ns). This component is assigned to the intermediate state in which the flavin is flexibly bound. This is in agreement with earlier studies (Barman and Tollin, 1972) which showed that binding of free FMN to the apoflavodoxin occurs via a two-step mechanism. In the first binding step the phosphate group is involved which then triggers a conformational change of the protein. At 4 °C the shortest fluorescence lifetime seems to be coupled with a rotational correlation time corresponding to the whole protein meaning that the flavin moiety responsible for the short lifetime is immobilized within the protein matrix.

The different conformational substates probably play a role in the electron transfer process. However, time-resolved polarized fluorescence studies in which the flavodoxin is bound to natural donor and acceptor redox partner proteins have to be performed to demonstrate the exact role of the fluctuations as found in this study.

Acknowledgements

The authors would like to thank dr. Ph. Bastiaens for valuable discussions and reading the manuscript.

References

Barman, B. G. & Tollin, G. (1972) *Biochemistry 11*, 4746-4754.

Bastiaens, P. I. H., van Hoek, A., van Berkel, W. J. H., de Kok, A. & Visser, A. J. W. G. (1992a) *Biochemistry 31*, 7061-7068.

Bastiaens, P. I. H., van Hoek, A., Benen, J. A. E, Brochon, J.-C. & Visser, A. J. W. G. (1992b) *Biophys. J. 63*, 839-853.

Bastiaens, P. I. H., van Hoek, A., Wolkers, W. F., Brochon, J.-C. & Visser, A. J. W. G. (1992c) Biochemistry 31, 7050-7060.

Bastiaens, P. I. H., van Hoek, A., Brochon, J.-C. & Visser, A. J. W. G. (1992d) in *Proc. S.P.I.E. -Int. Soc. Opt. Eng*, Vol. 1640, pp. 138-147..

Beechem, J. M. & Brand, L. (1985) *Ann. Rev. Biochem. 54*, 43-71.

Benemann, J. R., Yoch, D. C., Valentine, R. C. & Arnon, D. I. (1969) *Proc. Nat. Acad. Sci. U.S. 64*, 1079-1086.

Burnett, R. M., Darling, G. D., Kendall, D. S., LeQuesne, M. E., Mayhew, S. G., Smith, W. W. & Ludwig, M. L. (1974) *J. Biol. Chem. 249*, 4383-4392.

Cundall, R. B. & Dale, R. E. (Eds.) (1983) *Time-resolved fluorescence spectroscopy in biochemistry and biology*, NATO ASI series, Ser. A: Life Sciences, Vol. 69, Plenum Press, New York.

Farnum, M. F., Magde, D., Howell, E. E., Hirai, J. T., Warren, M. S., Grimsley, J. K. & Kraut, J. (1991) *Biochemistry 30*, 11567-11579.

Föry, W., MacKenzie, R. E., Wu, F. Y.-H. & McCormick, D. B. (1970) *Biochemistry 9*, 515-525.

Hansen, L. K., Christoph, G. W., Hofrichter, J. & Ludwig, M. L. (1991) in *Flavins and Flavoproteins*, (Curti, B., Ronchi, S. & Zanetti, G., Eds.), pp. 405-408, Walter de Gruyter, Berlin.

Hatchikian, E. C., LeGall, J., Bruschi, M. & Dubourdieu, M. (1972) *Biochim. Biophys. Acta 258*, 701-708.

Irie, K., Kobayashi, K., Kobayashi, M. & Ishimoto, M. (1973) *J. Biochem. 73*, 353-366.

Jablonski, A. (1965) *Acta Phys. Polonica 28*, 717-725.

Jaynes, E. T. (1983) *Papers on Probability, Statistics and Statistical Physics*, (Reidel, D., Ed.), Dordrecht, The Netherlands.

Johnson, P. G. & McCormick, D. B. (1973) *Biochemistry 12*, 3359-3364.

Karplus, M. & McCammon, J.A. (1983) *Ann. Rev. Biochem. 53*, 263-300.

Knight, E., Jr. & Hardy, R. W. F. (1966) *J. Biol. Chem. 241*, 2752-2756.

Kraut, J. (1988) *Science 242*, 534-560.

Lakowicz, J. R. (1983) *Principles of fluorescence spectroscopy*, Plenum Press, New York.

Leenders, R., Bastiaens, Ph., Lunsche, R., van Hoek, A. & Visser, A. J. W. G. (1990) *Chem. Phys. Lett. 165*, 315-322.

Leenders, R. & Visser, A. J. W. G. (1991) in *Flavins and Flavoproteins* (Curti, B., Ronchi, S. & Zanetti, G., Eds.), pp. 393-398, Walter de Gruyter, Berlin.

Leenders, R., Kooijman, M., van Hoek, A., Veeger, C. & Visser, A. J. W. G. (1993) *Eur. J. Biochem. 211*, 37-45.

Lehrer, S. S. (1971) *Biochemistry 10*, 3254-3263.

Livesey, A. K., Licinio, P. & Delaye, M. (1986) *J. Chem. Phys. 84*, 5102-5107.

Livesey, A. K. & Brochon, J. C. (1987) *Biophys. J. 52*, 693-706.

Ludwig, M. L., Pattridge, K. A., Smith, W. W., Jensen, L. H. & Watenpaugh, K. D. (1982) in *Flavins and Flavoproteins* (Massey, V. & Williams, C. H., Eds.), pp. 19-28, Elsevier/North-Holland, Amsterdam.

MacKenzie, R. E., Föry, W. & McCormick, D. B. (1969) *Biochemistry 8*, 1839-1844.

Mayhew, S. G. (1971) *Biochim. Biophys. Acta 235*, 289-302.

Mayhew, S. G. & Ludwig, M. L. (1975) in *The Enzymes*, Vol. XII, (Boyer, P. D., Ed.), pp. 57-118, Academic Press, New York.

Mérola, F., Rigler, R., Holmgren, A. & Brochon, J. C. (1989) *Biochemistry 28*, 3383-3398.

Pueyo, J. J., Walker, M. C., Tollin, G. & Gómez-Moreno, C. (1991) in *Flavins and Flavoproteins*, (Curti, B., Ronchi, S. & Zanetti, G., Eds.), pp. 483-486, Walter de Gruyter, Berlin.

Rigler, R. & Ehrenberg, M. (1973) *Q. Rev. Biophys. 6*, 139-199.

Rigler, R. & Ehrenberg, M. (1976) *Q. Rev. Biophys. 9*, 1-19.

Smith, W. W., Burnett, R. M., Darling, G. D. & Ludwig, M. L. (1977) *J. Mol. Biol. 117*, 195-225.

van Lin, B. & Bothe, H. (1972) *Arch. Mikrobiol. 82*, 155-172.

van Hoek, A., Vervoort, J. & Visser, A. J. W. G. (1983) *J. Biochem. Biophys. Methods 7*, 243-254.

van Hoek, A. & Visser, A. J. W. G. (1985) *Anal. Instrum. 14*, 359-372.

van Hoek, A., Vos, K. & Visser, A. J. W. G. (1987) *IEEE J. Quantum Electron. QE-23*, 1812-1820.

van Hoek, A. & Visser, A. J. W. G. (1992) in *Time-resolved Laser Spectroscopy in Biochemistry, vol. 1640* (Lakowicz, J. R., Ed.), pp. 325-329, Proceedings of SPIE-The International Society for Optical Engineering, Bellingham, WA.

van Mierlo, C. P. M., Lijnzaad, Ph., Vervoort, J., Müller, F., Berendsen, H. J. C. & de Vlieg, J. (1990a) *Eur. J. Biochem. 194*, 185-198.

van Mierlo, C. P. M., van der Sanden, B. P. J., van Woensel, P., Müller, F. & Vervoort, J. (1990b) *Eur. J. Biochem. 194*, 199-216.

Vetter, H., Jr. & Knappe, J. (1971) *Hoppe-Seyler's Z. Physiol. Chem. 352*, 433-446.

Visser, A. J. W. G., Penners, N. H. G. & Müller, F. (1983) in *Mobility and recognition in cell biology*, (Sund, H & Veeger, C., Eds.), pp. 137-152, Walter de Gruyter, Berlin.

Visser, A. J. W. G., Ykema, T., van Hoek, A., O'Kane, D. J. & Lee, J. (1985) *Biochemistry 24*, 1489-1496.

Vos, K., van Hoek, A. & Visser, A. J. W. G. (1987) *Eur. J. Biochem. 165*, 55-63.

Wassink, J. H. & Mayhew, S. G. (1975) *Anal. Biochem. 68*, 609-616.

Chapter 4

Molecular dynamics simulations of oxidized and reduced *Clostridium beijerinckii* flavodoxin

Rik Leenders, Wilfred F. van Gunsteren, Herman J. C. Berendsen, and Antonie J. W. G. Visser

submitted to: *Biochemistry*

Abstract

Molecular dynamics simulations of oxidized and reduced *Clostridium beijerinckii* flavodoxin in water have been performed in a sphere of 1.4 nm radius surrounded by a restrained shell of 0.8 nm. The flavin binding site, comprising the active site of the flavodoxin, was in the center of the sphere. No explicit information about protein-bound water molecules was included. An analysis is made of the motional characteristics of residues located in the active site. Positional fluctuations, hydrogen bonding patterns, dihedral angle transitions, solvent behaviour, and time-dependent correlations are examined. The 375-ps trajectories show that both oxidized and reduced protein-bound flavins are immobilized within the protein matrix, in agreement with earlier obtained time-resolved fluorescence anisotropy data. The calculated time-correlated behaviour of the tryptophan residues reveals significant picosecond mobility of the tryptophan sidechain located close to the reduced isoalloxazine part of the flavin.

Introduction

Flavodoxins are small bacterial flavoproteins which function as low-potential electron-transfer proteins. Depending on the oxidation state of the flavin, flavodoxins can exist in different conformations (Mayhew & Ludwig, 1975; Watt et al., 1991). The nature of these conformational changes is difficult to derive from the crystal structure alone. Therefore, information on the dynamics of flavodoxin in its different oxidation states is required. The motional characteristics of FMN in the protein matrix of oxidized and reduced *Clostridium beijerinckii* flavodoxin have been studied earlier using time-resolved fluorescence anisotropy measurements (Leenders & Visser, 1991,1992; Leenders et al., 1993).

The protein-bound flavin, comprising the active site of the flavodoxin, can exist in three different oxidation states of which the oxidized and fully reduced state have been shown to be fluorescent (Visser et al., 1987; Visser, 1989; Leenders & Visser, 1991,1992; Leenders et al., 1993). An additional advantage for using the flavin chromophore is the fact that flavodoxin contains only one flavin residue per protein molecule, which may simplify the interpretation of experimentally obtained time-resolved fluorescence anisotropy data.

Computer simulations of macromolecular dynamics have been performed now for over 15 years. Early molecular dynamics simulations of proteins were performed in vacuo, in the absence of solvent molecules (McCammon et al., 1977; Northrup et al., 1980; Levitt, 1980; Ichiye and Karplus, 1983; Levy, 1985; Åqvist et al., 1985, 1986; Henry and Hochstrasser, 1987). These vacuum simulations describe motional features of buried residues rather well (van Gunsteren and Karplus, 1982a; Harris and Hudson, 1991), but the dynamics of residues located near the protein surface are distorted by the vacuum effect (Axelsen et al., 1988; Chen et al., 1988; MacKerell et al., 1988). Inclusion of solvent molecules in the simulations improves the behaviour of the latter residues resulting in realistic low-frequency collective motion of parts of the protein located at the periphery of the protein.

The results obtained with molecular dynamics (MD) simulations can be validated with different experimental studies and vice versa. The relation between these calculations and experiments can be illustrated with some examples. First, 2-dimensional nuclear magnetic resonance (NMR) measurements in combination with molecular dynamics simulations have been shown to be of great help in obtaining information about unresolved molecular structures (de Vlieg et al., 1986; van Mierlo et al., 1990a,b). The structure of the retinol binding apoprotein was determined in this way by using the related structure of the holoenzyme as a starting structure in the simulations (Åqvist et al., 1986). Secondly, Ichiye and Karplus (1983) showed that the fluorescence depolarization on the picosecond time scale of tryptophan residues of lysozyme could be calculated using the results of a molecular dynamics simulation. Because the resolution of the time-resolved fluorescence anisotropy experiments is limited to the picosecond time scale, only the effective zero-time anisotropies and/or fast decaying anisotropies with decay times in the picosecond range can be compared with the calculated values. Fluorescence anisotropy measurements can be related to the time correlation function, which describes the angular displacement of the emission transition dipole moment (Ichiye & Karplus, 1983). Comparison of MD calculations and fluorescence anisotropy decay measurements is normally limited to a few protein residues (e.g., tryptophans and tyrosines), but in case of flavodoxin an additional chromophoric group, the isoalloxazine ring system of the flavin, can be used.

In this study we have performed molecular dynamics simulations of the active sites of oxidized and reduced flavodoxin in a solvent environment. The calculated characteristics of both oxidation states are compared with each other

as well as with those obtained with time-resolved fluorescence measurements (Leenders & Visser, 1991,1992; Leenders et al., 1993).

Computational procedure

Molecular dynamics (MD) simulations were carried out using the GROMOS package (van Gunsteren and Berendsen, 1987) on the Cray Y-MP4/464 computer at SARA Scientific Computing Services Amsterdam. The GROMOS force field involves terms for bond stretching, bond-angle bending, dihedral angle bending and improper dihedral angle bending interactions, and non-bonded terms describing the Van der Waals' and electrostatic interactions. No explicit hydrogen-bonding term was included since this interaction is accounted for by the non-bonded interactions (Reiher, 1985), but the van der Waals' repulsion properties of polar atoms were increased as compared to the normal repulsion parameters (Hermans et al., 1984). MD simulations of both oxidized and reduced flavodoxin were performed in order to obtain a more detailed insight in the role of flexibility of the active site of flavodoxins in case of a redox change. The X-ray coordinates for oxidized and semiquinone *clostridial* flavodoxin have been determined with 0.19 nm and 0.18 nm resolution, respectively (Burnett et al., 1974; Smith et al., 1977). Comparison of the diffraction patterns from crystals of the semiquinone and fully reduced flavodoxin (Ludwig et al., 1971), 1D-NMR studies (James et al., 1973), and 2D-NMR studies (Leenders et al., unpublished data) showed that the tertiary structure of fully reduced *clostridial* flavodoxin is nearly identical to that of the semiquinone form. The coordinates of the two resolved crystal structures were used as starting conformations, where in reduced flavodoxin flavin atom N(1) was kept unhydrogenated in agreement with nuclear magnetic resonance studies (Vervoort et al., 1986). For oxidized flavin the standard GROMOS force field has been used. For reduced flavin the standard force field parameters were modified slightly, partioning the resulting negative charge over the flavin atoms N(1) and O(2) (see Figure 1). The partial charges used for atoms N(1), C(2), and O(2), were -0.635 q, +0.27 q and -0.635 q, respectively.

Molecular topologies for oxidized and reduced flavodoxin were generated using the GROMOS residue topologies of RT37C and interaction function parameters of IFP37C4. In the GROMOS force field hydrogens attached to non-polar carbon atoms are incorporated in the latter forming united atoms,

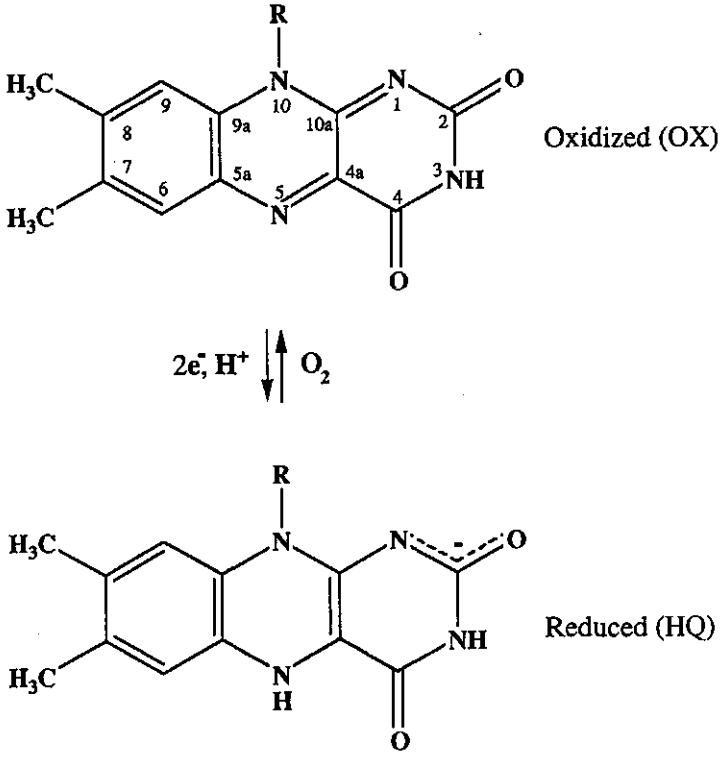

Figure 1. *The molecular structure of oxidized and two-electron-reduced flavin mononucleotide (FMN).* The molecule is composed of a isoalloxazine ring system and a ribityl sidechain, *R* (-CH_2-$(C(OH)H)_3$-CH_2-O-phosphate). Upon reduction the protein-bound flavin atom N(1) remains unhydrogenated; the resulting negative charge is delocalized (see text).

which reduces the required computer time significantly. Only the hydrogens able to form hydrogen bonds were included explicitly. Each flavodoxin was placed in a rectangular box filled with equilibrated simple point charge (SPC) water molecules (Berendsen et al., 1981). All solvent molecules which were positioned less than 0.23 nm from a flavodoxin atom were deleted. The best way to minimize edge effects caused by the vacuum is to use periodic boundary conditions, but because these simulations are still very computer intensive, only a solvent-sphere surrounding the active site has been simulated. The edge effects are then minimized by harmonically restraining the positions of the atoms in the outer shell of the protein-solvent system, whereas the atoms in the inner sphere

are simulated without any positional restraints. In case of the simulations performed in this study an inner sphere of 1.4 nm surrounding the centre of the flavin chromophore was simulated without any positional restraint, whereas a shell of 0.8 nm (the atoms located between 1.4 nm and 2.2 nm from the flavin) was position-restrained to confine the shell-atoms to the simulation region (see Figure 2). The force constant used for position-restraining was 10 $kcal.mmol^{-1}.Å^{-2}$. All residues which were partly located within the 1.4 nm sphere were totally included in the freely simulated region. Residues which are part of the α-helix directed towards the negatively charged flavin phosphate are included in the simulation because of their supposed stabilizing effect (Hol et al., 1978). The radius of the inner sphere was chosen large enough to include the three tryptophan residues located close to the flavin, enabling a comparison of the simulated tryptophan behaviour with experimental results (Leenders et al., to be published). The simulated systems consisted of 1034 protein (united) atoms with 1108 solvent molecules for the oxidized flavodoxin, and of 1027 protein atoms with 1090 solvent molecules for the reduced flavodoxin. For obtaining low-energy conformations, without local strain, the energy of the two systems was minimized for 100 steepest descent and 50 conjugate gradients steps. During energy minimization the solvent molecules located in the inner sphere were allowed to move freely, while the flavodoxin conformation was position restrained. The procedure was then repeated with the solvent molecules position-restrained and the flavodoxin atoms free. After this energy minimization no extra water molecules could be positioned indicating that a proper water density was achieved. The MD simulations were started by randomly assigning velocities (from a Maxwellian distribution) to the atoms yielding an overall kinetic energy corresponding to 300 K. Any residual transitional motion of and rotational motion about the center of mass was removed from the initial velocities to simplify analysis of the subsequent conformational fluctuations. The leap frog algorithm (Hockney and Eastwood, 1981) was used for integrating the equations of motion in cartesian coordinates. The SHAKE algorithm (Ryckaert et al., 1977; van Gunsteren & Karplus, 1982b) was used to constrain all covalent bonds allowing an integration time step of 2 fs. During the simulation the systems were coupled to an external bath with constant temperature (Berendsen et al., 1984), with temperature relaxation times of 0.1 ps. The systems were equilibrated until the total potential energy as well as the root mean square (rms) difference between the simulated structure and the initial X-ray positions remained constant. After these time points the coordinates, velocities, and energies were recorded every 25 steps (0.05 ps) until 375-ps trajectories were completed.

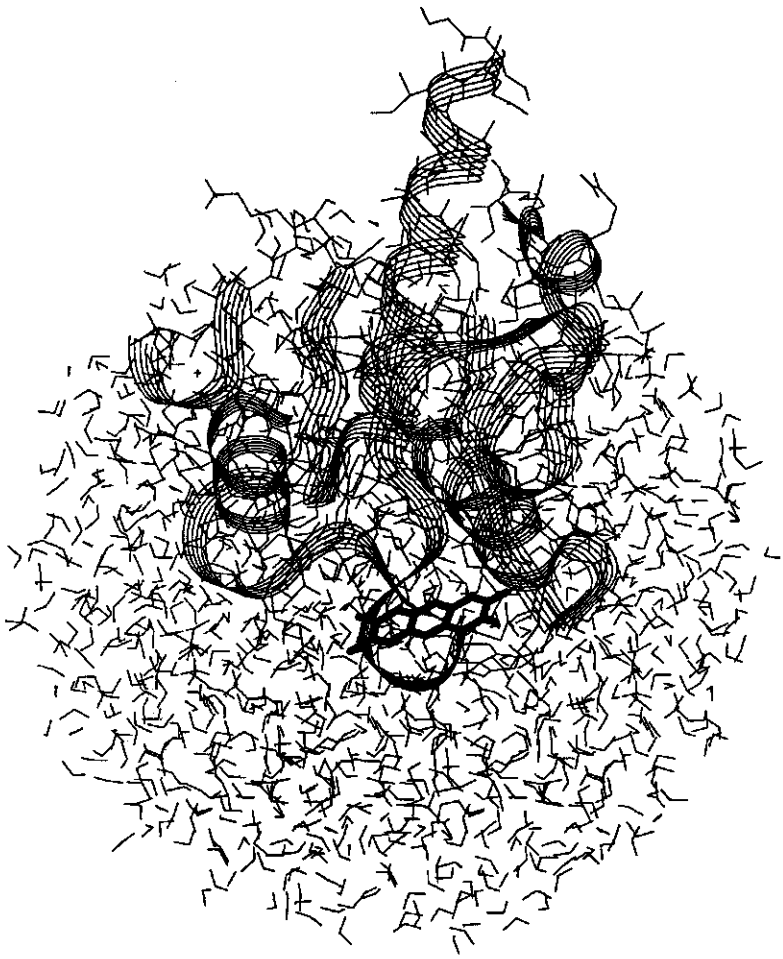

Figure 2. *Schematic representation of a simulated system.* The flavin isoalloxazine ring system is surrounded by a 2.2 nm sphere containing protein atoms and solvent molecules. The protein backbone is presented by a ribbon structure.

Before analysis of the successive protein structures in the trajectories, a least-squares fit was performed on the positions of the C(α) atoms. In the analyses only the freely simulated inner sphere of 1.4 nm is considered to avoid disturbing effects resulting from the applied position restraints or from the vacuum outside the simulated 2.2 nm sphere.

Results and Discussion

Structure comparison and dynamics

Energy-minimization of the oxidized and reduced flavodoxins had reduced the potential energy to about $-3.3*10^4$ kJ/mol. The molecular dynamics simulations were started and the total potential energy as well as the root mean square deviation between initial X-ray and MD-structure were monitored (van Gunsteren and Mark, 1992). The oxidized flavodoxin equilibrated within 60 ps, whereas the reduced flavodoxin reached equilibrium somewhat earlier (after 50 ps). The root mean square (rms) positional fluctuations, ΔR, were calculated according to:

$$\Delta R = \left[\frac{1}{N_{at}} \sum_{i=1}^{N_{at}} <\{(\Delta x_i)^2 + (\Delta y_i)^2 + (\Delta z_i)^2\}>\right]^{1/2} \qquad (1)$$

where Δx_i, Δy_i, and Δz_i are the differences between the instantaneous and averaged atomic coordinates for the i-th atom, the brackets (<...>) represent a time average, and the summation is over backbone and sidechain atoms of the individual solute residues surrounding the center of the isoalloxazine ring system (inner 1.4 nm sphere). The backbone rms fluctuation, ΔR_B, averaged over C, O, C(α), and N atoms of the 51 residues located in the freely simulated inner sphere, was almost identical for oxidized and reduced flavodoxin (ΔR_B is 0.037 and 0.041 nm, respectively), indicating quite rigid overall structures in both oxidation states (see Figure 3A and 3C). This is in accordance with earlier results obtained with several spectroscopic techniques. From crystallographic studies (Burnett et al., 1974; Smith et al., 1977) it is known that *clostridial* flavodoxin has a compact structure with a central anti-parallel β-sheet embedded by four α-helices. Furthermore, two-dimensional NMR studies of the *clostridial* flavodoxin (Leenders et al., unpublished data) and the closely related *Megasphaera elsdenii* flavodoxin (van Mierlo et al., 1990a,b) showed that these flavodoxins have compact structures without great fluctuations. The average rms fluctuation of the amino acid sidechain atoms, ΔR_S, is somewhat larger than for the backbone atoms (Figures 3A and 3C). For oxidized and reduced flavodoxin, ΔR_S was 0.058 nm and 0.073 nm, respectively. The absence of sterically hindering bulky sidechains in the glycines adjacent to residue Trp90 combined with the fact that this tryptophan residue is located at the periphery of the protein result in large fluctuations of the tryptophan indole group in both

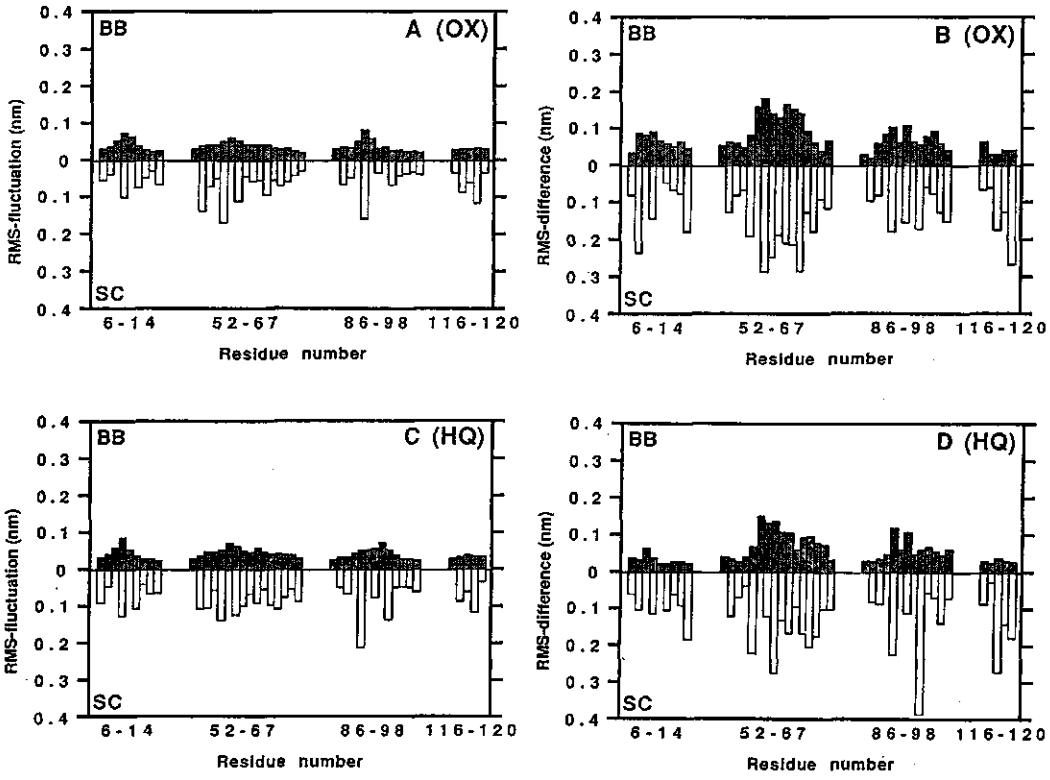

Figure 3. *Rms fluctuations and differences for oxidized and reduced flavodoxin.* **A**, rms fluctuations of oxidized flavodoxin (OX); **B**, rms difference between time-averaged and X-ray structure for OX; **C**, rms fluctuation of reduced flavodoxin (HQ); **D**, rms difference between time-averaged and X-ray structure for HQ. The values for backbone (BB) and sidechain (SC) atoms are drawn with filled and open bars, respectively. Only the amino acids are presented of which both neighbours were simulated without any positional restraints.

oxidation states (Figures 3A and 3C). This flexibility is examined in more detail in the section about tryptophan motional characteristics.

The rms fluctuation of oxidized and reduced flavin is 0.079 nm and 0.065 nm, respectively, and indicates that the flexibility of the protein-bound flavin is comparable to fluctuations of the backbone and sidechain atoms of amino acid residues located in the vicinity of the chromophore. The magnitude of the flavin fluctuations does not appear to be influenced by less mobile amino acids that are

part of α-helices and/or β-sheet. The rms fluctuations are distributed rather uniformly over the isoalloxazine ring system and ribityl sidechain of both oxidized and reduced flavin. The only significant difference is found within the flavin phosphate group in the oxidized flavodoxin, which has higher rms fluctuations than the rest of the flavin. This behaviour will be discussed later in some detail.

It is interesting to examine if any correlation exists between the motional freedom of the flavin chromophore and the amino acids surrounding it. Therefore, atomic fluctuation cross-correlations were calculated using:

$$C(F,a) = \frac{< \Delta R_F \,.\, \Delta R_a >}{< (\Delta R_F)^2 >^{1/2} \,.\, < (\Delta R_a)^2 >^{1/2}} \qquad (2)$$

where ΔR_F and ΔR_a is the (atomic) displacement from the mean position of the atoms of the flavin mononucleotide and amino acid residue, respectively. For both simulations three parts of the protein are found that show atomic fluctuations which are (positively) correlated with the flavin fluctuations (see Table 1); these regions are bounded by residues 7 to 9, 54 to 60, and 87 to 89. The first region is part of the phosphate binding site, and the other residues are part of the isoalloxazine binding site. The correlations, which are found to propagate to approximately 1.1 nm in both oxidized and reduced flavodoxin, are always somewhat higher in reduced protein (see Table 1), except for residue Trp90. From the crystallographically obtained three-dimensional flavodoxin structures the sidechain of residue Trp90 seems to be stacked to the isoalloxazine part of the flavin. However, from the simulation of oxidized and reduced flavodoxin there is no sign of correlated motion of the two ring systems.

For oxidized and reduced flavodoxin the rms differences between the X-ray structure and the averaged MD structure are obtained using:

$$\Delta r = \left[\frac{1}{N_{at}} \sum_{i=1}^{N_{at}} (r_i^X - \langle r_i \rangle^{MD})^2\right]^{1/2} \qquad (3)$$

where r_i^X and $\langle r_i \rangle^{MD}$ are the atomic position of atom i in the crystal structure and in the averaged MD structure, respectively, and the summation is over all atoms

Table 1. *Equal-time cross-correlations of the flavin chromophore positional fluctuationswith those of amino acid residues in the oxidized and reduced flavodoxin.* The average distance, R_{av}, between amino acid and flavin chromophore calculated from both oxidation states is indicated.

Residue	C_{OX}	C_{HQ}	R_{av} (nm)	Residue	C_{OX}	C_{HQ}	R_{av} (nm)
Trp6	0.05	0.13	1.02	Gly86	0.08	0.07	1.02
Ser7	0.09	0.33	1.07	Ser87	0.10	0.26	0.67
Gly8	0.15	0.31	0.85	Tyr88	0.18	0.26	0.80
Thr9	0.10	0.30	0.86	Gly89	0.32	0.48	0.55
Gly10	0.15	0.13	1.02	Trp90	0.16	0.06	0.67
Asn11	0.29	0.11	0.87	Gly91	0.17	0.21	0.89
Thr12	0.10	0.21	0.92	Asp92	0.08	0.05	1.20
Glu13	0.09	0.17	1.31	Gly93	0.04	0.05	1.13
				Lys94	0.07	0.19	1.38
Gly52	0.06	0.07	1.30	Trp95	0.06	0.18	0.92
Cys53	0.00	0.04	0.94	Met96	0.04	0.10	1.26
Ser54	0.20	0.28	0.56				
Ala55	0.32	0.38	0.41	Val117	0.12	0.12	1.07
Met56	0.17	0.30	0.58	Gln118	0.18	0.24	0.97
Gly57	0.29	0.50	0.77	Asn119	0.14	0.19	0.73
Asp58	0.23	0.43	0.97	Glu120	0.05	0.14	1.10
Glu59	0.25	0.43	0.90				
Val60	0.20	0.27	0.96				
Leu61	0.08	0.08	1.14				

located in the 1.4 nm inner sphere. Figures 3B and 3D show that the averaged MD structures of both oxidized and reduced flavodoxin have a high resemblence with their starting X-ray structures. The average rms differences of the backbone atoms, Δr_B, are 0.072 nm and 0.056 nm for oxidized and reduced flavodoxin, respectively. However, in both oxidation states the backbone of loop 57-63 has significantly higher average rms differences (Δr_B of about 0.15 nm) suggesting that this part of the protein has a solution structure which is different from the crystal structure. This difference is even larger for the sidechains of these residues (Δr_S's more than 0.2 nm).

The average rms difference of the protein-bound flavin, Δr_F, is 0.104 nm and 0.145 nm for the oxidized and reduced flavin. Inspection of Figure 4 shows that in the average simulated structures the oxidized flavin isoalloxazine ring system is translated and the reduced flavin ring system is somewhat rotated as compared to the initial X-ray structures. These findings were confirmed by comparison of the structures on a graphical display system. This slight rotation (of about 11°) could be a result of the choice of the charge partitioning on flavin

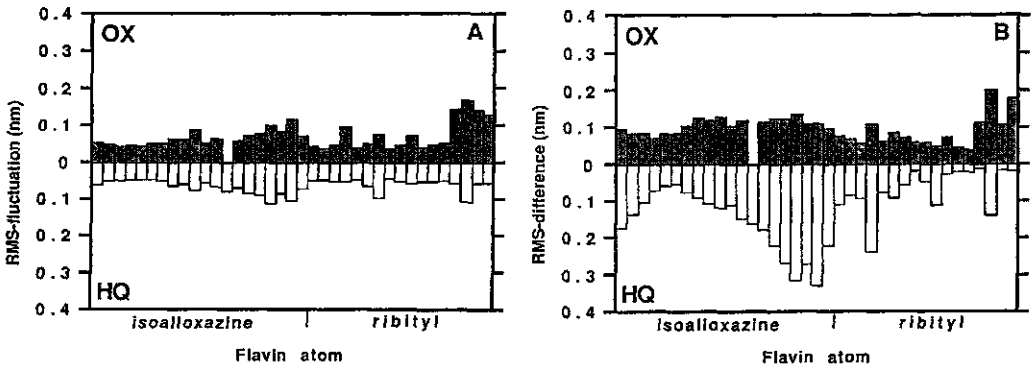

Figure 4. *Rms fluctuations (A) and differences (B) of the oxidized and reduced protein-bound flavin (OX and HQ, respectively).* Atom numbering is clockwise (see Figure 1). The isoalloxazine atom sequence is C(9a), N(10), C(10a), N(1), C(2), O(2), etc. The reduced flavin contains one extra hydrogen (at position N(5)). The solvent accessible side of the reduced flavin ring system (the dimethyl ring) is somewhat shifted as compared to the position in the initial crystal structure.

atoms N(1) and O(2). However, since the apoprotein-to-flavin distances in the averaged MD structures are comparable to the distances in the solution structure of the related *M. elsdenii* flavodoxin (van Mierlo et al., 1990a), it is more likely that the flavin in the reduced flavodoxin has a solution structure which is slightly different from the initial X-ray structure. This could mean that the semiquinone and fully reduced flavodoxin have somewhat different active site conformations.

Comparison of the averaged MD structure of oxidized flavodoxin with that of fully reduced flavodoxin (data not shown) yields a backbone rms difference of 0.063 nm indicating that the overall structure of flavodoxin is more or less independent of its oxidation state (the backbone rms difference between the initial X-ray structures is 0.028 nm). The backbone atoms in specific regions have rms differences up to 2.0 nm (residues 56 to 64 and residues 90 and 91). The former difference is explained by the fact that in the reduced state the carbonyl of residue Gly57 is rotated towards the flavin as was demonstrated for the semiquinone state (Smith et al., 1977). This rotation is compensated by movement of backbone atoms located near residue Gly57. The latter difference

is mainly the result of a change in backbone conformation near residue Trp90 in the simulated reduced flavodoxin.

The flavin rms difference between the averaged oxidized and reduced MD structures is 0.107 nm, which is of the order of the flavin rms difference between the initial crystal structures (0.073 nm). This means that the flavin as well as residues surrounding it occupy comparable positions in oxidized and reduced flavodoxin. The active site structure and dynamics of the flavodoxin in the oxidized and reduced state is examined in terms of hydrogen bonding patterns, dihedral angle transitions, solvent behaviour, and flavin and tryptophan motional characteristics.

Table 2. *Average backbone dihedral angles of oxidized (OX) and reduced (HQ) flavodoxin with their corresponding rms fluctuations.* The fluctuations were calculated similar to Eq. 1.

	OX		HQ	
dihedral angle	aver.	rms.	aver.	rms.
ω (C(α)-C-N-C(α))	177.9	5.4	178.6	5.5
ϕ (C-N-C(α)-C)	-79.8	9.6	-83.2	9.8
ψ (N-C(α)-C-N)	24.5	10.5	31.1	9.5

Dihedral angles

All active site dihedral angles (including the flavin dihedrals) of oxidized and reduced flavodoxin were monitored. As found earlier the solvent has a damping effect on the dihedral angle motion (van Gunsteren and Karplus, 1982a). The average backbone dihedral angles with their corresponding rms fluctuations are listed in Table 2. It is obvious that the backbone dihedrals show relatively small fluctuations, dihedral angle ω in particular. Attention was focussed on dihedral angle transitions in order to locate regions with higher backbone flexibility. To define a transition, the dihedral angle has to cross the minimum between two adjacent dihedral potential wells. Furthermore, this transition should have a long enough lifetime. Since dihedral angle transitions occur typically in about 1 ps, an arbitrary choice for the minimum transition

lifetime should at least be 2 ps. With this strict definition only a few backbone dihedral angle transitions occurred during the 375-ps trajectories.

In the oxidized flavodoxin 10 backbone dihedral angle transitions occurred involving dihedrals ψ9 (backbone dihedral angle ψ of residu Thr9), ϕ10, ψ90, ϕ91, whereas in the reduced flavodoxin only 2 short-lived transitions occurred which involved dihedrals ψ9 and ϕ10. This is in accordance with the relatively high backbone rms fluctuations around these residues and results in different average backbone dihedral angles in these regions in oxidized and reduced flavodoxin. For example, dihedral angle ψ10 in oxidized flavodoxin has an average value of 40.8°, whereas in reduced flavodoxin this dihedral is 5.2° (the rms fluctuations in this dihedral angle were similar in both oxidation states: 23.5° and 17.8°, respectively). Another significant difference is found at backbone dihedral angles near residue Trp90: ϕ89(OX) is -98.0° ± 17.1° and ϕ89(HQ) is -66.3° ± 16.5° and ψ90(OX) is 9.9° ± 47.9° and ψ90(HQ) is -34.0° ± 15.0°. A similar large fluctuation as in ψ90(OX) was found in the average dihedral angle ϕ91(OX): -105.9° ± 43.4°. The correlation between the fluctuations in dihedral angles ψ90 and ϕ91 was calculated similar to Eq. 2. From the normalized crosscorrelation coefficients, C(OX) is -0.94 and C(HQ) is -0.44, it can be concluded that these dihedral angles have fluctuations which are anticorrelated in both oxidation states, in particular in the oxidized flavodoxin. Another backbone dihedral angle differs considerably between the two simulated oxidation states: ψ57(OX) is 99.9° ± 17.3° and ψ57(HQ) is -114.1° ± 12.8°. This indicates that, although an extra hydrogen bond is formed upon reduction, this does not result in an altered mobility of this backbone dihedral angle of residue Gly57.

The flavin was also monitored for dihedral angle transitions. The only transition that occured was of the ribityl sidechain dihedral angle, C(ε)-O(ζ)-P-O. From this behaviour it could be concluded that the phosphate group in the oxidized flavodoxin is bound more loosely than in the reduced protein, as was already demonstrated by the relatively high rms fluctuations of the atoms in the phosphate group. The dihedral angle switches between roughly two values: -60° and 60°. From the trajectories it can be calculated that in the oxidized state the value of this dihedral angle is -60° for 53% of the time, whereas in reduced flavodoxin this is 94%. This difference is also reflected in the difference in hydrogen bonding of the flavin phosphate with the apoprotein (Asn11); in oxidized flavodoxin this hydrogen bond exists for 50% of the trajectory and in reduced flavodoxin this is 91%.

This shows that in the active site region differences in both conformation and flexibility between the different oxidation states exist.

Table 3. *Selection of hydrogen bonds involving flavin atoms, frequently occurring during the 375-ps simulation of oxidized (OX) and reduced (HQ) flavodoxins.* Occurrences less than 10 % of the simulated time, are indicated (-).

Donor	-	Acceptor	Don	-	H	-	Acc	Occ_{OX}	Occ_{HQ}
Ser7	-	FMN	O(γ)	-	H(γ)	-	OT1	-	99
Gly8	-	FMN	N	-	H	-	OT1	37	10
Gly8	-	FMN	N	-	H	-	OH	-	87
Thr9	-	FMN	N	-	H	-	OH	37	10
Thr9	-	FMN	O(γ1)	-	H(γ1)	-	OT2	28	60
Gly10	-	FMN	N	-	H	-	OT2	42	54
Asn11	-	FMN	N	-	H	-	OT2	50	91
Thr12	-	FMN	N	-	H	-	OT1	16	91
Ser54	-	FMN	O(γ)	-	H(γ)	-	OT1	54	30
Glu59	-	FMN	N	-	H	-	O(4)	72	86
Gly89	-	FMN	N	-	H	-	N(1)	62	53
Gly89	-	FMN	N	-	H	-	O(2)	45	81
Trp90	-	FMN	N	-	H	-	N(1)	-	98
Gly91	-	FMN	N	-	H	-	O(2)	56	99
FMN	-	Ala55	O(β)	-	H(β)	-	O	56	-
FMN	-	Gly57	N(5)	-	H(5)	-	O	-	78
FMN	-	Ser87	O(δ)	-	H(δ)	-	O(γ)	79	91
FMN	-	Asn119	O(γ)	-	H(γ)	-	O(δ1)	15	-

Intramolecular hydrogen bonding

From crystallographic studies of *Cl. beijerinckii* flavodoxin (Burnett et al., 1974; Smith et al., 1977) it is known which parts of the polypeptide chain surround the non-covalently bound flavin chromophore. It is also known that upon reduction of the flavodoxin the carbonyl group of residue Gly57 rotates towards the flavin atoms N(5) and H(5) (Smith et al., 1977). This indicates a role for one or more intramolecular hydrogen bonds influencing the motional behaviour and characteristics of the isoalloxazine ring system in the reduced state. Therefore, the presence of hydrogen bonds during the simulations was investigated by scanning the 375-ps trajectories. The criteria for a hydrogen bond were taken as follows: the distance between hydrogen and acceptor atoms

should be less than 0.25 nm and the angle between donor, hydrogen, and acceptor atoms has to exceed 135°. Hydrogen bonds involving flavin atoms in oxidized and reduced flavodoxin are listed in Table 3. From this Table it is obvious that both oxidized and reduced flavin are bound to the apoprotein by a large number of hydrogen bonds. An average overall number of hydrogen bonds can be calculated: the reduced flavin is bound by 14 H-bonds and the oxidized flavin by 11 H-bonds. The flavin phosphate group, which is surrounded by residues 8-12 and 54, is bound more firmly in the reduced flavodoxin as compared to the oxidized flavodoxin. The reduced flavin pyrimidine ring, surrounded by residues 59 and 89-91, is also bound in a more rigid manner than in oxidized flavodoxin as can be extracted from the hydrogen bonds involving flavin atom O(2) (Table 3).

The stability of the flavodoxin is indicated by the presence of a large number of (equivalent) hydrogen bonds within the oxidized and reduced apoprotein itself (data not shown). A selection of some differences in hydrogen bonding involving nonflavin atoms located in the freely simulated inner sphere is shown in Table 4. The protein structure, judging from analysis of all occurring hydrogen bonds, is nearly identical in the two oxidation states as was found when comparing the averaged atomic positions in both oxidation states.

Table 4. *Selection of hydrogen bonds involving nonflavin atoms which have large differences in occurrence between oxidized* (OX) *and reduced* (HQ) *flavodoxin.*

Donor - Acceptor	Don - H - Acc	Occ_{OX}	Occ_{HQ}
Trp6 - Glu65	N(ε1) - H(ε1) - O(ε1)	43	-
Ser7 - Glu13	O(γ) - H(γ) - O(ε1)	99	-
Glu13 - Ser7	N - H - O(γ)	-	72
Asp92 - Glu59	N - H - O(ε2)	67	-
Asp92 - Glu59	N - H - O(ε1)	59	-
Gly93 - Glu59	N - H - O(ε1)	99	-
Lys94 - Glu59	N - H - O(ε1)	99	-

Solvent behaviour

In the dynamics calculations no information was included about specific protein-bound (crystal) water molecules. All solvent molecules were initially part of the bulk solvent. The solvent molecules located between 1.4 nm and 2.2

nm from the center of the flavin were position-restrained to minimize distortions which are the result of the vacuum beyond the outer sphere. In the oxidized and reduced flavodoxin, 194 and 201 solvent molecules were simulated without any positional restraints (inner sphere). These solvent molecules show rms fluctuations ranging from 0.03 nm to 1.18 nm, indicating that some water molecules are almost immobilized, whereas others exhibit considerable motion. The overall solvent rms fluctuations are similar in both runs (ΔR_{sol} is 0.53 and 0.48 nm for the oxidized and reduced flavodoxin, respectively). The solvent molecules which have the smallest rms fluctuations are possibly bound to the protein, as some water molecules were demonstrated in the crystal structures of oxidized and semiquinone flavodoxin (Burnett et al., 1974; Smith et al., 1977). Therefore, the protein-solvent hydrogen bonding behaviour was calculated from the 375-ps trajectories (we will call these interactions intermolecular).

The trajectories have been scanned for interactions between oxygen atoms in solvent molecules and any polar atom in the flavodoxin. The same criteria as for intramolecular hydrogen bonds were used. In both oxidation states some water molecules are located at close distance from the flavin during the entire run.

In the oxidized flavodoxin 7 water molecules form hydrogen bonds with flavin atoms. During the span of the simulation flavin atom N(3) forms hydrogen bonds with two water molecules which are both involved in other intermolecular hydrogen bonds (with the backbone oxygen of residue Trp90 and with the sidechains of residues Asp58 and Glu59). The two hydrogen bonds between flavin atom N(3) and the two water molecules exist for 16% and 43% of the simulation time. The other five water molecules form hydrogen bonds with oxygen atoms of the ribityl sidechain. In particular, atom O(γ) interacts with three different water molecules, one of which is bridged to the sidechain of residues Asn11 (29%) and Asn119 (28%). In the crystal structure of oxidized flavodoxin this water molecule is called W-2 (Burnett et al., 1974). The hydrogen bond involving the water molecule bridged to residue Asn119 exists for 42% of the simulation time, whereas the other two H-bonds occur 10% of the time. The latter water molecule and two other water molecules form hydrogen bonds with the ribityl phosphate group. One of these water molecules is not only bound to a oxygen atom of the phosphate group (43%) but is also bound to the sidechain of residue Ser7 (65%) and the backbone nitrogens of residues Asn11 and Glu13 (28% and 99% of the time, respectively). This water molecule is called W-1 in the crystal structure of oxidized flavodoxin (Burnett et al., 1974).

In the reduced flavodoxin also 7 water molecules are found to form hydrogen bonds with the flavin chromophore. Contrary to oxidized flavodoxin flavin atom O(2) is involved in a relatively strong hydrogen bond (present for 63% of the time) with a water molecule, which also interacts with the backbone nitrogen of residue Gly93 (19%). This water molecule is called W-3 in the crystal structure of semiquinone flavodoxin (Smith et al., 1977). Ribityl-sidechain atom O(β) forms a hydrogen bond with a water molecule (18%) which is also involved in H-bonds with residues Ser54 (26%) and Ala55 (13%). As in oxidized flavodoxin flavin atom O(γ) forms H-bonds with three water molecules (47%, 18%, and 10%), that are also bridged to the sidechains of residues Asn11 (39%) and Asn119 (36%), and the backbone oxygen of Ala55 (11%). Two of these water molecules were demonstrated to be present in the crystal structure of semiquinone flavodoxin (W-2 and W-4). The flavin phosphate group in reduced flavodoxin is surrounded by three water molecules that form H-bonds for part of the simulation time (35%, 29%, and 21%, respectively). These water molecules also form hydrogen bonds with residues Thr9 (26%), Ser54 (25%), and Ala55 (22%). The water molecule involved in H-bonds with the flavin phosphate group and residue Thr9 is called W-1 in the crystal structure.

In contrast with what might be expected from the crystal structures the protein-bound water molecules are not bound all of the time. Generally, the strongest hydrogen bonds between water molecules and protein atoms exist for 40-50% of the time, but the majority of the protein-solvent hydrogen bonds is present for shorter periods indicating a dynamic active site, in which the noncovalently bound flavin chromophore is stabilized by a combination of interactions between flavin, protein, and solvent atoms.

Flavin and tryptophan motional characteristics

With time-resolved fluorescence depolarization measurements the mobility of chromophores can be determined from the decay of the anisotropy:

$$r(t) = \frac{i_{\parallel}(t) - i_{\perp}(t)}{i_{\parallel}(t) + 2i_{\perp}(t)} \tag{4}$$

where $i_{\parallel}(t)$ and $i_{\perp}(t)$ are the fluorescence intensities polarized parallel and perpendicular with respect to the polarization direction of excitation. The

anisotropy decay, $r(t)$, can be described by the time-correlation function of the reorientation of the emission transition dipole moment (Ichiye & Karplus 1983, and references cited therein):

$$r(t) = \frac{2}{5} <P_2[\hat{\mu}_a(0) \cdot \hat{\mu}_e(t)]> e^{-t/\phi_r} \quad (5)$$

where the factor $\frac{2}{5}$ accounts for the maximum theoretical anisotropy as a result of photoselection, $P_2[...]$ is the second-order Legendre polynomial, $\hat{\mu}_a(0)$ is the direction of the absorption transition moment at time t=0 and $\hat{\mu}_e(t)$ is the direction of the emission transition moment at time t. These directions may be considered separately because light absorption occurs in about 10^{-15} s, which is much faster than the process of internal conversion (~10^{-12} s) before emission starts. The brackets, <...>, denote an ensemble average. Because overall rotational motion of the flavodoxin (with rotational correlation time ϕ_r) is on a different, much longer, time scale, Eq. 5 becomes:

$$r(t) = \frac{2}{5} <P_2[\hat{\mu}_a(0) \cdot \hat{\mu}_e(t)]> \quad (6)$$

In case the $P_2[...]$ correlation function reaches a plateau value the comparison between the results obtained with experiment and simulation are given to a good approximation by (Axelsen et al., 1988):

$$<P_2[\hat{\mu}_a(0) \cdot \hat{\mu}_e(t)]> = P_2[cos\delta] \cdot <P_2[\hat{\mu}(0) \cdot \hat{\mu}(t)]> \quad (7)$$

where δ is the angle between the absorption and emission transition moments and $\hat{\mu}$ is the direction of either the absorption or emission transition moment. The anisotropy can then be calculated by substitution of Eq. 7 in Eq. 6.

The direction of the absorption transition moments in the oxidized flavin chromophore is deduced from the work of Johansson et al. (1979). When calculating the P_2 correlation function the emission transition moment was taken parallel with the first absorption transition moment (δ is 0°). From Figure 5 it is evident that the P_2 correlation function reaches a plateau for both the oxidized and reduced protein-bound flavin. The high plateau values indicate that the flavin chromophore is more or less immobilized within the protein matrix. For reduced flavodoxin a plateau value was found which was somewhat higher (P_2=0.95). From the work of Leenders et al. (1993; Chapter 2) the angle δ

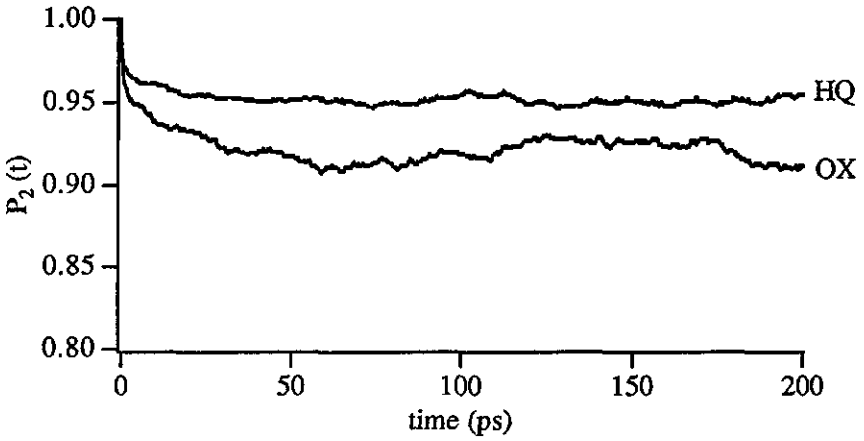

Figure 5. *Time-correlation function $P_2(t)$ describing the reorientation of the first absorption transition dipole moment of oxidized (OX) and reduced (HQ) flavin.* The orientation of the transition moment of reduced flavin is assumed to be identical to that of oxidized flavin (see text).

between the absorption and emission transition moment in reduced *clostridial* flavodoxin was determined to be 30.1°. Substitution of these values in Eqs. 6 and 7 yields a calculated anisotropy of 0.250, in excellent agreement with the experimentally determined value of 0.249 ± 0.002 (Leenders et al., 1993). Using the fact that angle δ is 10.5° in oxidized flavin (Chapter 7; Bastiaens and Visser, unpublished results), the plateau value of P_2=0.91 corresponds with an initial anisotropy value of 0.346 which perfectly matches the experimentally determined initial anisotropy of 0.35 ± 0.01 (Chapter 3). Since the calculated and experimentally determined initial anisotropies match very well, this confirms the motional rigidity of the protein-bound flavin as described by the dynamics calculations.

The simulation of the oxidized flavin did not reveal any nanosecond rotational motion as was demonstrated with fluorescence anisotropy measurements. This anisotropy decay component, which is thought to be an intermediate between the protein-bound and dissociated flavin chromophore, is an order of magnitude slower than the timescale of the calculations. Therefore, much longer simulations, without positional restraints within the protein matrix, would have to be performed to allow the non-covalently bound flavin to evolve to more loosely bound configurations.

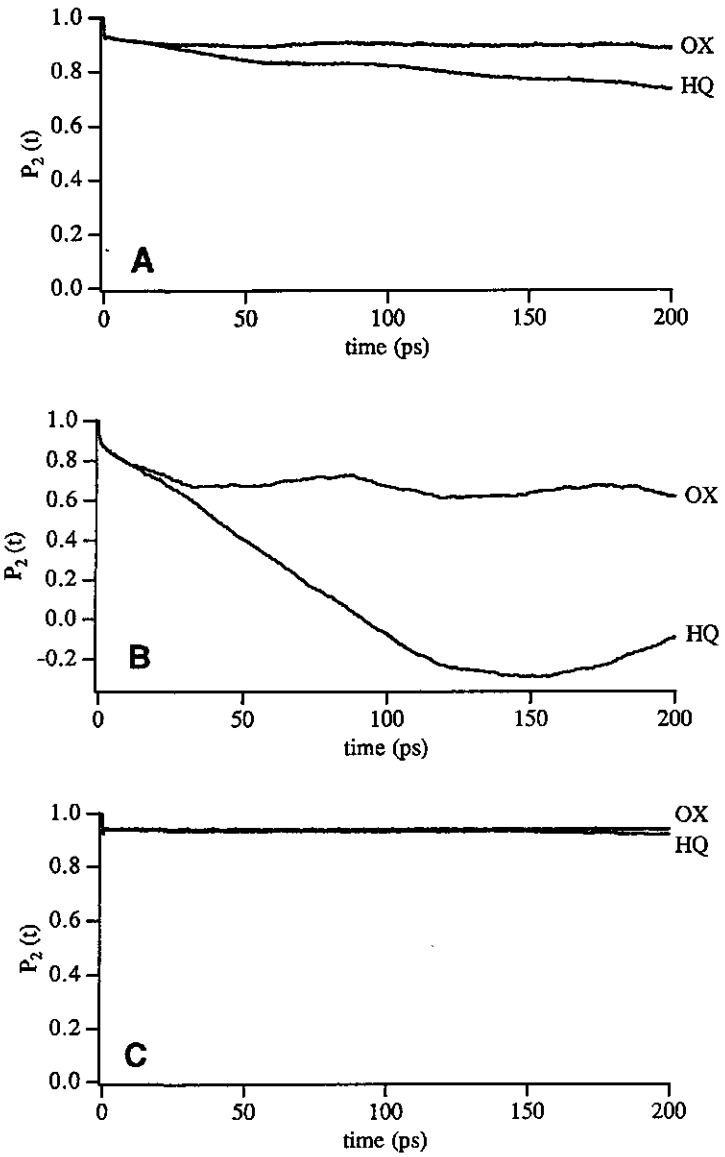

Figure 6. *Time-correlation function $P_2(t)$ describing the reorientation of the ^1L_a absorption transition dipole moment of the three tryptophan sidechain in oxidized and reduced flavodoxin* (no significant differences were detected between the time correlation functions of ^1L_a and ^1L_b). **A**, Trp6; **B**, Trp90; **C**, Trp95. It is clear that residue Trp90 has considerable motional freedom, whereas residues Trp6 and Trp95 are bound more firmly (see text for details).

Because the freely simulated inner sphere was chosen large enough the three tryptophan residues were also allowed to undergo unrestrained motion. Analysis of the time correlation functions therefore can yield valuable information about the mobility of the tryptophan residues in a *pasteurianum* flavodoxin, since polarized fluorescence studies of tryptophan dynamics in flavodoxin have only been reported for *rubrum* class of flavodoxins (Leenders et al., 1990b). The location of the absorption moments in the molecular frame are known from earlier work (Yamamoto and Tanaka, 1972). To gain insight in the dynamic behaviour of the tryptophan indole sidechains, the $P_2(t)$ was calculated for the ^1L_a and ^1L_b transition moments of the three tryptophans in the oxidized and reduced flavodoxins. From Figure 6 it can be deduced that the three tryptophans have different motional freedom. In oxidized flavodoxin residue Trp6 shows slight motion on a long time scale, whereas residue Trp95 seems to be almost completely immobilized. Residue Trp90, however, shows a large motional flexibility. In reduced flavodoxin Trp95 is also immobilized. Residues Trp6 and Trp90 have significantly more motional freedom than in oxidized flavodoxin.

From the crystal structure it is known that the indole sidechain of Trp90 and the isoalloxazine ring system of the flavin are coplanar. The differences in motional flexibility of residue Trp90 and the flavin chromophore, however, indicate that both residues have rather uncorrelated motion (this was already demonstrated in Table 1).

Tryptophan-to-flavin energy transfer

The three tryptophan residues and the flavin in the *clostridial* flavodoxin are separated by an average distance of about 1.2 nm. The interaction between the tryptophan residues and the flavin is monitored by calculating the Förster-type of energy transfer, which occurs due to dipole-dipole coupling. The rate of energy transfer from tryptophan donor to flavin acceptor, k_{ET} (in ns^{-1}), can be expressed by:

$$k_{ET} = \tau_{ET}^{-1} = (8.79 * 10^{17})\ \kappa^2 \frac{1}{\tau_r} R^{-6} J n^{-4} \qquad (8)$$

In this equation, τ_R is the (radiative) fluorescence lifetime of the tryptophan donor in the absence of the flavin acceptor, n is the refractive index of the

medium between donor and acceptor, and J is the spectral overlap integral given by:

$$J = \int_0^\infty \frac{F(\nu)\,\varepsilon(\nu)}{\nu^4}\,d\nu \tag{9}$$

where $F(\nu)$ is the normalized fluorescence spectrum of tryptophan as a function of frequency ν, and $\varepsilon(\nu)$ is the molar extinction coefficient of the flavin. The geometric parameters are the tryptophan-flavin center to center distance R (in nm), and κ^2, which is the orientation factor for the dipole-dipole interaction given by:

$$\kappa^2 = [\sin\theta_d \,.\, \sin\theta_a \,.\, \cos\zeta - 2(\cos\theta_d \,.\, \cos\theta_a)]^2 \tag{10}$$

Here ζ is the angle between the plane through the emission transition moment of the tryptophan donor and the separation vector and the plane through the second absorption transition moment of the flavin acceptor and the separation vector, and θ_d and θ_a are the polar angles made by these transition moments, respectively, with the separation vector.

Experimental measurements of tryptophan-to-flavin energy transfer involve averages over large ensembles of flavodoxin molecules. These results can be directly compared with those obtained from the simulations if the entire protein was simulated in a solvated state for a long period. The structural fluctuations of the flavodoxin would then be sampled with statistically significant frequencies. Because of computational limitations only the active site of the flavodoxin was simulated in a solvent sphere; however, the effects of internal motion upon the energy-transfer rates can be estimated from our calculations.

Since tryptophan has two potentially involved excited states, ^1L_a and ^1L_b, both rates of energy transfer to the flavin were calculated. The location of the ^1L_a and ^1L_b emission transition moments was assumed parallel with the absorption transition moments determined by Yamamoto and Tanaka (1972), and the second flavin absorption moment in oxidized flavodoxin was taken from the work of Johansson et al. (1979). For reduced flavodoxin no exact location has been reported in literature for the latter transition moment. Therefore, energy transfer calculations can only be performed for oxidized flavodoxin.

Since R and κ^2 are the only variables in the ensemble, averaging over κ^2/R^6 is equivalent to averaging over k_{ET} (see Eq. 8). We calculated the values of

Table 5. *The calculated κ^2/R^6 ratio averaged over the 7500 subsequent oxidized flavodoxin structures.* The ratio for the initial crystal structure is given for comparison. The fluorescence lifetime, τ_{ET}, as a result of the tryptophan-to-flavin energy-transfer are also given (in ps). For details see text.

			MD		X-ray	
Donor	→	Acceptor	κ^2/R^6	τ_{ET} (ps)	κ^2/R^6	τ_{ET} (ps)
Trp6 (^1L_a)	→	FMN	0.679	15.3	0.667	15.6
Trp6 (^1L_b)	→	FMN	0.040	247.0	0.026	400.0
Trp90 (^1L_a)	→	FMN	13.108	0.79	14.882	0.70
Trp90 (^1L_b)	→	FMN	170.91	0.06	422.01	0.02
Trp95 (^1L_a)	→	FMN	0.807	12.9	0.674	15.4
Trp95 (^1L_b)	→	FMN	0.081	128.0	0.103	101.0

κ^2/R^6 directly from the X-ray structure and compared these with the ones averaged over all subsequent MD-structures (see Table 5). It is obvious that different energy-transfer rates are calculated for the crystal structure and averaged over the structures from the trajectory. Since the flavin ring system is relatively immobilized, this difference is mainly the result of dynamic effects of the tryptophan indole ring. Using the κ^2/R^6 ratio in combination with the radiative lifetime and the overlap integral the energy transfer rate can be calculated (Eq. 8). The radiative lifetime of tryptophan fluorescence was taken as 20 ns (Hochstrasser and Negus, 1984), and the refractive index was taken as 1.4 (Eisinger et al., 1969). The overlap integral was determined for the somewhat different *D. gigas* and *D. vulgaris* flavodoxins (Leenders et al., 1990b). Taking the overlap integral for *clostridial* flavodoxin as the average of the two *Desulfovibrio* overlap integrals (i.e., $0.84*10^{-14}$ cm^3/M), energy-transfer times in the sub-picosecond to sub-nanosecond range could be calculated (see Table 5). These values are in the order of the ones determined experimentally (Chapters 5 and 6).

Conclusions

From the simulations it clearly follows that the overall active site conformation is similar in the averaged MD structures and the initial crystal structures. In particular, regions comprising α-helices and β-sheet have almost identical structures. However, regions with a somewhat altered conformation are also found. The backbone conformation of residues 57 to 63 shows rms differences of 0.15 nm (with sidechains rms differences of up to 0.3 nm). These regions are located in the active site, near the flavin chromophore. The oxidized flavin only shows small rms differences, whereas the reduced flavin ring system has larger rms differences. This effect might be the result of the chosen charge separation for the non-protonated atom N(1) in reduced flavin. The simulations further indicate that, on the time scale of the calculations, the flavin in oxidized as well as in reduced flavodoxin is immobilized in the protein matrix. The tryptophan residues have different motional flexibility. Residues Trp6 and Trp95 are almost immobilized, whereas residue Trp90, which is located at the periphery of the flavodoxin, has a large motional freedom, particularly in the reduced flavodoxin. This could be deduced from the large rms fluctuations of the Trp90 sidechain atoms as well as from the fast decay of the P_2 time-correlation function. This flexibility may play a role in optimising the electron transfer pathway to suitable electron acceptor proteins.

Earlier performed in vacuo simulations yielded anisotropies for the flavin which differed from the values found experimentally. Solvent inclusion mainly effects residues located at the periphery of the protein and is therefore necessary when comparing calculated and experimentally determined parameters, as was demonstrated when describing the motional behaviour of the protein-bound flavin. In our simulations all initial solvent molecules were part of the bulk. No information about crystal water molecules was added. During the simulations the water molecules partitioned into two groups: solvent molecules in bulk with high rms fluctuations and solvent molecules which are protein-bound (small fluctuations). It was demonstrated that the latter solvent molecules are located similarly to the water molecules found in the crystal structures.

From fluorescence and fluorescence anisotropy experiments it is sometimes very difficult to explain all the contributions in the decay profiles. From the simulations energy transfer rates could be calculated for the separate tryptophan residues. This is hardly possible in case of the experiments where one has to use proteins with selectively modified or changed residues.

In the case of flavodoxin, which has a compact and rigid structure, the use of spherical boundary conditions led to good results. However, one should keep in mind that spherical boundary conditions can only be used with considerable care, especially when little is known about dynamic properties of the protein under investigation.

Acknowledgements

We thank Dr. Jacob de Vlieg for his assistance in starting the molecular dynamics calculations. We also thank for the service provided by SARA Scientific Computing Services Amsterdam.

References

Åqvist, J., van Gunsteren, W. F., Leijonmarck, M. & Tapia, O. (1985) *J. Mol. Biol. 183*, 461-477.

Åqvist, J., Sandblom, P., Jones, T. A., Newcomer, M. E., van Gunsteren, W. F. & Tapia, O. (1986) *J. Mol. Biol. 192*, 593-604.

Axelsen, P. H., Haydock, C. & Prendergast, F. G. (1988) *Biophys. J. 54*, 249-258.

Berendsen, H. J. C., Postma, J. P. M., van Gunsteren, W. F. & Hermans, J. (1981) in *Intermolecular Forces* (Pullmann, D., Ed.), pp. 331-342, Reidel, Boston.

Berendsen, H. J. C., Postma, J. P. M., van Gunsteren, W. F., DiNola, A. & Haak, J. R. (1984) *J. Chem. Phys. 81*, 3684-3690.

Burnett, R. M., Darling, G. D., Kendall, D. S., LeQuesne, M.E., Mayhew, S. G., Smith, W. W. & Ludwig, M. L. (1974) *J. Biol. Chem. 249*, 4383-4392.

Chen, L. X.-Q., Engh, R. A., Brünger, A. T., Nguyen, D. T., Karplus, M. & Fleming, G. R. (1988) *Biochemistry 27*, 6908-6921.

de Vlieg, J., Boelens, R., Scheek, R. M., Kaptein, R & van Gunsteren, W. F. (1986) *Isr. J. Chem. 27*, 181-188.

Eisinger, J., Feuer, B. & Lamola, A. A. (1969) *Biochemistry 8*, 3908-3914.

Harris, D. L. & Hudson, B. S. (1991) *Chem. Phys. 158*, 353-382.

Henry, E. R. & Hochstrasser, R. M. (1987) *Proc. Natl. Acad. Sci. USA 84*, 6142-6146.

Hermans, J., Berendsen, H. J. C., van Gunsteren, W. F. & Postma, J. P. M. (1984) *Biopolymers 23*, 1513-1518.

Hochstrasser, R. M. & Negus, D. K. (1984) *Proc. Natl. Acad. Sci. USA 81*, 4399-4403.

Hockney, R. W. & Eastwood, J. W. (1981) *Computer Simulation using Particles*, McGraw-Hill, New York.

Hol, W. G. J., van Duijnen, P. T. & Berendsen, H. J. C. (1978) *Nature 273*, 443-446.

Ichiye, T. & Karplus, M. (1983) *Biochemistry 22*, 2884-2893.

James, T. L., Ludwig, M. L. & Cohn, M. (1973) *Proc. Natl. Acad. Sci. USA 70*, 3292-3295.

Johansson, L. B.-Å., Davidsson, Å., Lindblom, G. & Razi Naqvi, K. (1979) *Biochemistry 18*, 4249-4253.

Leenders, R., Bastiaens, Ph., Lunsche, R., van Hoek, A. & Visser, A. J. W. G. (1990a) *Chem. Phys. Lett. 165*, 315-322.

Leenders, R., Vervoort, J., van Hoek, A. & Visser, A. J. W. G. (1990b) *Eur. Biophys. J. 18*, 43-55.

Leenders, R. & Visser A. J. W. G. (1991) in *Flavins and Flavoproteins* (Curti, B., Ronchi, S. & Zanetti, G., Eds.), pp. 393-398, Walter de Gruyter, Berlin.

Leenders, R. & Visser A. J. W. G. (1992) in *Time-resolved Laser Spectroscopy in Biochemistry, vol. 1640* (Lakowicz, J. R., Ed.), pp. 212-219, Proceedings of SPIE-The International Society for Optical Engineering, Bellingham, WA.

Leenders, R., Kooijman, M., van Hoek, A., Veeger, C. & Visser, A. J. W. G. (1993) *Eur. J. Biochem. 211*, 37-45.

Levitt, M. (1980) in *Protein Folding* (Jaenicke, R., Ed.), pp. 17-39, Elsevier-North-Holland, Amsterdam.

Levy, R. M. (1985) in *Proceedings of the Workshop on Molecular Dynamics and Protein Structure* (Hermans, J., Ed.), pp. 62-64, Polycrystal Book Service, Western Springs, Illinois.

Ludwig, M. L., Andersen, R., Apgar, P. A. & LeQuesne, M. (1971) in *Flavins and Flavoproteins* (Kamin, H., Ed.), pp. 171-184, University Park Press, Baltimore, MD.

MacKerell, A. D., Nilsson, L., Rigler, R. & Saenger, W. (1988) *Biochemistry 27*, 4547-4556.

Mayhew, S. G. & Luwdig, M. L. (1975) in *The Enzymes (3rd Ed.) 12B*, (Boyer, P. D., Ed.), pp. 57-118, Academic Press, New York.

McCammon, J. A., Gelin, B. R. & Karplus, M. (1977) *Nature (London) 267*, 585-590.

Northrup, S. H., Pear, M. R., McCammon, J. A. & Karplus, M. (1980) *Nature (London) 286*, 304-305.

Reiher, W. E. (1985) *Theoretical Studies of Hydrogen Bonding*, PhD-thesis, Harvard University, Cambridge, MA, *Diss. Abstr. Int. B. 47, 229-230.*

Ryckaert, J.-P., Ciccotti, G. & Berendsen, H. J. C. (1977) *J. Comp. Phys. 23*, 327-341.

Smith, W. W., Burnett, R. M., Darling, G. D. & Ludwig, M. L. (1977) *J. Mol. Biol. 117*, 195-225.

van Gunsteren, W. F. & Karplus, M. (1982a) *Biochemistry 21*, 2259-2274.

van Gunsteren, W. F. & Karplus, M. (1982b) *Macromolecules 15*, 1528-1544.

van Gunsteren, W. F. & Berendsen, H. J. C. (1987) *Groningen molecular simulation (GROMOS) library manual*, Biomos, Groningen.

van Gunsteren, W. F. & Mark, A. E. (1992) *Eur. J. Biochem. 204*, 947-961.

van Mierlo, C. P. M., Lijnzaad, Ph., Vervoort, J., Müller, F., Berendsen, H. J. C. & de Vlieg, J. (1990a) *Eur. J. Biochem. 194*, 185-188.

van Mierlo, C. P. M., van der Sanden, B. P. J., van Woensel, P., Müller, F. & Vervoort, J. (1990b) *Eur. J. Biochem. 194*, 199-216.

Vervoort, J., van Berkel, W. J. H., Mayhew, S. G., Müller, F., Bacher, A., Nielsen, P. & LeGall, J. (1986) *Eur. J. Biochem. 161*, 749-756.

Visser, A. J. W. G., van Hoek, A., Kulinski, T. & LeGall, J. (1987) *FEBS Lett. 224*, 406-410.

Visser, A. (1989) in *Fluorescent Biomolecules* (Jameson, D.M. & Reinhardt, G. D., Eds.), pp. 319-341, Plenum Press, New York.

Watt, W., Tulinsky, A., Swenson, R. P. & Watenpaugh, K. D. (1991) *J. Mol. Biol. 218*, 195-208.

Yamamoto, Y. & Tanaka, J. (1972) *Bull. Chem. Soc. Jpn. 45*, 1362-1366.

Chapter 5

Time-resolved fluorescence studies of flavodoxin. Fluorescence decay and fluorescence anisotropy decay of tryptophan in *Desulfovibrio* flavodoxins

Rik Leenders, Jacques Vervoort, Arie van Hoek, and Antonie J. W. G. Visser

published in: *European Biophysics Journal 18* (1990) 43-55

Abstract

The time-resolved fluorescence characteristics of tryptophan in flavodoxin isolated from the sulfate-reducing bacteria *Desulfovibrio vulgaris* and *Desulfovibrio gigas* have been examined. By comparing the results of protein preparations of normal and FMN-depleted flavodoxin, radiationless energy transfer from tryptophan to FMN has been demonstrated. Since the crystal structure of *D. vulgaris* flavodoxin is known, transfer rate constants from the two excited states ^1L_a and ^1L_b can be calculated for both tryptophan residues (Trp60 and Trp140). Residue Trp60, which is located close to the flavin, transfers energy very rapidly to FMN, whereas the rate of energy transfer from the remote Trp140 to FMN is much smaller. Both tryptophan residues have the indole rings oriented in such a way that transfer will preferentially take place from the ^1L_a excited state. The fluorescence decay of all protein preparations turned out to be complex, the parameter values being dependent on the emission wavelength. Several decay curves were globally analyzed using a model in which tryptophan is involved in some nanosecond relaxation process. A relaxation time of about 2 ns was found for both *D. gigas* apo- and holo-flavodoxin. The fluorescence anisotropy decay of both *Desulfovibrio* FMN-depleted flavodoxins is exponential, whereas that of the two holoproteins is clearly non-exponential. The anisotropy decay was analyzed using the same model as applied for fluorescence decay. The tryptophan residues turned out to be immobilized in the protein. A time constant of a few nanoseconds results from energy transfer from tryptophan to flavin, at least for *D. gigas* flavodoxin. Because of the close resemblance of steady-state and time-resolved fluorescence properties of tryptophan in both flavodoxins, the location of the remote tryptophan residue seems preserved in both flavodoxins. The center-to-center distance between this tryptophan and the flavin in *D. gigas* flavodoxin is probably very similar to the distance between Trp140 and the flavin in *D. vulgaris* flavodoxin (i.e. 20 Å).

Introduction

Time-resolved fluorescence spectroscopy has gained considerable attention because precise information about structure and dynamics of various biopolymers can be obtained (for general references see: Rigler and Ehrenberg,

1973, 1976; Cundall and Dale, 1983; Lakowicz, 1983; Beechem and Brand, 1985). Particularly, protein fluorescence decay measurements have been widely used for probing tryptophan microenvironment and dynamics (Munro et al., 1979; Longworth, 1983; Beechem and Brand, 1985; Brand et al., 1985). Flavodoxins are low-potential electron-carrying proteins (molecular weight 15-25 kDa), which contain, as well as tryptophan, another chromophoric molecule, namely the noncovalently bound prosthetic group flavin mononucleotide (FMN) (for reviews on flavodoxins see: Mayhew and Ludwig, 1975; Simondson and Tollin, 1980; Tollin and Edmondson, 1980). The chemical and physical properties of flavodoxins, isolated from various organisms, have been extensively investigated with several spectroscopic techniques (Edmondson and Tollin, 1971; D'Anna and Tollin, 1972; Ryan and Tollin, 1973; Eaton et al., 1975; Visser et al., 1977, 1980, 1983a, 1987; Irwin et al., 1980; Vervoort et al., 1985, 1986). The crystal structures of a few flavodoxins in different redox states have been reported at high resolution (Watenpaugh et al., 1973; Burnett et al., 1974; Smith et al., 1983; Watt et al., 1991).

In this paper the results of time-resolved fluorescence of tryptophan residues determined in two flavodoxins are reported. The flavodoxins were isolated from the sulfate-reducing bacteria *Desulfovibrio vulgaris* and *Desulfovibrio gigas*. The three-dimensional structure of *D. vulgaris* flavodoxin is known (Watenpaugh et al., 1973). This flavodoxin contains two tryptophan residues, one of which is adjacent to FMN and the other remote from FMN. *D. gigas* flavodoxin also has two tryptophan residues (Helms and Swenson, 1992). Both apo- and holo-flavodoxins were examined in order to monitor radiationless energy transfer from tryptophan to flavin. For *D. vulgaris* flavodoxin the results can be compared with theoretical transfer rates derived from the distances and orientations derived from the crystal structure.

Time-resolved fluorescence spectra of the tryptophans in apo- and holoproteins were measured in order to investigate rapid relaxation processes in these proteins. The results are discussed with reference to the peculiar photophysics of tryptophan (Andrews and Forster, 1974; Szabo and Rayner, 1980; Chang et al., 1983; Petrich et al., 1983; Cross et al., 1983; Ichiye and Karplus, 1983; Creed, 1984). Polarized fluorescence decay measurements were used to investigate the rotational motion of the tryptophans in both flavodoxins.

Experimental procedures

Isolation and purification of flavodoxins

Desulfovibrio flavodoxins, purified as described earlier (LeGall and Hatchikian, 1967; LeGall and Forget, 1978), were a gift of Prof. J. LeGall (University of Georgia). They were distributed into vials and kept as stock solutions at -20 °C. Prior to experiments a vial was thawed and gel-filtrated over Sephadex G25 with either 0.1 M Tris-HCl buffer pH 7.5 or 0.05 M potassium phosphate pH 7.0 (for temperature-dependent measurements) to concentrations in the 1-10 μM region. Published extinction coefficients (Dubourdieu and LeGall, 1970) were used to determine the concentrations. Apoproteins were prepared by the trichloroacetic acid precipitation method followed by dissolution in neutral buffer (Wassink and Mayhew, 1975).

Steady-state fluorescence

Fluorescence spectra were measured on an Aminco-SPF 500 spectrofluorimeter with excitation wavelength at 295 nm and band widths of 4 nm both in excitation and emission. The absorbance at 295 nm was adjusted to 0.06. Both emission and excitation spectra were corrected. Fluorescence quenching experiments with KI were performed as described by Lehrer (1971). N-acetyl-L-tryptophan amide (NATA) served as a reference compound in both spectral and quenching experiments. In the quenching experiments integrated spectra were compared with the integrated spectrum of NATA taken under similar conditions.

Time-resolved fluorescence

Fluorescence decay measurements using a mode-locked argon-ion laser/synchronously-pumped dye laser system as the source of excitation, inherent data collection and subsequent data analysis have been described in detail elsewhere (van Hoek et al., 1983, 1987; van Hoek and Visser, 1985; Visser et al., 1985; Vos et al., 1987; van Hoek and Visser, 1992). Tryptophan was selectively excited at 300 nm. Time- and wavelength-resolved fluorescence

emission spectroscopy was performed at 20 °C with a double monochromator (band width 6 nm) having a polarizer set at the magic angle in front of the entrance slit. Fluorescence decays were measured as a function of emission wavelength every 10 nm between 320 and 400 nm. Three-dimensional presentation of the results was as described by Easter et al. (1976). The wavelength- and time-resolved fluorescence intensity $I(\lambda,t)$ is given by:

$$I(\lambda,t) = h(\lambda) \,.\, s(\lambda,t) \tag{1}$$

where

$$h(\lambda) = \frac{F(\lambda)}{\int_0^\infty s(\lambda,t)\, dt} \tag{2}$$

with the corrected steady-state fluorescence $F(\lambda)$ and the decay function $s(\lambda,t)$ which is taken into first approximation as a triple-exponential function with amplitudes α_i and lifetimes τ_i:

$$s(\lambda,t) = \sum_i \alpha_i\, e^{-t/\tau_i} \tag{3}$$

For fluorescence decay and anisotropy decay at a single wavelength a Schott 339 nm line filter (half band width 5 nm) was used.

Global analysis of fluorescence decay curves of apo- and holo-flavodoxins was performed using the procedure previously outlined by Knutson et al. (1983) and Beechem et al. (1985a, b).

Energy transfer

Energy transfer is assumed to occur via the Förster mechanism of very weak dipole-dipole coupling (Förster, 1965). The rate of transfer between tryptophan (donor) and flavin (acceptor) is given by:

$$k_{DA} = (8.79 \,.\, 10^{23})\, \tau_r^{-1}\, R^{-6}\, \kappa^2\, J\, n^{-4} \tag{4}$$

In this equation, τ_r is the radiative lifetime of tryptophan fluorescence taken as 20 ns (Hochstrasser and Negus, 1984), n is the refractive index of the medium between donor and acceptor taken as 1.4 (Eisinger et al., 1969), and J is the spectral overlap integral given by:

$$J = \int_0^\infty \frac{F(\nu)\,\varepsilon(\nu)}{\nu^4}\,d\nu \tag{5}$$

where $F(\nu)$ is the normalized fluorescence spectrum of tryptophan on a wavenumber scale, $\varepsilon(\nu)$ is the molar decadic extinction coefficient of the flavin acceptor. From spectral data we determined the overlap integrals for the two flavodoxins as $J(D.\ gigas) = 0.91*10^{-14}$ cm^3/M and $J(D.\ vulgaris) = 0.77*10^{-14}$ cm^3/M. The geometric parameters are the distance R between the centers of donor and acceptor, given in Å in Eq.4, and the so-called orientation factor κ^2 given by:

$$\kappa^2 = [sin\theta_d\,.\,sin\theta_a\,.\,cos\zeta - 2(cos\theta_d\,.\,cos\theta_a)]^2 \tag{6}$$

where ζ is the dihedral angle between the transition moments of donor and acceptor and θ_d and θ_a are the polar angles made by the donor and acceptor transition moments, respectively, with the separation vector.

Geometry of chromophores in D. vulgaris flavodoxin

Center-to-center distances and the polar and dihedral angles between the relevant tryptophan and FMN transition moments in *D. vulgaris* flavodoxin were calculated using the CHEM-X package, developed and distributed by Chemical Design Ltd., Oxford, England. The location of the transition moments in tryptophan and flavin was taken from the work of Yamamoto and Tanaka (1972) and of Johansson et al. (1979), respectively.

Results and Discussion

The outline of this section is as follows. We first present some results of steady-state fluorescence spectroscopy of apo- and holo-flavodoxins to characterize qualitatively the polarity of the tryptophan environment and its accessibility for iodide. Then the time-resolved fluorescence and fluorescence anisotropy of *D. gigas* flavodoxin at a single emission wavelength are described using global analysis with 'arbitrary' multi-exponential functions leading to the best fit. A survey of decay parameters is then obtained. Fluorescence decays across the tryptophan emission band of apo- and holo-flavodoxins are analyzed to yield three-dimensional representations of time-resolved fluorescence, from which spectra at distinct times after the pulse are obtained. Theoretical rates of energy transfer between tryptophan and flavin are calculated from the 'known' *D. vulgaris* flavodoxin. Finally, a model is proposed to discuss the time-resolved fluorescence and fluorescence anisotropy: the data were re-analyzed globally to investigate the validness of the model.

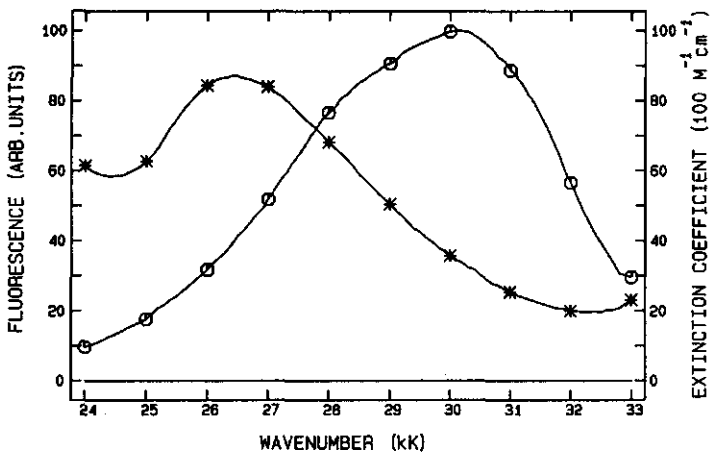

Figure 1. *Demonstration of the overlap between the emission spectrum of tryptophan (o) and the absorption spectrum of FMN (*) in D. gigas flavodoxin.* The emission maximum of tryptophan in *D. gigas* FMN-depleted flavodoxin is located at 30.3 kK (330 nm). The molar extinction coefficient for FMN is 8700 $M^{-1}cm^{-1}$ at 26.4 kK (379 nm).

Steady-state fluorescence

We have selectively excited the tryptophan residues of apo- and holo-flavodoxins at 295 nm. An example of absorption and emission spectra of *D. gigas* flavodoxin preparations is presented in Figure 1. Fluorescence quenching experiments are given in Figure 2 in the form of a Stern-Volmer and a modified Stern-Volmer plot. The results, relative quantum efficiencies, emission maxima and Stern-Volmer constants, are collected in Table 1. The most important features of Table 1 can be summarized as follows. From the emission maximum

Table 1. *Steady-state fluorescence properties of Desulfovibrio flavodoxins at 20 °C* [a].

sample	λ_{em} [b]	Q_r [c]	K_{SV} [d]
	(nm) (±0.02)	(M^{-1}) (±0.02)	
NATA	358	1.00	10.40
apo *D. gigas*	330	0.73	0.30
holo *D. gigas*	330	0.19	n.d.
apo *D. vulgaris*	332	0.61	0.51
holo *D. vulgaris*	330	0.10	n.d.

a) samples dissolved in 0.1 M Tris-HCl pH 7.5, apo is FMN-depleted flavodoxin, holo is native flavodoxin
b) wavelength of maximum fluorescence
c) relative quantum efficiency
d) Stern-Volmer constant

near 330 nm it can be concluded that the tryptophan residues are located in a rather apolar environment in both apo- and holoproteins. The fact that there is hardly any change in emission maxima with or without FMN, indicates that in first approximation the flavin does not perturb the electronic energy levels of the indole moiety. From the relative fluorescence efficiencies it is evident that FMN-binding results in a significant decrease of tryptophan fluorescence. This

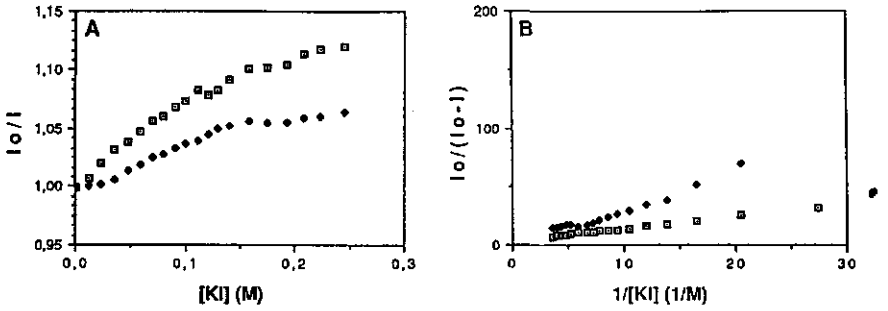

Figure 2. *Stern-Volmer plot (A) and modified Stern-Volmer plot (B) for quenching experiments of D. gigas and D. vulgaris FMN-depleted flavodoxin* (see text for details). ♦♦♦: *D. gigas* flavodoxin, ▫▫▫: *D. vulgaris* flavodoxin.

must be ascribed to radiationless excited-state energy transfer from tryptophan to flavin (Visser and Santema, 1981). In Figure 1 it is shown that there is a good overlap between the fluorescence spectrum of the single tryptophan (donor) and the absorption spectrum of the bound FMN (acceptor). The small initial slope in the Stern-Volmer plot (Figure 2A) of the apo-flavodoxins should indicate that the tryptophan residues are accessible to the bulky iodide ion for low efficiency quenching. However, the ordinate intercept in the modified Stern-Volmer plot (Figure 2B), reflecting the reciprocal fraction of accessible tryptophans indicates that a fraction of the tryptophan is totally inaccessible to quencher.

Fluorescence decay and fluorescence anisotropy decay

In contrast to the exponential fluorescence decay of NATA (Vos et al., 1987), the fluorescence decay pattern of tryptophan in the flavodoxin is more complex. At least three exponentials are needed to fit the experimental decay. We have selected *D. gigas* apo- and holo-flavodoxin at 20 °C to demonstrate the fit quality using a linear combination of exponential functions. An example of a best-fit decay analysis is shown in Figure 3 for *D. gigas* holo-flavodoxin. Decay and statistical parameters for the various models have been collected in Table 2. The fluorescence decay of the holoprotein is distinctly more rapid than that of apo-flavodoxin. This is demonstrated in Figure 4 where fluorescence decay profiles and their fits for *D. gigas* apo- and holoprotein are presented together.

The more rapid fluorescence decay of the holoprotein arises from the much larger amplitude of the shortest lifetime component (cf. Table 2).

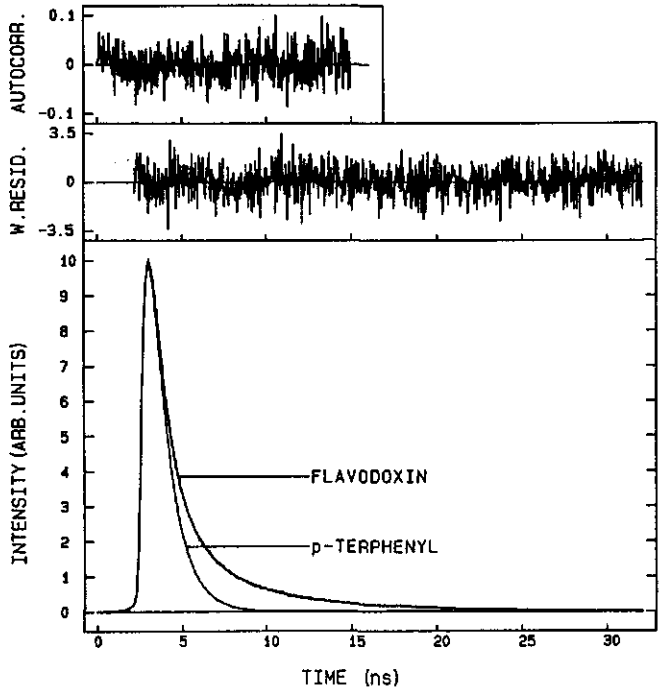

Figure 3. *Typical example of a fluorescence intensity decay analysis of D. gigas holo-flavodoxin in 0.1 M Tris-HCl pH 7.5 at 20 °C.* Excitation and emission wavelengths were 300 nm and 339 nm, respectively. Both the fluorescence response of p-terphenyl in ethanol (τ_{ref} is 1.06 ns) and the experimental and calculated fluorescence decays (1000 channels, time equivalence 31 ps per channel) of *D. gigas* holo-flavodoxin are shown. The (three) fluorescence decay times, pre-exponential factors, and statistical parameters are collected in Table 2.

The fluorescence anisotropy decay of both *D. gigas* apo- and holo-flavodoxin was globally analyzed as well, using single- and double-exponential functions. For apo-flavodoxin a double-exponential decay law does not improve the quality of the fit significantly (Figure 5A). For the holoprotein a double-exponential decay law was required to obtain a good fit to the data (see Figure 5B). Parameter values and statistical parameters are collected in Table 2. From the results in Table 2 it is clear that the anisotropy decay of holo-flavodoxin is characterized by a short and a long correlation time.

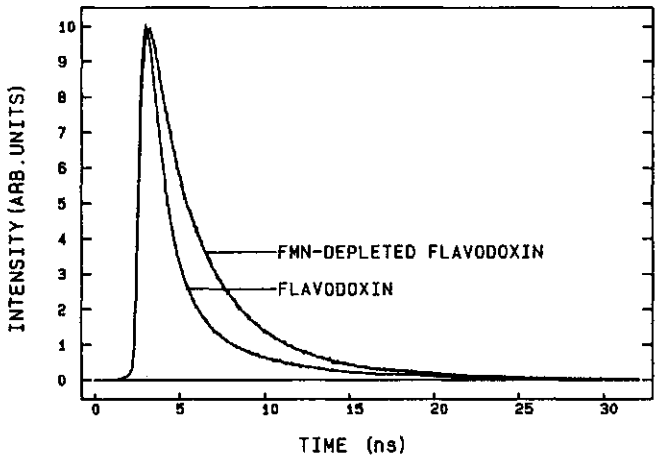

Figure 4. *Normalized fluorescence intensity decays of D. gigas FMN-depleted and holo-flavodoxin in 0.1 M Tris-HCl pH 7.5 at 20 °C.* Both experimental and calculated fluorescence intensity decays for both flavodoxin preparations are shown. Experimental conditions were identical to those described in the legend to Figure 3. The fluorescence decay times, pre-exponential factors, and statistical parameters are listed in Table 2.

Time-resolved fluorescence spectra

We have also analyzed the fluorescence decay of the four protein preparations as a function of emission wavelength. A three-dimensional representation of one data set is given in Figure 6. From such a data set one can easily retrieve peak normalized spectra as a function of time. The average fluorescence lifetime increases at longer fluorescence wavelengths implicating a spectral change during the decay. In Figure 7 examples of fluorescence spectra at different times after a δ-pulse excitation are given for *D. gigas* apo- and holo-flavodoxin. It can be clearly seen that the fluorescence maximum shifts to the red from 330 nm to approximately 340 nm in the apoprotein. In the holoprotein it is evident that two maxima appear in the time-dependent emission. Similar changes were observed in *D. vulgaris* flavodoxin (Visser and van Hoek, 1988).

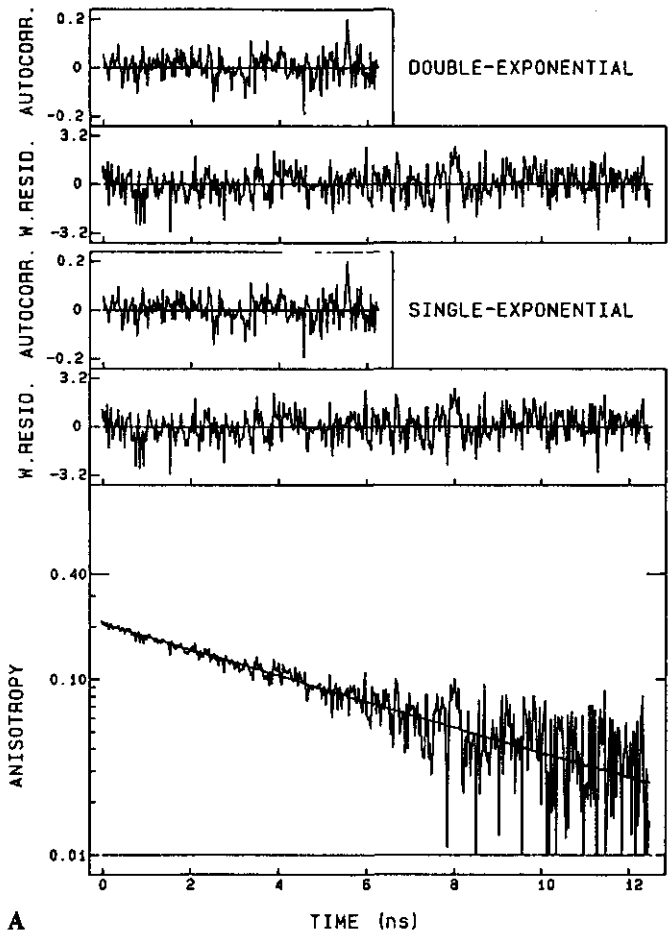

Figure 5. *An example of fluorescence anisotropy decay analyses of D. gigas apo-flavodoxin* (**A**) *and holo-flavodoxin* (**B**) *in 0.1 M Tris-HCl pH 7.5 at 20 °C.* Both experimental and calculated fluorescence anisotropy decays are shown. The weighted residuals and the autocorrelation of the residuals of fitting with a single- and a double-exponential function are shown in the top panels. The fluorescence anisotropy decay parameters and statistical data are listed in Table 2.

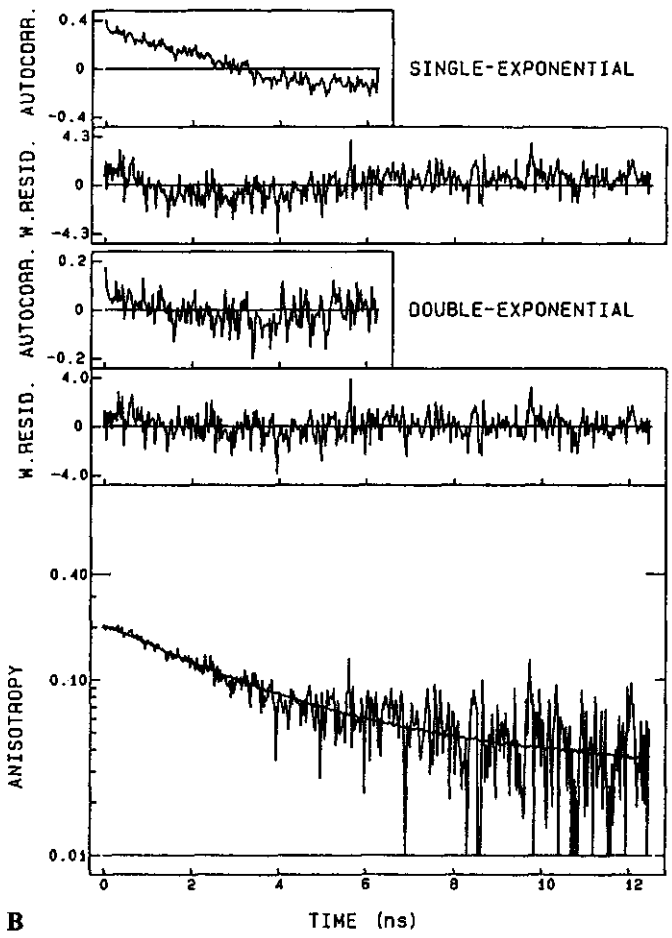
AUTOCORR.
W.RESID.
SINGLE-EXPONENTIAL
DOUBLE-EXPONENTIAL
ANISOTROPY
TIME (ns)
B

Figure 5B.

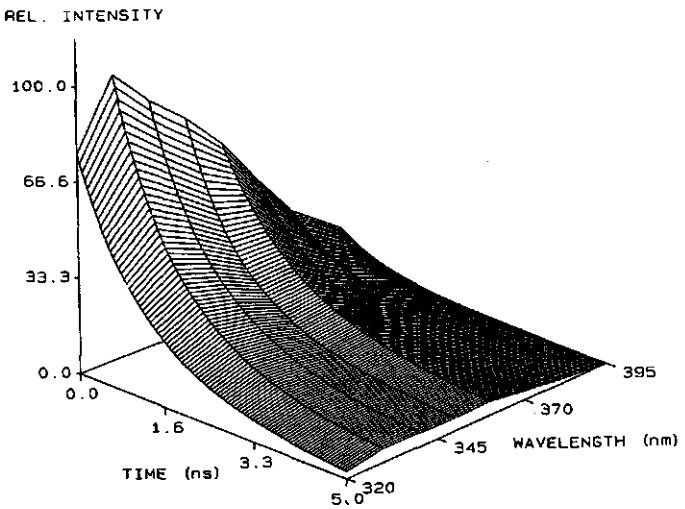

Figure 6. *Three-dimensional representation of a time-resolved fluorescence spectrum of D. gigas holo-flavodoxin*, constructed from a corrected steady-state fluorescence spectrum and deconvoluted fluorescence intensity decays for data collected at 320, 330, 340, 350, 360, 370, 380, and 395 nm.

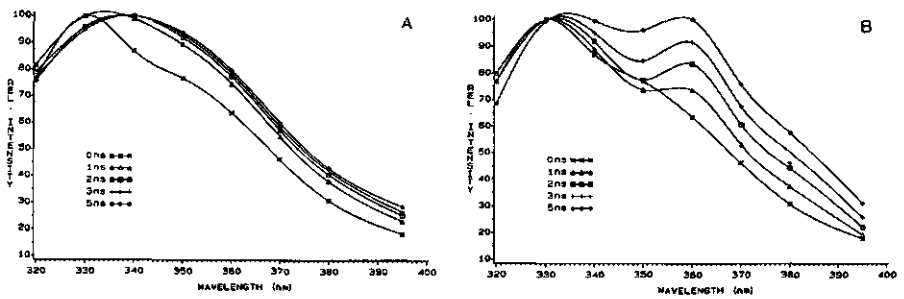

Figure 7. *Normalized fluorescence spectra of D. gigas FMN-depleted flavodoxin* (**A**) *and holo-flavodoxin* (**B**). The curves are extracted from three-dimensional graphs (as in Figure 6) by taking slices at times $t = 0,1,2,3$, and 5 ns. The fluorescence maximum shifts to the red from 330 nm to approximately 340 nm in the FMN-depleted flavodoxin. In the holo-flavodoxin two maxima appear (second maximum at about 359 nm). The spectral changes are completed after approximately 5 ns.

Table 2. *Parameters describing the fluorescence decay (A) and fluorescence anisotropy decay (B) of D. gigas apo- and holo-flavodoxin at 20 °C.* Parameters (standard deviations are listed in parentheses) were calculated using a linear combination of exponential functions (λ_{exc} is 300 nm, λ_{em} is 339 nm, and band width is 5 nm).

A. Fluorescence decay

sample	# [a]	α_1	τ_1	α_2	τ_2	α_3	τ_3	α_4	τ_4	χ_r^2	DW [b]	ZP [b]
			(ns)		(ns)		(ns)		(ns)			
D. gigas apo	1	1.00	3.75							27.3	0.06	2
		(0.01)	(0.01)									
	2	0.76	2.40	0.24	6.00					1.82	1.16	62
		(0.01)	(0.02)	(0.01)	(0.04)							
	3	0.18	0.41	0.67	2.79	0.15	6.67			1.13	1.81	199
		(0.01)	(0.04)	(0.01)	(0.03)	(0.01)	(0.08)					
	4	0.19	0.38	0.07	2.21	0.60	2.85	0.14	6.70	1.12	1.82	201
		(0.01)	(0.05)	(0.14)	(0.72)	(0.13)	(0.15)	(0.02)	(0.13)			
D. gigas holo	1	1.00	2.56							128.	0.01	1
		(0.01)	(0.01)									
	2	0.93	0.03	0.07	5.47					1.88	0.84	8
		(0.03)	(0.01)	(0.01)	(0.02)							
	3	0.74	0.89	0.18	2.80	0.08	6.74			0.98	1.84	226
		(0.01)	(0.02)	(0.01)	(0.12)	(0.01)	(0.12)					
	4	0.61	0.83	0.16	1.22	0.16	2.91	0.07	6.74	0.99	1.87	231
		(0.23)	(0.07)	(0.04)	(0.38)	(0.21)	(0.52)	(0.01)	(0.21)			

Table 2B. Fluorescence anisotropy decay [c]

sample	# [d]	β_1	ϕ_1 (ns)	β_2	ϕ_2 (ns)	χ_r^2	DW [b]	$ZP_{\parallel}$ [e]	$ZP_{\perp}$ [e]
D. gigas apo	1	0.22	5.81			1.12	1.84	201	205
		(0.01)	(0.08)						
	2	0.26	5.81	-0.04	5.89	1.12	1.84	203	205
		(0.29)	(2.10)	(0.29)	(14.30)				
D. gigas holo	1	0.21	4.74			1.10	1.63	140	164
		(0.01)	(0.08)						
	2	0.17	2.69	0.06	22.15	1.01	1.79	204	216
		(0.02)	(0.23)	(0.02)	(18.04)				

a) number of exponentials in the fluorescence decay function
b) DW is the Durbin-Watson parameter; ZP is the number of zero-passages of the autocorrelation function of the weighted residuals
c) calculated using three exponentials describing the fluorescence decay
d) number of exponentials in the fluorescence anisotropy decay function
e) $ZP_{\parallel}$ and $ZP_{\perp}$ are the number of zero-passages of the autocorrelation functions connected with parallel and perpendicular fluorescence intensity decays, respectively

Energy transfer

When the fluorescence decay characteristics of flavodoxin and FMN-depleted flavodoxin from both bacterial sources are compared, it is clear that the relative weight of the shorter lifetime component is increased in the holoprotein (cf. Table 2). Energy transfer from tryptophan to flavin can explain the enhanced contribution of the short lifetime component. The photophysical behaviour of tryptophan, however, is complex. Two potentially fluorescent states (^1L_a and ^1L_b, the ground state is denoted by ^1A) are closely spaced in energy, with widely different polarization directions in the molecular frame (Yamamoto and Tanaka, 1972) and with a high interconversion probability (Cross et al., 1983). The energy difference between the two states depends very

much on the polarity of the direct environment of the indole moiety (Andrews and Forster, 1974).

Table 3. *Energy transfer rate constants, k_{DA}, calculated for D. vulgaris flavodoxin* [a].

donor	→	acceptor	R [b]	κ^2 [c]	k_{DA} [d]	τ_{DA}
			(Å)		(s^{-1})	(ps)
^1L_a(Trp60)	→	FMN	5.5	1.20	$3.12*10^{12}$	0.32
^1L_b(Trp60)	→	FMN	5.5	0.06	$1.56*10^{11}$	6.4
^1L_a(Trp140)	→	FMN	19.8	0.60	$1.34*10^{9}$	750
^1L_b(Trp140)	→	FMN	19.8	0.17	$1.90*10^{8}$	5300

a) the constants were calculated from geometrical parameters using the 3-dimensional structure determined by Watenpaugh et al. (1973)
b) center to center distance
c) κ^2 is the orientation factor
d) $k_{DA}= 1/\tau_{DA}$

Since the 3-dimensional structure of the *D. vulgaris* flavodoxin is known (Watenpaugh et al., 1973), the energy transfer rate constants from each electronic level of both tryptophan residues to the single flavin acceptor can be evaluated, similarly to the assignments made for tryptophan-heme transfer in myoglobin (Hochstrasser and Negus, 1984). For simplicity we assumed in the calculations that the two excited states of the tryptophan can transfer independently and that both tryptophan residues exhibit Förster-type of energy transfer. Also, the same overlap integral for the two tryptophan-flavin couples is assumed. The flavin accepts the energy via the second electronic state, its absorption vector in the molecular plane is known (Johansson et al., 1979). Since the relative orientations of transition dipoles as well as distances can be determined, the transfer rate constants can be calculated (see Table 3). From inspection of Table 3 it is clear that the rate of energy transfer between the closest tryptophan (Trp60) and FMN is at least two orders of magnitude larger than the transfer rate associated with the other tryptophan residue (Trp140). The direct consequence is that fluorescence from this residue would be extinguished

very rapidly. Another interesting result is the fact that transfer from the ^1L_a electronic level is much more efficient than transfer from the ^1L_b state for both tryptophans. This difference in transfer rate can be mainly ascribed to the less favourable orientation factor κ^2 (Dale et al., 1979). For the purpose of discussion the calculated rates can qualitatively explain the fluorescence decay patterns and the time-resolved wavelength shifts of flavodoxin. The increase in amplitude of the short lifetime component, when comparing apo- with holoprotein, can be accounted for by the finite energy transfer process. If the reciprocal transfer rate constants (τ_{DA}, see Table 3) connected with the ^1L_a state are considered, it is evident that the time constant of transfer from Trp140 (the remote one) is relatively long, of the same order as found for the tryptophan-acceptor couple in lumazine protein (Kulinski et al., 1987).

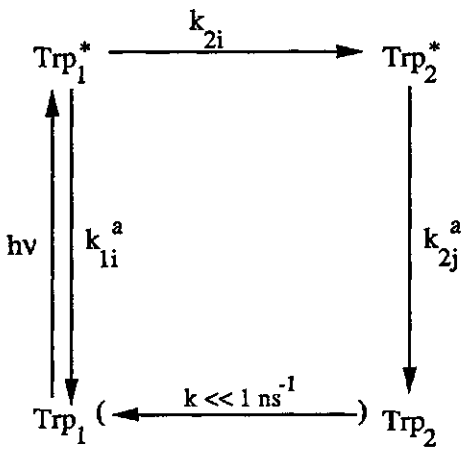

Figure 8. *Scheme describing an excited-state reaction of a tryptophan residue in a protein environment.* The rate constant for this process is given by the symbol k_{21}. Emission rate constants are indicated as well, with the superscript denoting either apoprotein (*a*) or in case of holoprotein (*h*).

Interpretation of fluorescence decay

The changes in emission spectra as a function of time observed for the single tryptophan in *D. gigas* flavodoxin indicate, in principle, two possibilities. The heterogeneity of the emission spectra arises either from at least two ground-state conformers with different excited-state behaviour or from the presence of an

excited-state reaction on nanosecond timescale. This reaction is not yet defined but it can originate from exciplex formation (Grinvald and Steinberg, 1974), solvent relaxation (Gudgin-Templeton and Ware, 1984), or in general, from relaxation into a different protein environment. A generalized scheme involving an uni-directional excited-state reaction and possibly consistent with the experimental data, for *D. gigas* at least, is given in Figure 8. Trp_1^* in Figure 8 is the primarily excited species, Trp_2^* being populated from Trp_1^*. The kinetics associated with this scheme are similar to that derived for comparable cases, e.g. the interconversion of peptide conformers during the lifetime of the excited state (Donzel et al., 1974), exciplex formation (Grinvald and Steinberg, 1974) or excited-state protonation (Laws and Brand, 1979). The fluorescence decay is expected to be bi-exponential when both species are characterized by single fluorescence rate constants. The pre-exponential factors and lifetimes are functions of all the rate constants involved, while the solution of the system depends on the initial boundary conditions. When the fluorescence decays of the two species are multi-exponential the expressions take the following form:

$$I_1(t) = [Trp_1^*](t) = \sum_i \alpha_{1i}^a \, e^{-k_{1i}^a \cdot t} \tag{7}$$

$$I_2(t) = [Trp_2^*](t) = \sum_i \sum_j \left\{ \frac{\alpha_{1i}^a \cdot \alpha_{2j}^a \cdot k_{2i}}{k_{1i}^a \cdot k_{2j}^a} \right\} * \left(e^{-k_{2j}^a \cdot t} - e^{-k_{1i}^a \cdot t}\right) \tag{8}$$

with

$$\sum_i \alpha_{1i}^a = \sum_i \alpha_{2j}^a = 1$$

In a first approximation we assume a general validity of the scheme for apo- and holoproteins (replace superscript a by h), i.e. any conformational change between apo- and holoprotein or resonance energy transfer in the holoprotein would not affect the scheme. When the microenvironments of the tryptophan residues in apo- and holoproteins are identical, the corresponding rate constants for the holoproteins are expected to be larger because of the additive involvement of the rate constant of energy transfer: $k^h = k^a + k_{DA}$. The two excited species, Trp_1^* and Trp_2^*, will have different spectral characteristics and the total fluorescence will be composed of two spectral contributions with

wavelength-dependent weighting factors f_1 and $f_2 = [1 - f_1]$, for [Trp_1^*] and [Trp_2^*]:

$$I(\lambda,t) = f_1(\lambda) \, . \, I_1(t) + [1 - f_1(\lambda)] \, I_2(t) \tag{9}$$

$f_1(\lambda)$ being the fraction of emission at given wavelength λ associated with Trp_1^* such that:

$$f_1(\lambda) = \frac{F_1(\lambda)}{\int_0^\infty I_1(t)\, dt} = \frac{F_1(\lambda)}{<\tau>} \tag{10}$$

where $F_1(\lambda)$ is the contribution of Trp_1^* fluorescence to the steady-state spectrum, $F(\lambda) = F_1(\lambda) + F_2(\lambda)$, and $<\tau>$ is the first-order average fluorescence lifetime of Trp_1^*. Global analytical approaches can be applied to resolve the two emission spectra from Eq. 9 since the rate constants of the decays at different emission wavelengths will be common. The next simplest case as compared to the bi-exponential decay model is for a mono-exponential fluorescence decay of Trp_1^* and a bi-exponential decay of Trp_2^*. Evaluation of Eq. 9 would result in a triple-exponential decay. A sum of three exponential functions, but with different pre-exponential factors, is also expected for the inverse case, namely a bi-exponential fluorescence decay of Trp_1^* and a single fluorescence rate constant for Trp_2^*. When both excited species are characterized by two fluorescence rate contants, the total fluorescence is expected to be composed of four exponential terms. The extension to a reversible excited-state reaction would result in more complicated rate equations and was not tried.

Although some parameters are also common between *D. gigas* apo- and holoproteins, global analysis across species was not carried out, because lifetimes of species taking part in energy transfer cannot be validly linked between apo- and holoprotein. In the global analysis two model functions were tried: a linear combination of either three or four exponential terms in which all the lifetimes (or reciprocal rate constants) were linked between nine decay experiments at emission wavelengths between 320 and 405 nm. Based on the values for the global reduced χ_r^2 for both models the four-exponential model turned out to be the best model of the two since it resulted into a significantly lower χ_r^2. The lifetimes and global reduced χ_r^2 values for both models have been listed in Table 4. As expected the relative amplitudes change with emission wavelength. The

Table 4. *Global lifetimes of the four different Desulfovibrio flavodoxin preparations, obtained by global analysis of fluorescence decay curves at different emission wavelengths.*

sample	τ_1	τ_2	τ_3	τ_4	$\chi_r^2{}_{(4)}$ [a]	$\chi_r^2{}_{(3)}$ [a]
	(ns)	(ns)	(ns)	(ns)		
apo *D. gigas*	0.13	1.23	3.67	9.10	1.63	2.25
holo *D. gigas*	0.12	1.11	3.84	10.0	1.33	2.63
apo*D.vulgaris*	0.09	0.81	2.86	6.53	1.34	1.86
holo*D.vulgaris*	0.09	0.82	4.41	10.8	1.46	2.79

a) global reduced $\chi_r^2(4)$ using a four-exponential decay function (with linked fluorescence lifetimes), $\chi_r^2(3)$ is the same but for a three-exponential decay function

two shorter lifetime components (tentatively assigned to [Trp_1^*]) have a relatively larger weight than the two longer lifetime components (assigned to [Trp_2^*]). The amplitudes of the longer lifetime components, however, increase significantly at longer emission wavelength (at the cost of those of the shorter lifetimes). This is taken to indicate that the (predominant) contribution of Trp_1^* emission differs from that of the Trp_2^* emission. Using the results of global analysis we were able to resolve the steady-state fluorescence spectrum into two contributions arising from Trp_1^* and Trp_2^*. The results are given in Figure 9. It can be noticed that the fluorescence of Trp_2^* is red-shifted as compared to that of Trp_1^*. This model is in complete agreement with the time-resolved spectral behaviour as presented in Figure 7. The second species Trp_2^* has a much longer average lifetime so that its presence becomes apparent after vanishing of Trp_1^*. The results summarized in Table 4 are also revealing with respect to energy transfer in the holoproteins. If attention is focussed to *D. gigas* flavodoxin, the rate constants are of comparable magnitude. Only Trp_1^* would be involved in energy transfer since the lifetimes are shorter in the holoprotein. Rate constants of energy transfer of 0.6 ns^{-1} and 0.1 ns^{-1} are obtained from the two lifetime components of Trp_1^* in *D. gigas* apo- and holo-flavodoxin. It is worth noting that these rates are in the same order of magnitude as those calculated for energy transfer between Trp140 and FMN in *D. vulgaris* flavodoxin. The lifetimes of

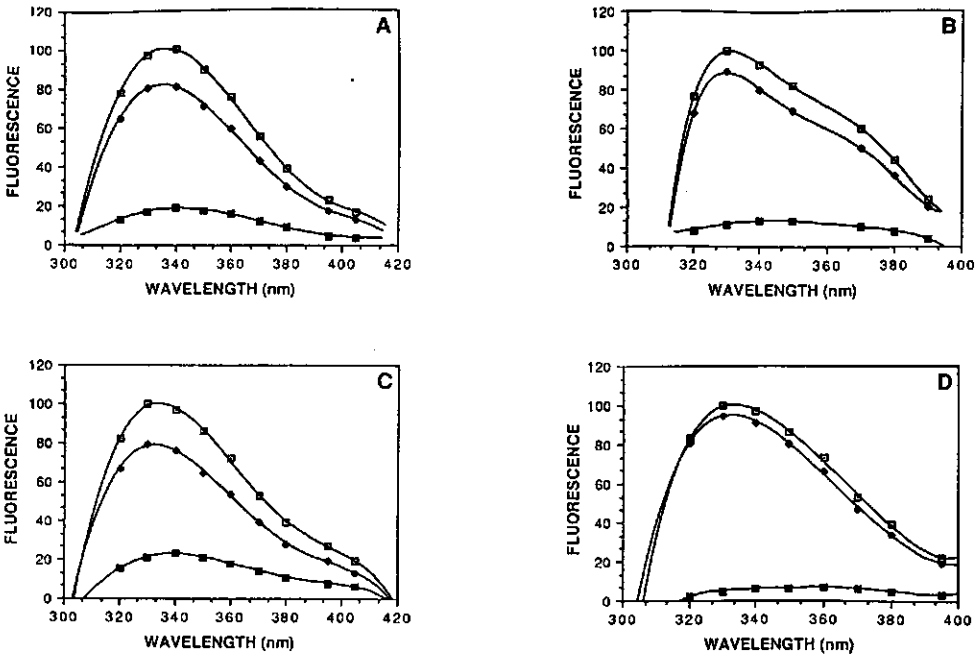

Figure 9. *Fluorescence spectra associated with Trp_1^* and Trp_2^* for four different Desulfovibrio flavodoxin preparations.* **A.** *D. gigas* apo-flavodoxin, **B.** *D. gigas* holo-flavodoxin, **C.** *D. vulgaris* apo-flavodoxin, and **D.** *D. vulgaris* holo-flavodoxin. ▫▫▫: total fluorescence, ♦♦♦: fluorescence of Trp_1^*, and ▪▪▪: fluorescence of Trp_2^*. See Figure 8 and text for details.

Trp_2^* are even slightly longer in the *D. gigas* holoprotein. The conclusion must therefore be that the microenvironment of the tryptophan is (slightly) altered upon binding of the flavin prosthetic group giving rise to somewhat different decay kinetics. Energy transfer is only manifested by quenching of the steady-state fluorescence spectrum of tryptophan and by an increase in amplitude of the short fluorescence lifetime component in the holoprotein (Table 2). Inspection

of Table 4 reveals that there is no good correlation between the results from *D. vulgaris* apo- and holo-flavodoxins (the longer lifetime components are significantly longer in the holo-flavodoxin). However, there is some correlation between the lifetimes of *D. gigas* and *D. vulgaris* holo-flavodoxins. This result is interesting because it implies that the remote tryptophan residues in the two *Desulfovibrio* flavodoxins are very similar. The results of *D. vulgaris* apo-flavodoxin can be accounted for by the fact that both tryptophans are fluorescent now with different lifetimes and the lifetime values in Table 4 should be considered average values of emission from Trp60 and Trp140. The rate constants k_{21} and k_{22} for the conversion of Trp_1^* into Trp_2^* can be obtained, in principle, from the pre-exponential factors of the exponential functions. Evaluation of these amplitudes leads to a system of nonlinear equations from which the rate constants can be obtained. We have estimated the rate constants for the case of *D. gigas* flavodoxin only at emission wavelengths between 320 and 370 nm. For apo-flavodoxin we found $k_{21} \cong 6 \pm 5$ ns^{-1} and $k_{22} = 0.52 \pm 0.20$ ns^{-1}, and for the holo-flavodoxin $k_{21} \cong 2 \pm 1$ ns^{-1} and $k_{22} = 0.55 \pm 0.18$ ns^{-1}. The rate constant k_{21} cannot be determined accurately because it can hardly be resolved, rate constant k_{22} on the other hand can be determined accurately and is identical for apo- and holo-flavodoxin. The reciprocal value of k_{22} indicates a relaxation time in the order of about 2 ns.

In the analysis of the fluorescence decay the assumption of two lifetime components for each species (two different microenvironments) is an over-simplification since the microenvironment of the tryptophan is probably more heterogeneous. For a more precise description a (multi-modal) distribution of fluorescence lifetimes should be taken into consideration (Alcala et al., 1987).

In principle, the expressions for the fluorescence decay (Eqs. 7 and 8) would also apply formally if Trp_1^* and Trp_2^* did actually correspond to ^1L_a and ^1L_b excited states produced. The ^1L_a excited state is then directly produced from one ground state, while the ^1L_b excited state is formed from the ^1L_a excited state. The reversible case would be completely consistent with internal conversion between ^1L_a and ^1L_b states (Cross et al., 1983). Equilibrium of the two transitions is expected to occur very rapidly in the temperature range used (Andrews and Forster, 1974; Ichiye and Karplus, 1983). In this case the observed rate constants of fluorescence and of energy transfer will then be average values over the ^1L_a and ^1L_b transitions.

Interpretation of fluorescence anisotropy decay

The rotational correlation times of the apo-flavodoxins (20 °C) obtained after single-exponential analysis are in good agreement with the molecular weight of the proteins (M_r = 15 kDa) using the empirical formula (Visser et al., 1983b):

$$\phi = 3.84 * 10^{-4} M_r \qquad (11)$$

with ϕ in ns and M_r in Da. The calculated correlation time is 5.8 ns. An important conclusion that can be drawn from the results presented in Table 2 is that the tryptophan residues in the apo-flavodoxins are immobilized on the nanosecond time-scale, thus they are rotating with the whole protein. On the other hand, the two holo-flavodoxins exhibit anomalous anisotropy decay with a short and a long correlation time. When the fluorescence anisotropy decay data of the holo-flavodoxins (at different temperatures) are analyzed using a bi-exponential decay model (single-exponential analysis did not result in good fits), it is found that the short correlation time is in the range of 1-3 ns and the long correlation time is in the range of 15-30 ns. In first approximation the long correlation time would indicate a large particle with molecular weight of 40-80 kDa. However, the protein preparation was shown to be homogeneous by a variety of analytical biochemical methods and no aggregation was found under the conditions used. Also, extreme elongation which can account for heterogeneous anisotropy decay can be ruled out since the protein shape is nearly spherical (Watenpaugh et al., 1973). This led us to seek for another explanation, which fits nicely in the concepts developed in the previous section.

Considering the proposed model to explain the fluorescence decay data (Figure 8), the fluorescence anisotropy decay will also be dependent on the emission wavelength:

$$r(\lambda,t) = \left\{ \frac{f_1(\lambda) \,.\, I_1(t) \,.\, r_1(0) + [1 - f_1(\lambda)] \,.\, I_2(t) \,.\, r_2(0)}{f_1(\lambda) \,.\, I_1(t) + [1 - f_1(\lambda)] \,.\, I_2(t)} \right\} * e^{-t/\phi_r} \qquad (12)$$

where ϕ_r is the rotational correlation time of the protein. This expression predicts nonexponential anisotropy decay for all wavelengths at which the two emission spectra overlap.

We have globally analyzed the polarized fluorescence decay curves of both apo- and holo-flavodoxins at different temperatures and at a single emission

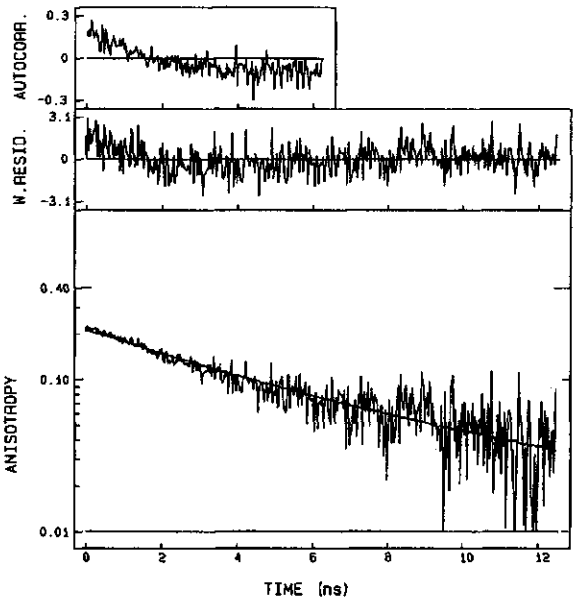

Figure 10. *Results of fitting of experimental fluorescence anisotropy decay data of D. gigas holo-flavodoxin (4 °C) with the model given in Eq.14.* Parameters and global reduced χ_r^2 are given in Table 5.

wavelength in order to recover an optimum correlation time ϕ and a value for $r(0)$ (we have ignored the 0.1 ns longer time arising from the contribution of FMN). We have tried to fit the anisotropy decay data according to Eq.12 for sets of apo- and holo-flavodoxins. As judged from the fitting criteria, however, the results were not satisfactory. The globally obtained correlation times were distinctly shorter than the ones obtained from separate analysis of the anisotropy decay of apo-flavodoxin. These results suggest that Eq. 12 is not adequate and that an extra depolarization process must be operative in the two holo-flavodoxins. This process is probably related to the type of energy transfer as described in the previous section. Therefore the data were re-analyzed using the

model as described in Eq. 12 for apo-flavodoxin and an empiric decay function which describes the anomalous decay in the holo-flavodoxin:

$$r^a(t) = \beta_1^a \,.\, e^{-t/\phi_r} \tag{13}$$

$$r^h(t) \approx [\beta_1^h + \beta_1^h \,.\, e^{-t/\phi_s}] \,.\, e^{-t/\phi_r} \tag{14}$$

where

$$\beta_1^h + \beta_2^h \approx \beta_1^a.$$

Here Eq. 13 is, in principle, identical to Eq. 12 and Eq. 14 contains an extra exponential term accounting for an additional depolarization with correlation time ϕ_s; superscripts *a* and *h* refer to apo- and holo-flavodoxin, respectively. The nature of this depolarization is not known, but it may arise from segmental motion or energy transfer. This decay model, though not exact, gave much better fits to the data. A typical example of the analysis of *D. gigas* holo-flavodoxin is given in Figure 10. If the additional depolarization is due to energy transfer, the correlation time ϕ_s contains information on the rate of energy transfer: $\phi_s^{-1} = k_{DA} + \phi_r^{-1}$. All anisotropy parameters including the rate constant of energy transfer are collected in Table 5. It should be stressed that the model described by Eq. 14 is not exact. The relaxation of the tryptophan residue into another microenvironment, already present in the apo-flavodoxin, is a complicating factor because it apparently takes place on the same time scale as the energy transfer process. Nonetheless, the analyzed anisotropy results yield a realistic rotational correlation time for apo- and holo-flavodoxins. Furthermore, the anisotropy analysis yields, for *D. vulgaris* flavodoxin, a rate constant of energy transfer in the same order of magnitude as the one determined from the crystal structure (cf. Table 3). In addition, for *D. gigas* flavodoxin, the rate constant of energy transfer turns out to be comparable to the ones obtained from time-resolved fluorescence decay analysis (0.6 ns^{-1} and 0.1 ns^{-1}).

Table 5. *Global correlation times and other anisotropy parameters of the four different Desulfovibrio flavodoxin preparations at various temperatures according to Eqs. 13 and 14.* The rotational correlation time ϕ of the apoprotein, as calculated in single-exponential decay analysis, has been linked with the correlation time ϕ of the holoprotein. The correlation times ϕ were fixed at the values of the apoprotein, which gave better fits.

sample		T	β_1	ϕ	β_2	ϕ_s	k_{DA}	$r(0)$	$\chi_r^{2\,a}$
		(°C)	(±0.01)	(ns) (-)	(±0.02)	(ns) (±0.3)	(ns^{-1})	(±0.03)	
D. gigas	apo	4	0.22	8.3				0.22	1.21
	holo	4	0.15	8.3	0.08	2.8	0.2	0.23	
	apo	20	0.22	5.8				0.22	1.36
	holo	20	0.18	5.8	0.04	1.3	0.6	0.22	
	apo	30	0.22	4.5				0.22	1.28
	holo	30	0.16	4.5	0.05	1.6	0.4	0.21	
D. vulgaris	apo	4	0.24	9.2				0.24	1.32
	holo	4	0.21	9.2	0.02	0.4	2.5	0.23	
	apo	20	0.24	5.3				0.24	1.30
	holo	20	0.23	5.3	0.01	0.5	1.7	0.24	
	apo	30	0.23	4.1				0.23	1.32
	holo	30	0.22	4.1	0.02	0.6	1.4	0.24	

a) global reduced χ_r^2, obtained after globally analyzing the decay curves of apo- and holo-flavodoxins at a certain temperature

Conclusions

The fluorescence decay kinetics of tryptophan can be modeled according to a scheme describing a relaxation process, in which the interaction of the tryptophan residue with its environment changes in the nanosecond time range. Such an excited-state reaction takes place in both apo- and holo-flavodoxin. Preferential energy transfer from the originally excited state of tryptophan to the flavin acceptor appears to be a realistic mechanism. An important conclusion

can be drawn from the fluorescence decay data of *D. gigas* flavodoxin. Because of the close resemblance of decay patterns and (time-resolved) fluorescence spectra between both flavodoxins, it is likely that the remote tryptophan residue is preserved in both flavodoxins. The center of this tryptophan must then be located at about 20 Å from the center of the isoalloxazine ring-system. *D. vulgaris* flavodoxin with its two tryptophan residues is a complex system for exact quantification of its fluorescence in apo- and holo-flavodoxin. On the other hand, the gene encoding the *D. vulgaris* flavodoxin has been cloned and brought to expression in *Escherichia coli* (Krey et al., 1988), so this flavodoxin lends itself for site-directed mutagenesis, in which either one of the tryptophans can be replaced by other non-fluorescent amino acids leading in this way to a complete understanding of the protein fluorescence.

A final concluding remark should be made on the comparison of tryptophan fluorescence in apo- and holo-flavodoxin. Removal of FMN results into an altered microenvironment of the tryptophan residue(s) which shows up as different fluorescence kinetics of the two protein preparations. This impedes a straightforward determination of, for instance, the rate constant of energy transfer between tryptophan and flavin.

Acknowledgements

We wish to acknowledge Prof. J.M. Beechem and Prof. L. Brand for kindly making available the global analysis programs. We thank Mrs. J.C. Toppenberg-Fang and Ms. E. Verberne for assistance in the preparation of the manuscript. Financial support was obtained from The Netherlands Organization for Scientific Research (N.W.O.) and from NSF grant DMB-8602789 (to J. LeGall).

References

Alcala, J. R., Gratton, E. & Prendergast, F. G. (1987) *Biophys. J. 51*, 597-604.

Andrews, L. J. & Forster, L. S. (1974) *Photochem. Photobiol. 19*, 353-360.

Beechem, J. M., Ameloot, M. & Brand, L. (1985a) *Chem. Phys. Lett. 120*, 466-472.

Beechem, J. M., Ameloot, M. & Brand, L. (1985b) *Anal. Instrum. 14*, 379-402.

Beechem, J. M. & Brand, L. (1985) *Ann. Rev. Biochem. 54*, 43-71.

Brand, L., Knutson, J. R., Davenport, L., Beechem, J. M., Dale, R. E., Walbridge, D. G. & Kowalczyk, A. A. (1985) in *Spectroscopy and the Dynamics of Molecular Biological Systems* (Bayley, P. M. & Dale, R. E., Eds.), pp. 259-309, Academic Press, London.

Burnett, R. M., Darling, G. D., Kendall, D. S., LeQuesne, M. E., Mayhew, S. G., Smith, W. W. & Ludwig, M. L. (1974) *J. Biol. Chem. 249*, 4383-4392.

Chang, M. C., Petrich, J. W., McDonald, D. B., Fleming, G. R. (1983) *J. Am. Chem. Soc. 105*, 3819-3824.

Creed, D. (1984) *Photochem. Photobiol. 39*, 537-562.

Cross, A. J., Waldeck, D. H. & Fleming, G. R. (1983) *J. Chem. Phys. 78*, 6455-6467.

Cundall, R. B. & Dale, R. E. (Eds.) (1983) *NATO ASI series, Ser A: Life sciences, vol. 69*, Plenum Press, New York.

Dale, R. E., Eisinger, J. & Blumberg, W. E. (1979) *Biophys. J. 26*, 161-194.

D'Anna, J. A. & Tollin, G. (1972) *Biochemistry 11*, 1073-1080.

Donzel, B., Gauduchon, P. & Wahl, Ph. (1974) *J. Am. Chem. Soc. 96*, 801-808.

Dubourdieu, M. & LeGall, J. (1970) *Bioch. Bioph. Res. Commun. 38*, 965-972.

Easter, J. H., DeToma, R. P. & Brand, L. (1976) *Biophys. J. 16*, 571-583.

Eaton, W. A., Hofrichter, J., Makinen, M. W., Andersen, R. D. & Ludwig, M. L. (1975) *Biochemistry 14*, 2146-2151.

Edmondson, D. E. & Tollin, G. (1971) *Biochemistry 10*, 124-133.

Eisinger, J., Feuer, B. & Lamola, A. A. (1969) *Biochemistry 8*, 3908-3914.

Förster, T. (1965) in *Modern Quantum Chemistry, part III* (Sinanoglu, O., Ed.), pp. 93-137, Academic Press, New York.

Grinvald, A. & Steinberg, I. Z. (1974) *Biochemistry 13*, 5170-5178.

Gudgin-Templeton, E. F. & Ware, W. R. (1984) *J. Phys. Chem. 88*, 4626-4631.

Helms, L. R. & Swenson, R. P. (1992) *Biochim. Biophys. Acta 1131*, 325-328.

Hochstrasser, R. M. & Negus, D. K. (1984) *Proc. Natl. Acad. Sci. USA 81*, 4399-4403.

Ichiye, T. & Karplus, M. (1983) *Biochemistry 22*, 2884-2893.

Irwin, R. M., Visser, A. J. W. G., Lee, J. & Carreira, L. A. (1980) *Biochemistry 19*, 4639-4646.

Johansson, L. B.-Å., Davidsson, Å., Lindblom, G. & Razi Naqvi, K. (1979) *Biochemistry 18*, 4249-4253.

Knutson, J. R., Beechem, J. M. & Brand, L. (1983) *Chem. Phys. Lett. 102*, 501-507.

Krey, G. D., Vanin, E. F. & Swenson, R. P. (1988) *J. Biol. Chem. 263*, 15436-15443.

Kulinski, T., Visser, A. J. W. G., O'Kane, D. J. & Lee, J. (1987) *Biochemistry 26*, 540-549.

Lakowicz, J. R. (1983) *Principles of Fluorescence Spectroscopy*, Plenum Press, New York.

Laws, W. R. & Brand, L. (1979) *J. Phys. Chem. 83*, 795-802.

LeGall, J. & Hatchikian, E. T. (1967) *C. R. Acad. Sci. Paris 264*, 2580-2583.

LeGall, J. & Forget, N. (1978) *Methods Enzymol. 53*, 613-634.

Lehrer, S. S. (1971) *Biochemistry 10*, 3254-3263.

Longworth, J. W. (1983) in *Time-resolved Fluorescence Spectroscopy in Biochemistry and Biology* (Cundall, R. B. & Dale, R. E., Eds.), pp. 651-725, Plenum Press, New York.

Mayhew, S. G. & Ludwig, M. L. (1975) in *The Enzymes* (Boyer, P. D., Ed.), pp. 57-118, Academic Press, New-York.

Munro, I., Pecht, I. & Stryer, L. (1979) *Proc. Natl. Acad. Sci. USA 76*, 56-60.

Petrich, J. W., Chang, M. C., McDonald, D. B. & Fleming, G. R. (1983) *J. Am. Chem. Soc. 105*, 3824-3832.

Rigler, R. & Ehrenberg, M. (1973) *Quart. Rev. Biophys. 6*, 139-199.

Rigler, R. & Ehrenberg, M. (1976) *Quart. Rev. Biophys. 9*, 1-19.

Ryan, J. & Tollin, G. (1973) *Biochemistry 12*, 4550-4554.

Simondson, R. P. & Tollin, G. (1980) *Molec. Cell. Biochem. 33*, 13-24.

Smith, W. W., Pattridge, K. A., Ludwig, M. L., Petsko, G. A., Tsernoglou, D., Tanaka, M. & Yasunobu, K. T. (1983) *J. Mol. Biol. 165*, 737-755.

Szabo, A. G. & Rayner, D. M. (1980) *J. Am. Chem. Soc. 102*, 554-563.

Tollin, G. & Edmondson, D. E. (1980) *Methods Enzymol. 69*, 392-406.

Valeur, B. & Weber, G. (1977) *Photochem. Photobiol. 25*, 441-444.

van Hoek, A., Vervoort, J. & Visser, A. J. W. G. (1983) *J. Biochem. Biophys. Methods 7*, 243-254.

van Hoek, A. & Visser, A. J. W. G. (1985) *Anal. Instrum. 14*, 359-378.

van Hoek, A., Vos, K. & Visser, A. J. W. G. (1987) *IEEE J. Quantum. Electr. QF-23*, 1812-1820.

van Hoek, A. & Visser, A. J. W. G. (1992) in *Time-resolved Laser Spectroscopy in Biochemistry, vol. 1640* (Lakowicz, J. R., Ed.), pp. 325-329, Proceedings of SPIE-The International Society for Optical Engineering, Bellingham, WA.

Vervoort, J., Müller, F., LeGall, J., Bacher, A. & Sedlmaier, H. (1985) *Eur. J. Biochem. 151*, 49-57.

Vervoort, J., Müller, F., Mayhew, S. G., van den Berg, W. A. M., Moonen, C. T. W. & Bacher, A. (1986) *Biochemistry 25*, 6789-6799.

Visser, A. J. W. G., Li, T. M., Drickamer, H. G. & Weber, G. (1977) *Biochemistry 16*, 4879-4882.

Visser, A. J. W. G., Carreira, L. A., LeGall, J. & Lee, J. (1980) *J. Phys. Chem. 84*, 3344-3346.

Visser, A. J. W. G. & Santema, J. S. (1981) *Photobiochem. Photobiophys. 3*, 125-133.

Visser, A. J. W. G., Vervoort, J., O'Kane, D. J., Lee, J. & Carreira, L. A. (1983a) *Eur. J. Biochem. 131*, 639-645.

Visser, A. J. W. G., Penners, N. H. G. & Müller, F. (1983b) in *Mobility and Recognition in Cell Biology* (Sund, H. & Veeger, C., Eds.), pp. 137-152, Walter de Gruyter, Berlin-New York.

Visser, A. J. W. G., Ykema, T., van Hoek, A., O'Kane, D. J. & Lee, J .(1985) *Biochemistry 24*, 1489-1496.

Visser, A. J. W. G., van Hoek, A., Kulinski, T. & LeGall, J. (1987) *FEBS Lett. 224*, 406-410.

Vos, K., van Hoek, A. & Visser, A. J. W. G. (1987) *Eur. J. Biochem. 165*, 55-63.

Wassink, J. H. & Mayhew, S. G. (1975) *Anal. Biochem. 68*, 609-616.

Watenpaugh, K. D., Sieker, L. C. & Jensen, L. H. (1973) *Proc. Natl. Acad. Sci. USA 70*, 3857-3860.

Watt , W., Tulinsky, A., Swenson, R. P. & Watenpaugh, K. D. (1991) *J. Mol. Biol. 218*, 195-208.

Yamamoto, Y. & Tanaka, J. (1972) *Bull. Chem. Soc. Jpn. 45*, 1362-1366.

Chapter 6

Time-resolved tryptophan fluorescence of flavodoxins

Rik Leenders, Johnny Roslund, and Antonie J. W. G. Visser

submitted to: *FEBS Letters*

Abstract

The time-resolved fluorescence characteristics of tryptophan in flavodoxins isolated from the bacteria *Desulfovibrio gigas*, *Desulfovibrio vulgaris*, *Clostridium beijerinckii*, and *Megasphaera elsdenii* have been examined. The fluorescence decays were recorded using synchrotron radiation. The results were analyzed into lifetime distributions using the maximum entropy method (MEM). In the present study comparison of the fluorescence decays of normal and FMN-depleted flavodoxins demonstrates that radiationless energy transfer from tryptophan to flavin probably occurs in all flavodoxins under investigation. By comparing the lifetime distribution patterns of apo- and holo-flavodoxins it can be concluded that in all holo-flavodoxin samples a certain amount of apoprotein is present.

Introduction

Flavodoxins are proteins which promote the transfer of electrons between two redox proteins as part of photosynthetic, nitrogen-reducing, sulfate-reducing or hydrogen-evolving systems (for a review: Mayhew and Ludwig, 1975). Flavodoxins are found in several aerobic and anaerobic bacteria and in some algae. The three-dimensional structure, in different oxidation states, has been determined for several flavodoxins using X-ray crystallography and nuclear magnetic resonance (Watenpaugh et al., 1973; Burnett et al., 1974; Smith et al., 1977; Ludwig et al., 1982; Smith et al., 1983; van Mierlo et al., 1990a,b; Watt et al., 1991). From these structures rate constants of energy transfer between tryptophan and flavin can be calculated and compared with the experimentally determined values. It is noted that this comparison is rather complicated in proteins with more than one tryptophan residu. In this study the time-resolved tryptophan fluorescence has been examined.

Materials and Methods

Preparation of the flavodoxins

The flavodoxins from *Desulfovibrio gigas*, *Desulfovibrio vulgaris*, *Clostridium beijerinckii*, and *Megasphaera elsdenii* were prepared as described earlier (LeGall and Hatchikian, 1967; Mayhew and Massey, 1969; Mayhew, 1971; Irie et al., 1973; Leenders and Visser, 1991). The flavodoxins were dissolved in 0.1 M KP_i pH 7.0 at protein concentrations of 10 μM. Apoflavodoxins were prepared as described by Wassink and Mayhew (1975). The measurements are performed at temperatures between 4 °C and 30 °C.

Time-resolved tryptophan fluorescence measurements

Fluorescence decay measurements were performed at beamline 32 at the MAX synchrotron in Lund, Sweden (Rigler et al., 1987). The apo- and holoflavodoxins were excited at 300 nm, and the fluorescence was detected using KV337 and OG330 filters (Schott, Mainz-Germany). The fluorescence decay was analyzed in terms of continuous lifetime distributions by means of the maximum entropy method (Livesey et al., 1986; Livesey and Brochon, 1987; Leenders et al., 1993).

Results and Discussion

The time-resolved fluorescence of *D. gigas*, *D. vulgaris*, *Cl. beijerinckii*, and *M. elsdenii* flavodoxin was measured. As an example the fluorescence decay of *Cl. beijerinckii* flavodoxin is presented in Figure 1. The decay of the *clostridial* apoflavodoxin is shown for comparison. It is obvious that the fluorescence of the holoflavodoxin decays faster than in the apoflavodoxin. For *D. vulgaris* flavodoxin this behaviour has been ascribed to energy transfer from the excited tryptophan to the flavin acceptor (Leenders et al., 1990). In the present study the

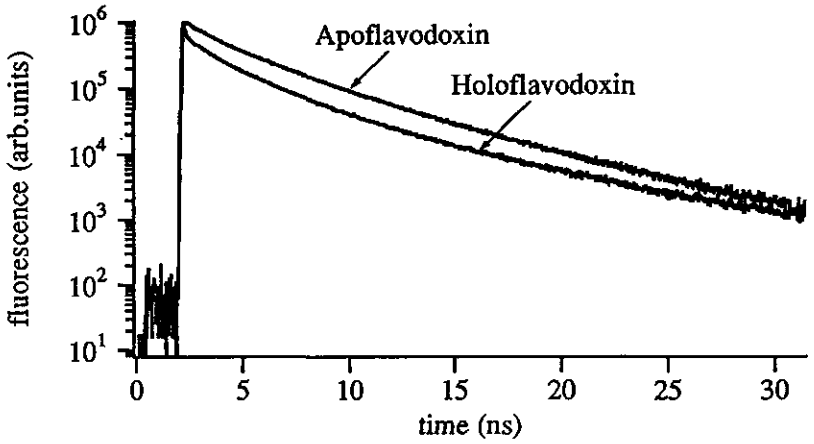

Figure 1. *Fluorescence decay of Cl. beijerinckii apo- and holo-flavodoxin (at 20 °C).*

fluorescence decay kinetics of the apo- and holoflavodoxins have been analyzed with the maximum entropy method. The results of these analyses are shown in Figure 2. The holoflavodoxin fluorescence decays contain one major distribution and a few less intense components. The most pronounced feature in the apoflavodoxin decays is the absence of the intense distribution, which was present in the holoflavodoxin decays. The barycenter of this intense lifetime distribution ($\Sigma\alpha_i\tau_i/\Sigma\alpha_i$ calculated over a limited range of τ_i values) in *D. vulgaris* flavodoxin is positioned at about 750 ps, which perfectly matches the lifetime calculated for energy transfer (Leenders et al., 1990). Therefore, this component is most likely coupled to energy transfer from tryptophan to flavin. The intense distribution in *Cl. beijerinckii* holoflavodoxin is located at about 35 ps. Since this flavodoxin contains three tryptophan residues near the flavin a more efficient energy transfer is expected. This results in a fluorescence lifetime which is shorter than in *D. vulgaris* flavodoxin. In the temperature range used (4-30 °C), the barycenter of the lifetime distribution is hardly influenced, in agreement with energy transfer. Furthermore, it was found that a large change in relative viscosity of the holoflavodoxin samples did not influence the position or lifetime

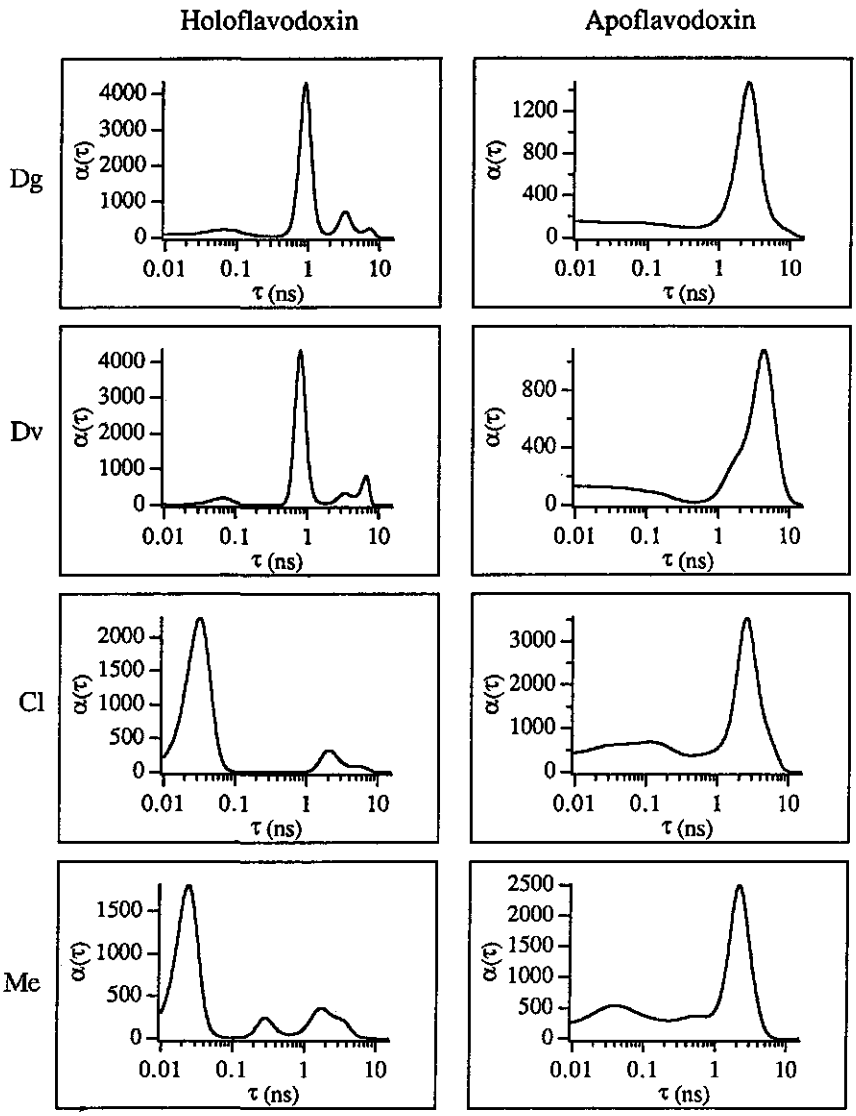

Figure 2. *Maximum entropy analyses of apo- and holo-flavodoxins (at 20 °C).* **Dg**, *D. gigas* flavodoxin; **Dv**, *D. vulgaris* flavodoxin; **Cl**, *Cl. beijerinckii* flavodoxin; **Me**, *M. elsdenii* flavodoxin. The quality of the fits was excellent, $1.00 \leq \chi^2 \leq 1.07$.

distribution of the short lifetime (data not shown), again indicating that it originates from energy transfer.

From comparison of the fluorescence decays of apo- and holo-flavodoxins it seems that in the holo-flavodoxin samples there is always a certain amount of apo-flavodoxin present.

It is noticed that the decay characteristics of the four flavodoxins can be divided into two groups. On one hand the two *Desulfovibrio* flavodoxins and on the other the *Cl. beijerinckii* and *M. elsdenii* flavodoxins. This is in accordance with results from earlier studies (D'Anna and Tollin, 1972; Leenders et al., 1993).

Acknowledgements

The authors wish to thank Dr. R. Nystrom of the MAX Laboratory for his hospitality and help in starting the synchrotron experiments. Furthermore, the European Molecular Biology Organization is thanked for providing a short-term EMBO-fellowship (to RL).

References

Burnett, R. M., Darling, G. D., Kendall, D. S., LeQuesne, M. E., Mayhew, S. G., Smith, W. W. & Ludwig, M. L. (1974) *J. Biol. Chem. 249*, 4383-4392.

D'Anna, J. A. & Tollin, G. (1972) *Biochemistry 11*, 1073-1080.

Irie, K., Kobayashi, K., Kobayashi, M. & Ishimoto, M. (1973) *J. Biochem. (Tokyo) 73*, 353-366.

Leenders, R., Vervoort, J., van Hoek, A. & Visser, A. J. W. G. (1990) *Eur. J. Biophys. 18*, 43-55.

Leenders, R. & Visser, A. J. W. G. (1991) in *Flavins and Flavoproteins* (Curti, B., Ronchi, S. & Zanetti, G., eds.) pp. 393-398, Walter de Gruyter, Berlin.

Leenders, R., Kooijman, M., van Hoek, A., Veeger, C. & Visser, A. J. W. G. (1993) *Eur. J. Biochem. 211*, 37-45.

LeGall, J. & Hatchikian, E. C. (1969) *C. R. Acad. Sci. Paris 264*, 2580-2583.

Livesey, A. K., Licinio, P. & Delaye, M. (1986) *J. Chem. Phys. 84*, 5102-5107.

Livesey, A. K. & Brochon, J. C. (1987) *Biophys. J. 52*, 693-706.

Ludwig, M. L., Pattridge, K. A., Smith, W. W., Jensen, L. H. & Watenpaugh, K. D. (1982) in *Flavins and Flavoproteins* (Massey, V. & Williams, C. H., Eds.), pp. 19-28, Elsevier/North-Holland, Amsterdam.

Mayhew, S. G. & Massey, V. (1969) *J. Biol. Chem. 244*, 794-802.

Mayhew, S. G. (1971) *Biochim. Biophys. Acta 235*, 289-302.

Mayhew, S. G. & Ludwig, M. L. (1975) in *The Enzymes*, vol. XII (Boyer, P. D., Ed.), pp. 57-118, Academic Press, New York.

Rigler, R., Kristenssen, O., Roslund, J., Thyberg, P., Oba, K. & Eriksson, M. (1987) *Physica Scripta T17*, 204-207.

Smith, W. W., Burnett, R. M., Darling, G. D. & Ludwig, M. L. (1977) *J. Mol. Biol. 117*, 195-225.

Smith, W. W., Pattridge, K. A., Ludwig, M. L., Petsko, G. A., Tsernoglou, D., Tanaka, M. & Yasunobu, K. T. (1983) *J. Mol. Biol. 165*, 737-755.

van Mierlo, C. P. M., Lijnzaad, Ph., Vervoort, J., Müller, F., Berendsen, H. J. C. & de Vlieg, J. (1990a) *Eur. J. Biochem. 194*, 185-198.

van Mierlo, C. P. M., van der Sanden, B. P. J., van Woensel, P., Müller, F. & Vervoort, J. (1990b) *Eur. J. Biochem. 194*, 199-216.

Wassink, J. H. & Mayhew, S. G. (1975) *Anal. Biochem. 68*, 609-616.

Watenpaugh, K. D., Sieker, L. C. & Jensen, L. H. (1973) *Proc. Nat. Acad. Sci, USA 70*, 3857-3860.

Watt, W., Tulinsky, A., Swenson, R. P. & Watenpaugh, K. D. (1991) *J. Mol. Biol. 218*, 195-208.

Chapter 7

Rotational resolution of methyl-group substitution and anisotropic rotation of flavins as revealed by picosecond-resolved fluorescence depolarization

Rik Leenders, Philippe Bastiaens, Renata Lunsche, Arie van Hoek, and Antonie J. W. G. Visser

published in: *Chemical Physics Letters 4* (1990) 315-322

Abstract

The rotational correlation times of the natural flavin compounds riboflavin and FMN and the flavin models lumiflavin, tetra-O-acetyl-riboflavin and their N(3)-methylated derivatives, dissolved in water, were determined with the time-resolved fluorescence depolarization technique. As a result of the currently possible time resolution the effect of methylgroup substitution could be determined as a few picoseconds longer correlation time in agreement with the slightly larger molecular volume. Anisotropic rotation of lumiflavin was demonstrated by observing the change in correlation time when excitation was in the second excited singlet state of the flavin. The angle between the emission transition moment and the long axis of the flavin ring system turned out to be approximately 22°.

Introduction

The experimental assessment of rotational diffusion is an important tool to investigate structure and dynamics of biomolecules and biopolymers. Extension of this method into the picosecond regime will provide the experimental counterpart of molecular dynamics simulations, which is particularly useful in testing theoretical descriptions of rotational diffusion (Ichiye and Karplus, 1983). Both experimental and theoretical approaches have gained considerable progress during the last years.

In this paper we have investigated rotational diffusion of several natural and synthetic flavin derivatives (Figure 1), all dissolved in aqueous solution. Two N(3)-methylated flavin compounds were compared with flavins nonmethylated at that position. It is demonstrated that the effect of methyl-substitution on the rotational diffusion is unambiguously present. As established earlier steady-state fluorescence depolarization of several flavins also revealed size-dependent changes (Weber, 1966). In Figure 1 the optical transitions from ground state to the first two singlet excited states have been indicated, as determined by Johansson et al. (1979). Also presented is the direction of the permanent dipole moment, calculated to be 7.8 D by Platenkamp et al. (1987). The flavin skeleton is intrinsically anisotropic. When the molecule possesses uniaxial symmetry, the fluorescence anisotropy decay profile should change when excitation is either in the first or in the second electronic state, since the anisotropy decay function

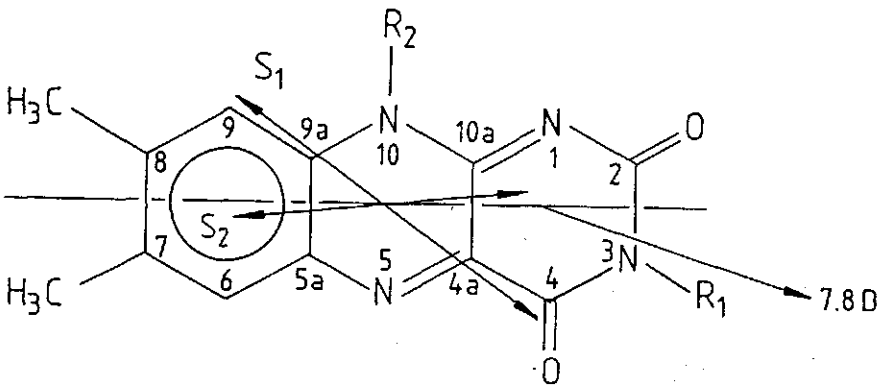

Figure 1. *Structure of flavins investigated.* R_1 = H and R_2 = CH_3: lumiflavin; R_1 = R_2 = CH_3: N(3)-methyllumiflavin; R_1 = H and R_2 = CH_2-[$CH(OCOCH_3)$]$_4$-H: tetra-O-acetylriboflavin; R_1 = CH_3 and R_2 = CH_2-[$CH(OCOCH_3)$]$_4$-H: N(3)-methyl-tetra-O-acetylriboflavin; R_1 = H and R_2 = CH_2-[CHOH]$_4$-H: riboflavin; R_1 = H and R_2 = CH_2-[CHOH]$_3$-$CHOPO_3$: FMN. The directions of dipole moment (7.8 D) and optical transition moments (from ground state to first two excited singlet states) are also indicated.

depends upon the angle of the absorption transition moment with the main symmetry axis. The theoretical background and experimental verification using similar molecules has been provided recently (Visser et al., 1989).

Since the time-resolution of pulse fluorimeters has been improved (Bebelaar, 1986), the time-dependent fluorescence behaviour of the flavins was re-investigated. The fluorescence of all compounds decays predominantly in an exponential fashion with lifetimes of about 5 ns, the exact value depending on the particular flavin used.

Experimental methods

Riboflavin and FMN were obtained from Sigma. FMN was purified with anion-exchange chromatography prior to use (Massey and Swoboda, 1963). Lumiflavin, N(3)-methyllumiflavin, tetra-O-acetyl-riboflavin and N(3)-methyl-tetra-O-acetyl-riboflavin were gifts of Dr. F. Müller (Basel). Water was purified on Millipore filters. Ethanol was fluorescent grade from Merck.

The time-correlated single photon counting equipment with the mode-locked continuous wave argon-ion laser, in combination with the frequency doubled, synchronously pumped dye laser, as excitation source has been amply described (Visser and van Hoek, 1979; van Hoek and Visser, 1985; Visser et al., 1985, 1988). The time resolution of the detection system has been improved by the incorporation of a microchannel plate detector (Hamamatsu R1645 U-01). The 476.7 nm line of the laser was selected for excitation in the first electronic absorption band since it is close to the 0,0-vibronic transition from ground state to the lowest excited singlet state (Platenkamp et al., 1980). Fluorescence was measured at 544.0 nm through an interference filter (Balzer 544) with half band width of 10 nm. Excitation in the second electronic absorption band of the flavin was performed by the output of the frequency doubled DCM dye laser at 340.0 nm. Data analysis was performed as recently described (Vos et al., 1987; Visser et al., 1988). To derive the instrumental response function we used erythrosin-B in water as reference compound (for experimental details see: Visser and van Hoek, 1988; van Hoek et al., 1987). Molecular volumes of the flavin compounds were obtained from the molecular weights and the density, which is taken as 1.60 g/cm^3 for each flavin derivative (Wang and Fritchie, 1973).

Van der Waals volumes of the different flavin compounds were determined using the Chem-X package, developed and distributed by Chemical Design Ltd., Oxford, England. The molecular dimensions were estimated from the van der Waals radii of each constituent atom taking into account the various bond lengths and assuming an extended conformation of the various side chains.

Results and discussion

Fluorescence lifetimes

From a close analysis of the fluorescence decay it turned out that, by comparing fitting criteria using single- and double-exponential decay models, the best fit was obtained for a bi-exponential function with a predominant relative contribution ($=\alpha_i\tau_i/\Sigma\alpha_i\tau_i$) of the long lifetime component of around 5 ns (the exact value depending on the flavin compound). The shorter lifetime component has a value of around 2 ns. Addition of the shorter lifetime

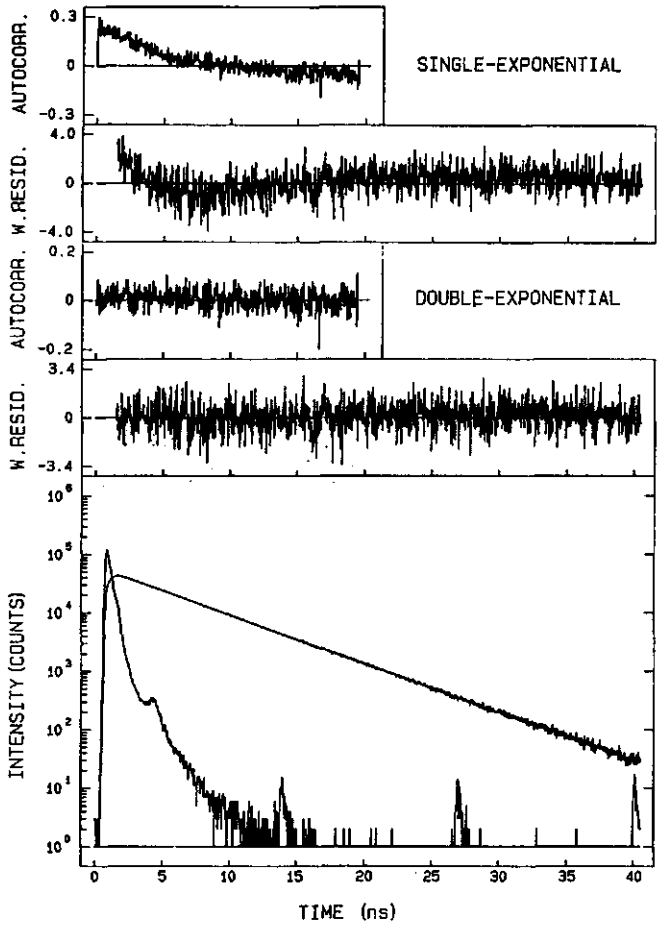

Figure 2. *Analysis of fluorescence decay of 1 μM lumiflavin in water at 20 °C.* The excitation and emission wavelengths were 476.7 and 544.0 nm, respectively. Fluorescence was measured through a polarizer set at the magic angle (54.7°). The time equivalence per channel was 39.6 ps/channel and the fit range was between channels 40 to 1024. The fluorescence response of Erythrosin-B in water and the experimental and calculated fluorescence response of lumiflavin according to a bi-exponential decay model are shown. The upper panels show the weighted residuals between calculated and observed fluorescence and the correlation function of the residuals. The recovered parameters are: $\alpha_1 = 0.956 \pm 0.003$, $\tau_1 = 5.21 \pm 0.01$ ns, $\alpha_2 = 0.044 \pm 0.003$, $\tau_2 = 2.1 \pm 0.2$ ns. Statistical parameters for this fit are: $\chi^2 = 1.05$, Durbin-Watson parameter DW = 2.04 and the number of zero passages in the autocorrelation function ZP = 252. For comparison the weighted residuals and autocorrelation function for a single-exponential decay analysis are also shown. The parameters for this fit are $\alpha = 1.000 \pm 0.001$, $\tau = 5.162 \pm 0.002$ ns with statistical parameters $\chi^2 = 1.37$, DW = 1.54 and ZP = 89.

Table 1. *Fluorescence lifetimes of flavin compounds in water or ethanol at 20 °C (λ_{exc} is 476.7 nm and λ_{em} is 544.0 nm).*

compound	solvent	τ (ns)	$\alpha \cdot \tau$ (%) [a]
		(±0.03 ns)	(±1%)
lumiflavin	water	5.20	98
	ethanol	6.55	99
N(3)-methyllumiflavin	water	4.67	96
	ethanol	5.88	98
tetra-O-acetylriboflavin	water	5.10	97
	ethanol	6.30	97
N(3)-methyl-tetra-O-acetyl-riboflavin	water	4.53	96
	ethanol	5.55	96
riboflavin	water	4.85	95
FMN	water	4.78	98

a) Percentage of fluorescence contribution, arising from the long lifetime component

component was required to obtain an optimum fit to the data, as illustrated in Figure 2, showing the fluorescence decay analysis of lumiflavin in water. This slight heterogeneity is observed for each flavin studied, independent of the concentrations within the range used, i.e. 0.4-11 μM. The long lifetimes and relative contributions are collected in Table 1. This observation also seems to be independent of the solvent, because ethanol instead of water yielded the same slight heterogeneity for flavins soluble in ethanol, (cf. Table 1). Since the instrumental response functions were inferior in the past (i.e. from 2 ns (Wahl et al., 1974) to 0.5 ns (Visser and van Hoek, 1979; van Hoek and Visser, 1985; Visser et al., 1985) until 0.1 ns (this work), this might be the reason for the fact that the effect remained unattended. The apparent heterogeneity remains to be investigated into more detail, but it might be related with the presence of different conformers in the ground state of the flavin, with different excited-state properties. It has been demonstrated recently, by geometry-optimized molecular orbital calculations (Hall et al., 1987), that the three-ring system is

highly flexible even in the oxidized state requiring only 1-2 kcal/mol for deformation.

Rotational correlation times

From experiments with polarized excitation and emission one can relate, in principle, the measured emission anisotropy, $r(t)$,

$$r(t) = \frac{i_{\parallel}(t) - i_{\perp}(t)}{i_{\parallel}(t) + 2i_{\perp}(t)} \tag{1}$$

to the correlation function describing the reorientation of the fluorescent molecule:

$$r(t) = \frac{2}{5} \langle P_2[\widehat{\mu}_a(0)\widehat{\mu}_e(t)] \rangle \tag{2}$$

with $\langle P_2[\widehat{\mu}_a(0)\widehat{\mu}_e(t)] \rangle$ the orientational correlation function expressed in terms of the second-order Legendre polynomial of the vector product of the absorption transition moment $\widehat{\mu}_a(0)$ at time t=0 and emission transition moment $\widehat{\mu}_e(t)$ at time t. For spherical molecules the anisotropy takes a relatively simple form:

$$r(t) = \frac{2}{5} P_2(cos\delta)\, e^{-t/\phi_r} \tag{3}$$

where $P_2(cos\delta)$ is the second-order Legendre polynomial of the cosine of the angle δ between absorption and emission transition moment; ϕ the rotational correlation time, $\phi = 1/(6D)$, with D the rotational diffusion coefficient. In Figure 3A an example of a fluorescence anisotropy decay analysis is presented for lumiflavin in water. The apparent anisotropy is smaller than the true one, which turned out to be close to the maximum value of 0.40. The lower apparent anisotropy is caused by the finite pulse width as shown by computer simulations (Papenhuijzen and Visser, 1983). In Figure 4A we have also plotted two statistical fit parameters versus fixed correlation times with preset initial anisotropy $r(0)$=0.38. The relatively sharp maximum and minimum, coinciding on the ϕ-axis, is indicative for a reliable value for the correlation time. In order to obtain consistent results for all flavin compounds, the initial anisotropy was

preset to 0.38 in all subsequent analyses while the correlation time was the adjustable parameter.

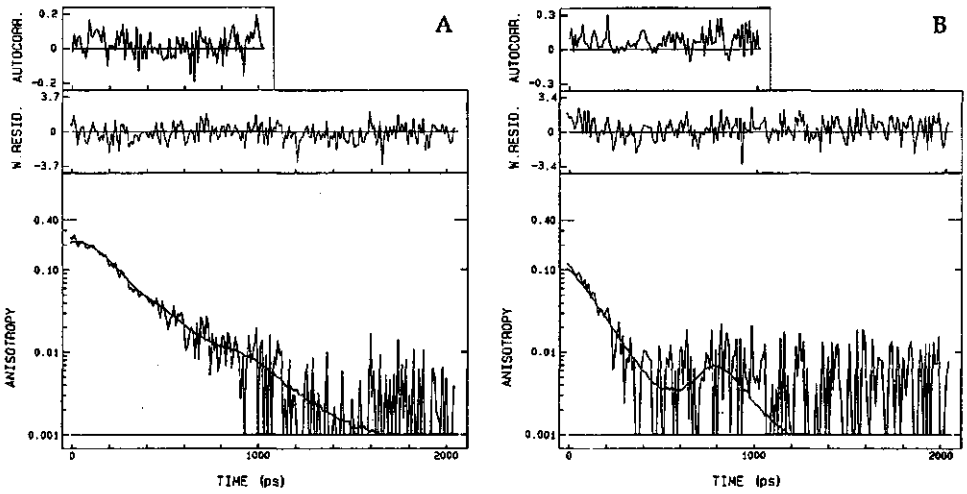

Figure 3. *Direct analyses of fluorescence anisotropy decay of 1 μM lumiflavin in water at 20 °C after excitation in the first (A) and second (B) absorption band, respectively.* **A.** Excitation and emission wavelengths were at 476.7 and 544.0 nm, respectively. The time equivalence was 10.5 ps/channel and the range for fitting was between channels 30 and 300. The experimental and calculated anisotropies are presented between channels 30 and 230. The initial anisotropy was fixed to 0.38 and the recovered correlation time is 82 ± 1 ps. Statistical parameters (see legend to Figure 2): χ^2=1.34, DW=1.66, $ZP_{\parallel}$ = 44 and, $ZP_{\perp}$ = 51. **B.** Excitation and emission wavelengths were at 340.0 and 544.0 nm, respectively. The time equivalence was 10.2 ps/channel and the range for fitting was between channels 57 and 257. The experimental and calculated anisotropies are presented between channels 57 and 257. The initial anisotropy was fixed to 0.25 and the recovered correlation time is 97 ± 2 ps. Statistical parameters: χ^2=1.86, DW=1.19, $ZP_{\parallel}$ = 40 and, $ZP_{\perp}$ = 29.

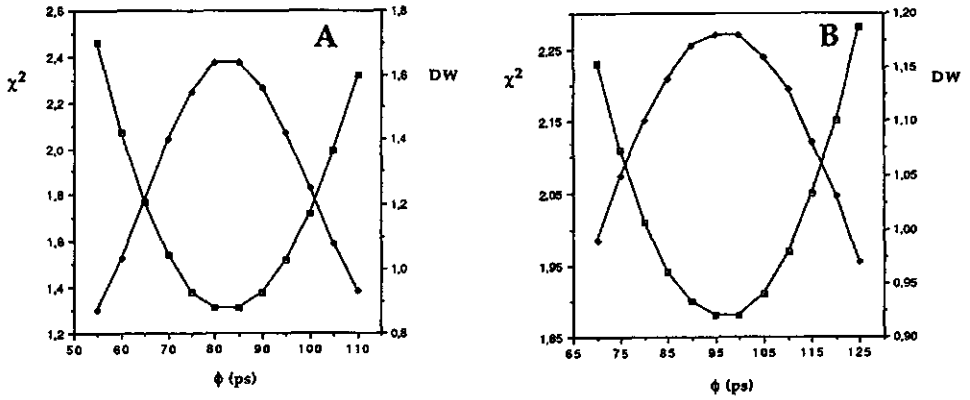

Figure 4. *Fixed correlation times analyses of fluorescence anisotropy decay of 1 μM lumiflavin in water at 20 °C after excitation in the first (A) and second (B) absorption band, respectively.* **A.** Curves of χ^2 and DW versus rotational correlation time ϕ for the experiment detailed in Figure 3A, with $r(0) = 0.38$ and correlation time fixed as indicated (●●●: χ^2 and □□□:DW). **B.** Same as Figure 4A but now for the experiment detailed in Figure 3B (fixed value for $r(0) = 0.25$).

Table 2. *Rotational correlation times and steady-state fluorescence anisotropies of flavins in water at 20 °C (λ_{exc} is 476.7 nm and λ_{em} is 544.0 nm).*

compound	ϕ_{obs}	ϕ_{calc} [a]	ϕ_{calc} [b]	r_0^{obs} [c]	r_0^{calc} [d]
	(ps,±1ps)	(ps)	(ps)	(-)	(-)
lumiflavin	82	66	44	0.005	0.006
N(3)-methyllumiflavin	85	69	45	0.007	0.007
tetra-O-acetylriboflavin	158	139	91	0.011	0.011
N(3)-methyl-tetra-O-acetyl-riboflavin	164	142	92	0.014	0.013
riboflavin	131	96	64	0.009	0.010
FMN	160	117	71	0.010	0.012

a) using Eq. 4 and the volume from molecular weight and density.
b) using Eq. 4 and the van der Waals volume.
c) from Weber (1969).
d) using Eq. 3.

In a previous publication (Visser and van Hoek, 1988) the initial anisotropy was preset to 0.4 in the analysis. From careful analysis of the fluorescence anisotropy of flavins in solid matrices it was found recently that the initial anisotropy is 0.38 ± 0.01 (Bastiaens and Visser, unpublished results). Prefixing the initial anisotropy to 0.38 in the analysis of the fluorescence anisotropy decay gave the same fit quality, but the correlation times were a few picoseconds longer than the previously reported ones. From Eq. 2 using $r(0)$=0.38 the angle between the transition moments of absorption and emission can be calculated directly, $\delta = 10.5°$ (excitation within the first electronic absorption band).

The correlation times of all flavin compounds have been collected in Table 2. The effective molecular volume of the flavins is correctly reflected by the correlation time. For instance, addition of a methylgroup at the N(3) position yields a few picoseconds longer correlation time. From these results it can be concluded that picosecond resolution can be obtained with time-correlated single photon counting and a relatively broad instrumental response function. Such a resolution was also obtained using phase fluorometry with GHz modulation frequencies (Lakowicz et al., 1987).

It is possible to calculate the steady-state fluorescence anisotropy $\langle r \rangle$ from the initial anisotropy, the fluorescence lifetime τ, and correlation time ϕ using the following relationship:

$$\langle r \rangle = \frac{\int_0^\infty r(0)\, e^{-t/\phi}\, e^{-t/\tau}\, dt}{\int_0^\infty e^{-t/\tau}\, dt} = r(0)\,\frac{\phi}{\tau + \phi} \qquad (4)$$

in which exponential functions describing anisotropy and total fluorescence decays were substituted into Eq.3. These data are also collected in Table 2. Experimental values, already reported more than twenty years ago (Weber, 1966), are included as well to demonstrate the excellent agreement.

A comparison with theoretically predicted values can be made by referring to the Stokes-Einstein relationship:

$$\phi = \frac{\eta V}{k T} = \frac{1}{6D} \qquad (5)$$

where η is the viscosity of water, k is the Boltzmann constant, T is the temperature, V is the molecular volume. The volumes were obtained as outlined in the experimental section. From the data collected in Table 2, it can be clearly observed that the calculated correlation times based on the van de Waals volumes are significantly shorter than the ones based on the molecular weight and density. Both calculated correlation times are shorter than the measured ones. An explanation can be found in the high polar character of the flavin molecule. The calculated ground-state dipole moment of the isoalloxazine ring is 7.8 D (Platenkamp et al., 1987) and it is directed between the two carbonyl residues at an angle of 16° with respect to the horizontal axis (see Figure 1). It has been concluded from the effect of pressure on the fluorescence spectral distribution of flavins that ground- and excited-state solvations are similar (Weber et al., 1974). Therefore, the results can be explained by assuming (weak) dipole-dipole interactions between the excited flavin molecules and water molecules. Stick-boundary conditions will certainly prevail in this system thereby increasing the effective volume of the flavin by solvent attachment. Another explanation could be the fact that the flavin molecule is not a spherical rotor. This aspect will be discussed in the following section.

Anisotropic motion

In order to detect anisotropic motion of the isoalloxazine moiety it is appropriate to consider only the lumiflavin case and not the compounds with the bulky side chains. For an irregularly shaped molecule the theoretical anisotropy decay function is composed of a combination of five exponential terms (Belford et al., 1972). If the shape of lumiflavin contains symmetry and can be approximated as that of a prolate ellipsoid of revolution, this is reduced to three correlation times (ϕ_i, i=1,2, and 3) connected with the anisotropy decay function (Tao, 1969):

$$r(t) = \beta_1 e^{-t/\phi_1} + \beta_2 e^{-t/\phi_2} + \beta_3 e^{-t/\phi_3} \qquad (6)$$

The pre-exponential factors β_i (i=1,2, and 3) are functions of the angles that the absorption and emission transition moments subtend with the main symmetry axis, and of the angle δ between the absorption and emission transition moments (for details see: Visser et al., 1989). The location of the absorption transition moments are known (Johansson et al., 1979). The first absorption transition

Table 3. *Parameters describing the fluorescence anisotropy decay of lumiflavin as prolate ellipsoid*[a].

Axial ratio:	$\rho = 2.1$
Diffusion constant:	$D_{\|} = 1.252$ D
Diffusion constant:	$D_{\perp} = 0.649$ D
Angle transition moment [b]:	$\delta = 32°$
correlation time 1:	$\phi_1 = 1.572\ \phi_{eff}$
correlation time 2:	$\phi_2 = 1.353\ \phi_{eff}$
correlation time 3:	$\phi_3 = 0.955\ \phi_{eff}$
$\lambda_{exc} = 476.7$ nm:	$\beta_1 = 0.185$
	$\beta_2 = 0.184$
	$\beta_3 = 0.011$
$\lambda_{exc} = 340.0$ nm:	$\beta_1 = 0.302$
	$\beta_2 = -0.052$
	$\beta_3 = 0.001$

a) detailed mathematical expressions are given in Visser et al. (1989).
b) from Johansson et al. (1979).

moment (λ_{exc} is 476.7 nm) makes an angle of 32° with respect to the long axis (the symmetry axis) of the three-membered ring system (see Figure 1). The total length of the axis is 9 Å. The short axis runs through the lines connecting N(5) with N(10) and the carbon atom of the methyl group adjacent to N(10). The length of the short axis amounts to 4.3 Å. The correlation times ϕ_i are functions of the two possible diffusion constants, namely for rotation about the long symmetry axis ($D_{\|}$) and for rotation about the short axis ($D_{\perp}$) (Tao, 1969). $D_{\|}$ and $D_{\perp}$ can be expressed in the axial ratio and in the rotational diffusion coefficient, D, of an equivalent sphere (Tao, 1969). Therefore the correlation times ϕ_i can be easily expressed in the effective correlation time, ϕ_{eff}, describing the correlation time of an equivalent sphere. The parameters of the anisotropy decay model according to Eq. 5 have been collected in Table 3. From inspection of Table 3 it can be immediately concluded that the anisotropy decay is close to an exponential function since the relative contributions ($=\beta_i/\Sigma\beta_i$) of the first two correlation times (ϕ_1 and ϕ_2) are similar, while the exponential term with the shorter correlation time (ϕ_3) only contributes for 3 % to the decay. We have used the experimental fluorescence anisotropy decay of lumiflavin for analysis according to the ellipsoidal model with the parameters listed in Table 3. The effective correlation time, ϕ_{eff}, was systematically varied until the best match

between experimental and calculated decay was obtained. The results, presented in Figure 5 as a plot of statistical parameters against ϕ_{eff}, are in favour of anisotropic rotation since the effective correlation time is shorter than the one obtained from direct analysis (i.e. 55 ps instead of 82 ps).

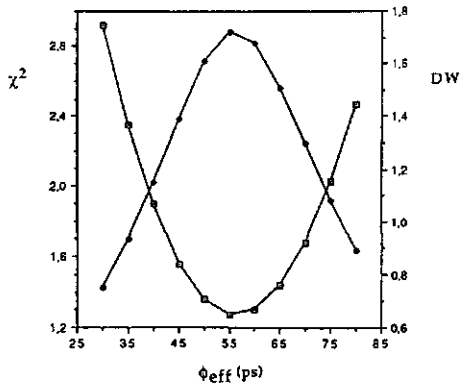

Figure 5. *Analysis of fluorescence anisotropy decay of lumiflavin according to a prolate ellipsoidal rotor.* The experiment detailed in Figure 3A was analyzed using the parameters summarized in Table 3. The effective correlation time, ϕ_{eff}, was systematically varied until an optimum fit was obtained (ϕ_{eff} = 55 ps). See text for details (•••: χ^2 and □□□:DW).

Anisotropic motion of lumiflavin was unambiguously demonstrated by also conducting experiments at 340.0 nm excitation, which encompasses the second electronic absorption band. The transition moment of this band makes an angle of 39° with the first optical transition moment and is nearly parallel to the symmetry axis (Johansson et al., 1979). The near colinearity of the second transition moment and the long axis would predict a slower, largely exponential anisotropy decay. At 340.0 nm excitation experiments with two flavin compounds were performed: FMN and lumiflavin. FMN has electronic properties identical to those of lumiflavin. Because of its much longer correlation time the establishment of the initial anisotropy using 340.0 nm excitation and 544.0 nm emission turned out to be very precise, $r(0) = 0.25 \pm 0.01$ (data not shown). The value of $r(0)$=0.25 was fixed in the analysis of the anisotropy decay of lumiflavin. From the analysis a distinctly longer correlation time of 97 ps was obtained (Figure 4B). Presented in a semilogarithmic way, the anisotropy taken with 340.0 nm excitation (Figure 3B) apparently shows a faster decay than the anisotropy with 476.7 nm excitation (Figure 3A). However, the

frequency doubled dye laser pulse width is 4 ps as compared to the 100 ps argon ion laser pulse, which leads to a distinctly smaller instrumental response function (about 100 ps as compared to 200 ps when excitation was at 476.7 nm). It is essential to apply proper deconvolution methods to retrieve the correct correlation times at high accuracy. A fixed correlation time analysis, similarly as performed in Figure 4A, revealed that the optimum correlation time is shifted to higher values, but the maximum Durbin-Watson- and minimum χ^2-values are much less pronounced than in the former case. The latter effect is due to the lower initial anisotropy, which decreases the dynamic range of measurable anisotropy.

From the initial anisotropies using two excitation wavelengths in combination with the directions of the absorption transition moments in the molecular framework of the isoalloxazine ring system as determined by Johansson et al. (1979), the angle between the emission transition moment and the symmetry axis could be determined, δ_e is $22 \pm 5°$.

Conclusions

The shortest rotational correlation times obtained in this study are approximately two or three times shorter than the width at half maximum of the instrumental response function. Both the precision and reproducibility (within a few picoseconds) of the method are excellent. The precision is demonstrated by the sensitivity of the correlation time for a slightly increasing molecular volume by a methyl group. Anisotropic rotation of the isoalloxazine moiety is clearly demonstrated by the fact that the correlation times turn out to be different when excitation was either within the first or second electronic absorption band.

Acknowledgements

We thank Dr. F. Müller for providing us with flavin compounds. Partial financial support was obtained from The Netherlands Organization for Scientific Research (N.W.O.).

References

Bebelaar, D. (1986) *Rev. Sci. Instrument. 57*, 1116-1125.

Belford, G. G., Belford, R. L. & Weber, G. (1972) *Proc. Natl. Acad. Sci. USA 69*, 1392-1393.

Hall, L. H., Bowers, M. L. & Durfor, C. N. (1987) *Biochemistry 26*, 7401-7409.

Ichiye, T. & Karplus, M. (1983) *Biochemistry 22*, 2884-2893.

Johansson, L. B.-Å., Davidsson, Å., Lindblom, G. & Razi Naqvi, K. (1979) *Biochemistry 18*, 4249-4253.

Lakowicz, J. R., Laczko, J. & Gryczynski, I. (1987) *Biochemistry 26*, 82-90.

Massey, V. & Swoboda, B. E. P. (1963) *Biochem. Z. 338*, 474-484.

Papenhuijzen, J. & Visser, A. J. W. G. (1983) *Biophys. Chem. 17*, 57-65.

Platenkamp, R. J., van Osnabrugge, H. D. & Visser, A. J. W. G. (1980) *Chem. Phys. Lett. 72*, 104-111.

Platenkamp, R.J., Palmer, M. H. & Visser, A. J. W. G. (1987) *Eur. Biophys. J. 14*, 393-402.

Tao, T. (1969) *Biopolymers 8*, 609-632.

van Hoek, A. & Visser, A. J. W. G. (1985) *Anal. Instrum. 14*, 359-372.

van Hoek, A., Vos, K. & Visser, A. J. W. G. (1987) *IEEE J. Quantum Electron. QE-23*, 1812-1820.

Visser, A. J. W. G. & van Hoek, A. (1979) *J. Biochem. Biophys. Methods 1*, 195-208.

Visser, A. J. W. G., Ykema, T., van Hoek, A., O'Kane, D. J. & Lee, J. (1985) *Biochemistry 24*, 1489-1496.

Visser, A. J. W. G. & van Hoek, A. (1988) in *Time-resolved Laser Spectroscopy in Biochemistry, vol. 909* (Lakowicz, J. R., Ed.), pp. 61-68, Proceedings of SPIE-The International Society for Optical Engineering, Bellingham, WA.

Visser, A. J. W. G., Kulinski, T. & van Hoek, A. (1988) *J. Molec. Struct. 175*, 111-116.

Visser, A. J. W. G., Vos, K., van Hoek, A. & Santema, J. S. (1988) *J. Phys. Chem. 92*, 759-765.

Visser, A. J. W. G., van Hoek, A., O'Kane, D. J. & Lee, J. (1989) *Eur. Biophys. J. 17*, 75-85.

Vos, K., van Hoek, A. & Visser, A. J. W. G. (1987) *Eur. J. Biochem. 165*, 55-63.

Wahl, Ph., Auchet, J.-C., Visser, A. J. W. G. & Müller, F. (1974) *FEBS Lett. 44*, 67-70.

Wang, M. & Fritchie, C. J. (1973) *Acta. Cryst. B29*, 2040-2045.

Weber, G. (1966) in *Flavins and Flavoproteins* (Slater, E. C., Ed.), pp. 15-31, Elsevier/North-Holland, Amsterdam.

Weber, G., Tanaka, F., Okamoto, B. Y. & Drickamer, H. G. (1974) *Proc. Natl. Acad. Sci. USA 71*, 1264-1266.

Chapter 8

General discussion

Until recently the conformational analysis of biomolecular structures was based on experiments performed with solid phase samples (X-ray diffraction, Fourier Transform Infrared spectroscopy, etc.). However, the development of techniques like nuclear magnetic resonance and time-resolved polarized fluorescence spectroscopy enables us to examine structure and dynamics of biomolecules in solution. Furthermore, molecular dynamics calculations of biomolecules in solvent environment can be used to examine processes which are difficult to approach experimentally.

This thesis deals with the dynamic properties of the active site of several flavodoxins. These proteins transfer electrons from one redox protein to another, whereby flavodoxin shuttles between fully reduced (hydroquinone) and semiquinone states. The mechanism of electron transfer is not yet elucidated, but it has become clearer in the last few years that both static and dynamic properties of the proteins influence the electron transfer rates.

In Chapter 2 the reduced flavin fluorescence characteristics of different flavodoxins are shown: *Desulfovibrio gigas*, *Desulfovibrio vulgaris*, *Clostridium beijerinckii*, and *Megasphaera elsdenii* flavodoxin. The results are compared with those of reduced flavin mononucleotide in solution. The fluorescence decays are analyzed both as a sum of exponentials with classical iterative non-linear least-squares reconvolution and using the inverted Laplace transform accomplished by the maximum entropy method. These two approaches yield highly similar results. The fluorescence decay is always composed of three lifetime distributions, where the shortest fluorescence lifetime is influenced by the protein environment. The results indicate that the active site of *Desulfovibrio* flavodoxins resembles that of reduced flavin in solution more than in the other two flavodoxins. Based on the results of the fluorescence decays of reduced flavodoxins, the proteins can be classified into two groups: the *rubrum*-like flavodoxins (the two *Desulfovibrio* proteins) and the *pasteurianum*-like flavodoxins (the other two proteins). It is suggested that the position of the shortest lifetime can be used as a marker for the environment of the reduced flavin. Analysis of the fluorescence anisotropy decays shows that the protein-bound reduced flavin is immobilized within the apoprotein matrix. The rotational correlation time of the *rubrum* class of flavodoxins is somewhat longer than for *pasteurianum* flavodoxins which is explained by a small difference in molecular weight and volume. The dynamic properties of reduced flavin bound in flavodoxin indicate that a specific fixed rotation of the flavin may be required for electron transfer between flavodoxin and other redox proteins.

Chapter 3 describes the fluorescence intensity decay of oxidized *clostridial* flavodoxin as analyzed using the maximum entropy method. Two short lifetimes (30 ps and 0.5 ns) are demonstrated which are not present in the fluorescence decay of oxidized flavin mononucleotide in solution. The third fluorescence lifetime (4.8 ns) coincides with the single lifetime found in free oxidized flavin. The fluorescence lifetime distribution is highly temperature dependent. At higher temperatures (more than 20 °C) the contribution of the 4.8 ns lifetime component increases dramatically. This behaviour can be explained by a small shift in equilibrium from protein-bound (low fluorescence quantum yield) to dissociated oxidized flavin (high quantum yield). This is confirmed by adding stoechiometric amounts of apoflavodoxin to the flavodoxin sample. The equilibrium then shifts to protein-bound flavin, even at elevated temperatures (more than 30 °C). The dissociation constant is determined, $K_D = 2.61*10^{-10}$ M^{-1} (at 20 °C). Addition of an excess of apoflavodoxin did not result in the complete disappearance of the 4.8 ns fluorescence lifetime. Collisional quenching experiments show that this flavin moiety in the flavodoxin fluorescence decay is solvent accessible, since it is significantly quenched by iodide. Associative analysis of the fluorescence and fluorescence anisotropy decays shows that the shortest fluorescence lifetime is probably coupled to a rotational correlation time similar to overall protein tumbling. However, the lifetime is far too short to contain accurate information on relatively slow protein tumbling. A part of the flavodoxin solution seems to be composed of dissociated flavin since the 4.8 ns lifetime can be linked to the rotational correlation time of free flavin in solution. This fluorescence lifetime, however, is also partly coupled to a correlation time slightly longer than that of free FMN. This moiety might then be intermediate between dissociated flavin and flavin which is loosely bound to the protein. Since its fluorescence lifetime is similar to that of free flavin this indicates that the flavin is probably bound to the protein via its ribityl-phosphate sidechain. This is in accordance with studies in which it is demonstrated that the phosphate group is essential for flavin binding to the apoprotein of flavodoxin (Barman and Tollin, *Biochemistry 11* (1972) 4746-4754). The correlation time is longer than for free flavin as a result of sterical hindrance.

The molecular dynamics of oxidized and fully reduced *Cl. beijerinckii* flavodoxin are calculated and described in Chapter 4. From the simulations of the flavodoxins in a solvent environment it is clear that the conformation of the active site of the flavodoxin in solution is very similar to the three-dimensional structure as determined by X-ray diffraction studies. However, some differences were found in the backbone conformation of the loop composed of residues 57

to 63. This loop is located near the flavin chromophore. Another difference is the direction of the plane through the reduced isoalloxazine ring system which is tilted about 11° as compared to its initial structure. This might be explained by the fact that the initial structure of semiquinone flavodoxin was used. Another explanation could be the choice of the distribution of the negative charge over flavin atoms N(1) and O(2). On the time scale of the calculations (hundreds of picoseconds), the oxidized as well as reduced flavin is immobilized within the protein matrix. This is in accordance with the experimentally determined initial fluorescence anisotropies. Comparison with earlier results of MD simulations in vacuo demonstrated that solvent inclusion is necessary for a correct description of the motional behaviour of the flavin. From the calculations the time-correlation functions of the three tryptophan sidechains were determined. Residues Trp6 and Trp95 are almost immobilized in both oxidation states, whereas residue Trp90 has a fast decaying time-correlation function, indicating a large motional freedom. This flexibility, present in both oxidation states, is most pronounced in reduced flavodoxin. A possible role for this flexibility in electron transfer is suggested. Based on the coplanarity of the flavin isoalloxazine ring and the indole sidechain of Trp90 in the initial crystal structures, it might be extracted that the ring systems have correlated motion. However, from the MD calculations it is demonstrated that hardly any correlation in positional fluctuations of both ring systems exists.

The tryptophan fluorescence decay kinetics of apo- and holo-flavodoxins (from *D. gigas, D. vulgaris, Cl. beijerinckii,* and *M. elsdenii*) are described in Chapters 5 and 6. The fast decaying fluorescence in the holoflavodoxins can be explained by energy transfer from the excited state of the tryptophan to the flavin acceptor. Energy transfer rate constants could be calculated from the known three-dimensional structure of *D. vulgaris* flavodoxin, which are present in the analysis of the fluorescence decays (see additional results summarized in the Appendix). Based on the steady-state and time-resolved characteristics it is suggested that the remote tryptophan (at about 20 Å from the center of the flavin) is preserved in both *Desulfovibrio* flavodoxins. Quantification of the fluorescence of flavodoxins with more than one tryptophan residues is extremely complex (tryptophan in aqueous solution already exhibits multi-exponential fluorescence decay). It is noted that a straightforward comparison of the fluorescence decays of apo- and holo-flavodoxins is difficult, since removal of the flavin chromophore results in a changed microenvironment of the tryptophan residues. However, strong indications have been found that in holo-flavodoxin samples, always contain a certain amount of apoflavodoxin.

In Chapter 7 the rotational correlation times of natural flavin compounds as well as some flavin models are reported. These time-resolved polarized fluorescence experiments were performed to examine the rotational characteristics of flavins in solution. This information can be used for comparison with protein-bound flavins (e.g., in flavodoxin (see Chapter 3)). An extra methyl group at flavin N(3) resulted in a few picoseconds longer correlation, in agreement with the slightly larger molecular volume and illustrating the high time-resolution of the picosecond laser fluorescence system used. Analyzing the decays after excitation in the first and second excited states demonstrated anisotropic motion of the lumiflavin. The angle between the long axis of the isoalloxazine ring system and the emission transition moment is approximately 22°, in fair agreement with the value obtained by Bastiaens et al. (*Biophys. J. 63* (1992) 839-853).

Samenvatting

Dit proefschrift behandelt de beweeglijkheid in een bepaald soort eiwit. Bij de term 'eiwit' denken velen in eerste instantie aan de doorzichtige massa rondom een ei-dooier. Hoewel deze eiwit-rijk is, komen eiwitten in de natuur veel vaker voor. Alle levende wezens op aarde bestaan deels uit allerlei verschillende eiwitten. Deze eiwitten hebben vele verschillende functies. Afhankelijk van hun functie hebben eiwitten een bepaalde structuur en vorm. Daarnaast kan het zo zijn dat de functie niet alleen afhankelijk is van de structuur maar ook van de beweeglijkheid binnen zo'n eiwit. Het in dit proefschrift beschreven eiwit is het flavodoxine. Het flavodoxine is een eiwit met als functie negatieve lading, in de vorm van electronen, te transporteren van het ene naar het andere eiwit. De electronen worden hierbij getransporteerd door een in het flavodoxine gebonden pigment, flavine genaamd. Dit flavine kan in verschillende oxidatie-toestanden of redox-toestanden voorkomen. Het flavodoxine wordt derhalve een redox-eiwit genoemd. Iedereen kent een aantal stoffen die in verschillende redox- of oxidatie-toestanden kunnen voorkomen. Het meest bekend is ijzer. Dit kan voorkomen als blank metaal (neutrale toestand) of als roest (het ijzer is dan positief geladen). Deze positieve lading wordt gecompenseerd door de negatief geladen electronen van het zuurstof waarmee het ijzer een reactie is aangegaan. Een ander voorbeeld is een dakgoot van zink. Het zink lost een beetje op wanneer het in aanraking komt met regenwater. Hierbij verandert de oxidatie-toestand van neutraal naar positief, waardoor het reageert met negatieve ionen uit het water. Dit geeft een neerslag op de dakgoot die daardoor dof wordt.

Zoals gezegd spelen beweeglijkheden in eiwitten mogelijkerwijs een rol bij hun functie. Deze flexibiliteit is het beste voor te stellen door te denken aan een boom in de winter. Alle takken zijn zichtbaar als een soort geraamte. Als er een flinke bries waait zie je dat de boom niet star is. Alle takken bewegen mee met de wind. De kleinste takken het snelst en de zwaarste takken het langzaamst. Ook is het zo dat als het uiteinde van een tak ver doorbuigt, dat dan het dikke basis-gedeelte ook enigszins meegaat. Dit wordt een gecorreleerde beweging genoemd. De structuur van een eiwit lijkt op het eerste gezicht ook een beetje op die van een kale boom. Ook de bewegingen van de delen van het eiwit zijn te vergelijken met die van de takken.

Net zoals zout of suiker oplost in water zo zijn ook de meeste eiwitten water-oplosbaar. In de natuur komen eiwitten voornamelijk opgelost voor. Bij

het ophelderen van de drie-dimensionale structuur van een eiwit wordt vaak gebruik gemaakt van eiwit-kristallen of poeders. Ondanks het feit dat dit een goede methode is om de structuur vrij nauwkeurig te weten te komen, levert het toch niet helemaal de structuur zoals die in oplossing is. Recentelijk zijn een aantal technieken ontwikkeld en verbeterd die het mogelijk maken de structuur en dynamica van eiwitten in oplossing te onderzoeken. Bekende voorbeelden zijn de kernspin-resonantie (NMR) en tijd-opgeloste fluorescentie. Daarnaast is het mogelijk om de dynamica van een eiwit te simuleren. Hierbij wordt gebruik gemaakt van krachtige (super)computers. Voorwaarden zijn wel dat de ruimtelijke structuur van het eiwit redelijk nauwkeurig bekend is en dat de parameters die in de berekening worden gestopt met de werkelijkheid in overeenstemming zijn. Bij deze technieken wordt geprobeerd de natuurlijke omstandigheden zo goed mogelijk te benaderen.

In Hoofdstuk 2 worden de fluorescentie-karakeristieken beschreven van gereduceerde flavines in flavodoxines uit verschillende bacteriën: *Desulfovibrio gigas*, *Desulfovibrio vulgaris*, *Clostridium beijerinckii* en *Megasphaera elsdenii*. De verkregen resultaten worden vergeleken met die van gereduceerd flavine vrij in oplossing. Het fluorescentie-verval is geanalyseerd met een som van exponenten en met de maximum entropie methode. Beide analyses leveren soortgelijke resultaten. Het fluorescentie-verval bestaat steeds uit drie levensduur-componenten. De kortste levensduur is erg afhankelijk van de omgeving van het flavine. In *Desulfovibrio* flavodoxines lijkt de flavine-omgeving meer op die van gereduceerd flavine in oplossing, dan bij de andere flavodoxines. Gebaseerd op de verkregen karakteristieken zijn de vier flavodoxines te verdelen in twee groepen: de *rubrum*-klasse (met de *Desulfovibrio* flavodoxines) en de *pasteurianum*-klasse (met de andere twee eiwitten). De positie van de kortste levensduur kan gebruikt worden als een marker voor de omgeving van het gereduceerde flavine. De rotatie-correlatie-tijden van de flavodoxines uit de *rubrum*-klasse zijn ietwat langer dan voor de andere twee flavodoxines. Dit kan verklaard worden door de verschillen in grootte en volume: *rubrum*-flavodoxines bevatten ongeveer 10 aminozuren meer dan *pasteurianum*-flavodoxines. De flavine-dynamica in de gereduceerde flavodoxines wijst op het belang van een specifieke gefixeerde oriëntatie van de flavine-chromofoor.

Hoofdstuk 3 beschrijft de tijd-opgeloste fluorescentie-metingen verricht aan geoxideerd *Cl. beijerinckii* flavodoxine. De resultaten van de maximum entropy analyse tonen dat er twee fluorescentie-levensduren (van 30 ps en 0.5 ns) in het flavodoxine voorkomen, welke niet aanwezig zijn bij geoxideerd flavine vrij in oplossing. Een derde levensduur van 4.8 ns komt zowel in het

flavodoxine als in vrij flavine voor. De levensduur-verdeling is sterk temperatuur-afhankelijk. Het aandeel van de langere levensduur neemt aanzienlijk toe bij hogere temperatuur (boven de 20 °C). Dit gedrag valt te verklaren door een kleine verschuiving van het evenwicht tussen eiwit-gebonden en gedissocieerd flavine. De dissociatie constante is berekend, $K_D = 2.61*10^{-10}$ M^{-1} (20 °C). Het vrije flavine, wat door de lage dissociatie-constante in zeer kleine hoeveelheden aanwezig is, heeft een veel hogere fluorescentie quantum-opbrengst dan het flavine dat in het flavodoxine gebonden is. Hierdoor lijkt het of het evenwicht een grote verschuiving ondergaat. Het toevoegen van kleine hoeveelheden apoflavodoxine aan de flavodoxine-oplossing resulteert in een terug-verschuiving van het evenwicht (dit blijft zo bij hogere temperatuur). Het toevoegen van nog grotere hoeveelheden apoflavodoxine heeft echter niet tot gevolg dat de 4.8 ns fluorescentie-levensduur volledig verdwijnt. Quenching-experimenten tonen aan dat de langste levensduur in flavodoxine gekoppeld is met flavine dat toegankelijk is voor oplosmiddel-moleculen. De andere twee levensduren worden door het iodide nagenoeg niet beïnvloedt. Associatieve analyse van de fluorescentie en fluorescentie anisotropie verval-curves toont dat de kortste levensduren gekoppeld zijn met een rotatie-correlatie-tijd zoals verwacht voor het gehele eiwit. De langste levensduur (4.8 ns) is deels gekoppeld aan de rotatie-correlatie-tijd van vrij flavine en deels aan een langere rotatie-correlatie-tijd. Deze laatste groep flavine-moleculen is mogelijk het intermediair tussen eiwit-gebonden en gedissocieerd flavine. Daar de fluorescentie-levensduur gelijk is aan die van vrij flavine is het waarschijnlijk dat het flavine in het intermediair met de fosfaat-groep is gebonden aan het apoflavodoxine. De langere correlatie-tijd, in vergelijking met flavine vrij in oplossing, wordt verklaard door sterische hindering.

De moleculaire dynamica van geoxideerd en gereduceerd *Cl. beijerinckii* flavodoxine is gesimuleerd en beschreven in Hoofdstuk 4. Uit de berekeningen van het flavodoxine in een oplosmiddel-omgeving is het duidelijk dat de conformatie van het actieve centrum goed overeenkomt met die in de kristalstructuur. Er worden enkele verschillen beschreven, zoals de conformatie van de aminozuren 57 tot en met 63. Een ander klein verschil is de richting van het vlak door het gereduceerde isoalloxazine. Deze is namelijk ongeveer 11° anders gericht dan in de oorspronkelijke structuur. Een mogelijke oorzaak hiervan is het feit dat de initiële structuur van het semiquinon flavodoxine is gebruikt. Een andere mogelijkheid is de wijze waarop de negatieve lading is verdeeld over de flavine atomen N(1) en O(2). Het is gebleken dat de simulaties uitgevoerd dienen te worden met oplosmiddel-moleculen omdat bij vacuum-

berekeningen de beweeglijkheid van het flavine niet correct wordt beschreven. Op de tijdschaal van de berekeningen zijn zowel het geoxideerde als gereduceerde flavine geïmmobiliseerd in het eiwit. Dit is in overeenstemming met de experimenteel bepaalde initiële anisotropiën. De calculaties van de tijd-correlatie functie van de zijketens van de drie tryptofaan-residuen tonen aan dat Trp6 en Trp95 redelijk geïmmobiliseerd zijn in de eiwit-matrix. Residu Trp90 daarentegen bezit een grote flexibiliteit in beide oxidatie-toestanden, gezien het snelle verval van de tijd-correlatie functie. Uit de kristalstructuur zou op grond van de parallel gerichte isoalloxazine-ring en de tryptofaan-indol (Trp90) veronderstelt kunnen worden dat de beweeglijkheid van beide ringsystemen gecorreleerd is. Uit de MD simulaties is echter geen significante correlatie in de ruimtelijke fluctuaties aantoonbaar.

De tijd-opgeloste tryptofaan-fluorescentie van de apo- en holoflavodoxines (uit *D. gigas* en *D. vulgaris*) worden beschreven in de Hoofdstukken 5 en 6. Het snelle verval van de fluorescentie van de holoflavodoxines kan verklaard worden door een energie-overdracht van het aangeslagen tryptofaan naar het flavine. Uit de kristalstructuur van het *D. vulgaris* flavodoxine kunnen energie-overdrachts-constanten berekend worden, die in het experimentele fluorescentie-verval aanwezig zijn. Op grond van 'steady-state' en tijd-opgeloste fluorescentie-karakteristieken wordt gesteld dat de ver van het flavine afgelegen tryptofaan (afstand flavine-tryptofaan is ongeveer 20 Å) geconserveerd is in beide *Desulfovibrio* flavodoxines. Het dient opgemerkt te worden dat quantificering van de fluorescentie-parameters van flavodoxines met meer dan één tryptofaan erg complex is (één tryptofaan residu heeft al een multi-exponentieel verval). Een bijkomstige factor is dat het moeilijk is om de fluorescentie-karakteristieken van apo- en holoflavodoxines zonder meer te vergelijken, daar mogelijk een conformatie-verandering geïnduceerd wordt door de verwijdering van het flavine.

In Hoofdstuk 7 wordt verslag gedaan van experimenten met verschillende natuurlijke flavines en enkele flavine-modellen. De tijd-opgeloste fluorescentie experimenten zijn uitgevoerd om de gepolariseerde fluorescentie-karakeristieken van vrije flavines te onderzoeken. Deze informatie kan worden gebruikt ter vergelijking met de fluorescentie-eigenschappen van eiwit-gebonden flavines (zoals in flavodoxine, Hoofdstuk 3). Een extra methyl-groep op de flavine-positie N(3) heeft een aantoonbare verlenging van de rotatie-correlatie-tijd tot gevolg. Dit is in overeenstemming met het enigszins grotere volume. Uit excitatie in de eerste en tweede absorptie-band wordt een anisotrope beweging van het lumiflavine afgeleid. Verder bedraagt de hoek tussen het emissie transitiemoment en de lange as van het isoalloxazine 22°.

Curriculum vitae

Henricus Robertus Maria Leenders is geboren op 24 mei 1963 te Ubbergen. In 1981 behaalde hij het diploma ongedeeld VWO aan het Carolus Borromeus College te Helmond. In datzelfde jaar werd de studie Scheikunde aangevangen aan de Katholieke Universiteit te Nijmegen. Het kandidaatsdiploma werd behaald in januari 1985. De daaropvolgende doctoraalfase bestond uit een hoofdvak Biochemie (Prof. dr. H. Bloemendal; recombinant-DNA onderzoek naar de interactie tussen DNA-promotoren) en de bijvakken Biofysische chemie (Prof. dr. C. Hilbers; 2-dimensionale NMR-metingen en moleculaire mechanica berekeningen aan circulaire dinucleotiden) en Zoölogie (Prof. dr. J. M. Denucé; chemisch endocrinologisch onderzoek aan het gonaden inhiberend hormoon van de kreeft). Het doctoraalexamen werd afgelegd in october 1987.

Van 1 november 1987 tot 1 februari 1992 is hij als promovendus verbonden geweest aan de vakgroep Biochemie van de Landbouwuniversiteit te Wageningen. In deze periode is het onderzoek verricht dat heeft geleid tot dit proefschrift.

Vanaf 1 juni 1992 is hij als adviseur verbonden aan de Stichting Academisch Rekencentrum Amsterdam (SARA).